

Non-isocyanate poly(hydroxyurethane)s and polycarbonates derived from *N*-substituted eight membered cyclic carbonates

Alexander Yik Ming Yuen

University of the Basque Country (UPV/EHU)
Donostia-San Sebastián
(2017)



POLYMAT

*To family, friends, and
colleagues.*

Acknowledgments

First and foremost, I would like to thank Professor David Mecerreyes and Dr. Haritz Sardon for selecting me as their student and their mentorship along the way. The experiences I had in San Sebastian not only broadening my knowledge in the field of polymer science, but also opened my eyes to the different cultures in Europe and beyond.

I am deeply thankful to my family (especially mom and dad) for their love and support. I am also grateful to have met so many great people who helped me fit in and adapt to the way of life in San Sebastian:

Isabel, Ana M., Luca, Paolin, Daniele, Ivan, Guiomar, Inaki, Sara, Stefano,
Francesca, Naroa, Leire, Amaury, Mehmet, Ana P., ... and many more

I will miss you guys and I hope we will stay in touch.

Finally, I would like to express my appreciation for the financial support from European commission through the OrgBIO-ITN project (607896). Additionally, I would like to thank the University of the Basque Country and POLYMAT for providing the laboratories, equipment, and other resources to conduct the research work in this thesis.

TABLE OF CONTENTS

Chapter 1. Introduction	2
1.1. Cyclic carbonates	2
1.2. Non-isocyanate polyurethanes (NIPUs) derived from the step growth polyaddition of bis-cyclic carbonates and diamines	4
1.3. Preparation of functional polycarbonates through the ring opening polymerization (ROP) of cyclic carbonates	7
1.4. Motivations.....	11
Chapter 2. Non-isocyanate poly(hydroxyurethane)s	16
2.1. Introduction.....	16
2.2. Results and discussion	18
2.2.1. Comparative study of different cyclic carbonates reactivity towards n-hexylamine	18
2.2.2. Comparative study with low reactivity amines	20
2.2.3. Computational modeling.....	21
2.2.4. Synthesis of NIPUs based on bis <i>N</i> -8-C and diamines	24
2.3. Conclusions	29
2.4. Experimental part	29
Chapter 3. Antimicrobial polycarbonates obtained by post-functionalization	36
3.1. Introduction.....	36
3.2. Results and discussion	39
3.2.1. Synthesis of the charged linear polycarbonate	39
3.2.2. Synthesis of the charged polycarbonate hydrogels	44
3.2.3. Antimicrobial and hemolysis studies with linear polycarbonates.....	46
3.2.4. Antimicrobial and hemolysis studies with polycarbonate gels	49

3.3. Conclusion	50
3.4. Experimental part	50
Chapter 4. Antimicrobial polycarbonates obtained by ROP of ionic monomers	58
4.1. Introduction	58
4.2. Results and discussion	59
4.2.1. Synthesis and polymerization of charged monomers	59
4.2.2. Computational modeling of charged monomers	64
4.2.3. Charged polycarbonate hydrogels derived from charged monomers	66
4.2.4. Assessing the swelling and degradation behavior of the charged polycarbonate gels	68
4.2.5. Antimicrobial studies	70
4.2.6. Hemolysis studies	73
4.3. Conclusion	74
4.4 Experimental part	74
Chapter 5. Synthesis, polymerization, and post-modification of allyl functional monomers	82
5.1. Introduction	82
5.2. Results and Discussion	84
5.2.1. Monomer preparation.....	84
5.2.2. Model polymerizations with allyl bearing monomers.....	86
5.2.3. Exploration of the polymerization conditions with 8-ACfm.....	88
5.2.4. Photo-induced thiol-ene reactions with allyl bearing polycarbonates	91
5.2.5. Exploration of copolymerization	94
5.3. Conclusions	98
5.4. Experimental section.....	98

Chapter 6. Polycarbonate iongels as electrodes for electrophysiology....	110
6.1. Introduction.....	110
6.2. Results and discussion	111
6.2.1. Preparation of ion gels	111
6.2.2. Characterization of the iongels with FTIR-ATR.....	114
6.2.3. Rheology testing.....	115
6.2.4. Biodegradability study.....	117
6.2.5. Ionic conductivity measurements	120
6.2.6. Electrode fabrication and testing	123
6.3. Conclusions	127
6.4. Experimental part	128
Chapter 7. Conclusions	134
Chapter 8. References and lists	138
8.1 References	138
8.2 List of figures.....	144
8.3 List of tables.....	149
8.4 List of publications from this thesis.....	150

Chapter 1



Introduction

Chapter 1. Introduction

1.1. Cyclic carbonates

Cyclic carbonates are a very intriguing and promising class of material that have been commercially available since the mid-1950's.¹ Since then, five membered cyclic carbonates have found numerous applications due to their biodegradability, high solvency, high boiling points (up to 240°C), high flash points (up to 160°C), low odor levels, low evaporation rates, and low toxicities¹. Moreover, the use of five membered cyclic carbonates as a solvent in degreasing, paint stripping, and cleaning applications has risen in the past few years.²⁻⁴ Cyclic carbonates such as ethylene carbonate (EC) and propylene carbonate (PC) are also utilized as electrolytes for lithium ion batteries.⁵ Furthermore, PC has also been studied as a carrier solvent for topically applied medications and cosmetics (Figure 1).⁶

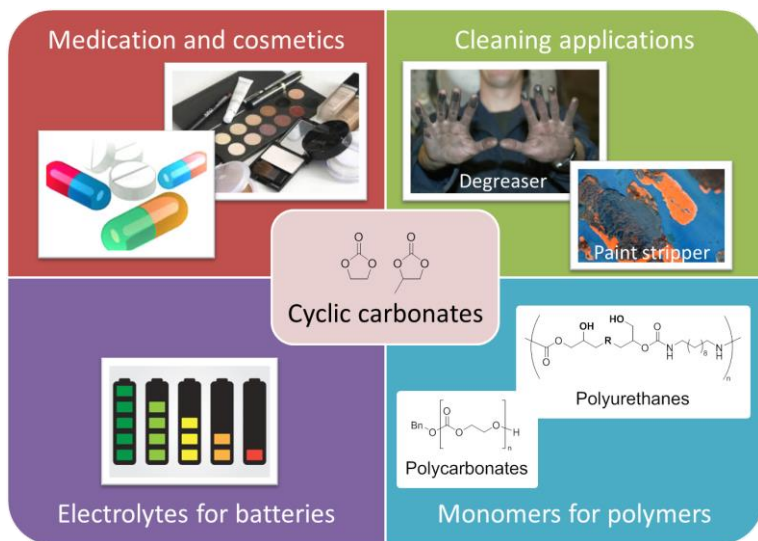


Figure 1. Applications of cyclic carbonates are far and wide ranging. The work in this thesis will focus on using cyclic carbonates as starting materials for polymers.

In the past, these materials were extensively produced through reactions with diol(s) and phosgene (or a phosgene derivative). Lately, much attention has been given to seek out alternative phosgene-free methods, due to the phosgene's toxicity, which include the use of high pressure CO₂, 1,1'-carbonyldiimidazole (CDI), and dimethylcarbonate (DMC).

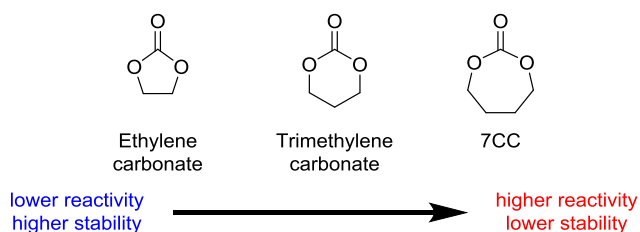


Figure 2. Examples of five, six, and seven membered cyclic carbonates (from left to right). As the ring size increases, the overall trend is higher reactivity and lower stability.

Although much can be said concerning the use of cyclic carbonates, their potential as monomers for the preparation of polymers will be the primary focus of this thesis. Nowadays, cyclic carbonates are used as monomers in polymer chemistry to synthesize poly(hydroxyurethane)s and biodegradable polycarbonates. The first, poly(hydroxyurethane)s, belongs to a family of polymers known as non-isocyanate polyurethanes (NIPUs). The reactivity of the different sized cyclic carbonates as shown in Figure 2 is an important issue in the preparation of poly(hydroxyurethane)s, and it will be discussed later in the thesis. On the other hand, cyclic carbonates can be used in ring-opening polymerization (ROP) towards biodegradable polycarbonates. The most typical examples include the ROP of ethylene carbonate and trimethylene carbonates, which are examples of five and six membered cyclic carbonates respectively. Additionally, some attention has also been given to the larger seven membered cyclic carbonates (7CC) which are much more reactive than the smaller cyclic carbonates. With further thought, Tomita *et al.* attributed the difference in

reactivity amongst these cyclic carbonates to higher ring-strain in the larger cyclic molecules.⁷ The higher reactivity is certainly advantageous for polymerizations, where high reactivity and monomer conversions can lead to high molecular weight polymers. Both NIPUs and polycarbonates are high valued polymers, which can be used in our daily lives and each type of polymer will be discussed more in detail in the following sections.

1.2. Non-isocyanate polyurethanes (NIPUs) derived from the step growth polyaddition of bis-cyclic carbonates and diamines

Polyurethanes (PUs) are considered one of the most important classes of polymeric materials due to their versatility and wide applications. The demand for PUs is rising on average of 4.5% per year, and their production was estimated at 18 kilotons for 2016.^{8,9} Traditionally, PUs are prepared by the reaction of diols and diisocyanates in the presence of a metal based catalyst, and this method is still currently in use in industries. However, the isocyanates reactants are known to be very toxic and harmful towards the environment. Furthermore, the continued use of isocyanates is under revision by the European Union and faces a possible ban. For this reason, 'greener' and more sustainable approaches towards PUs are currently under investigation.

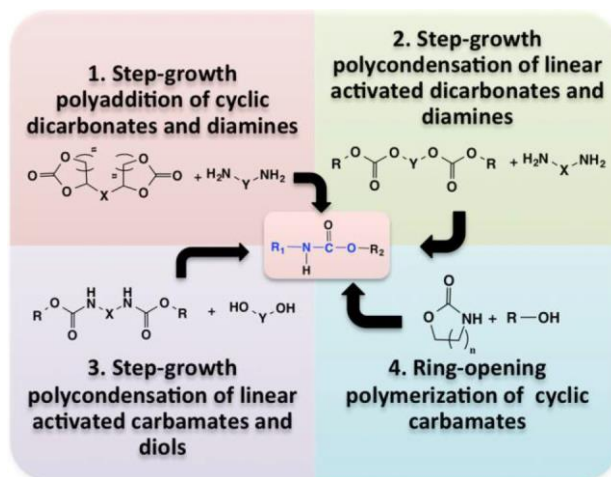
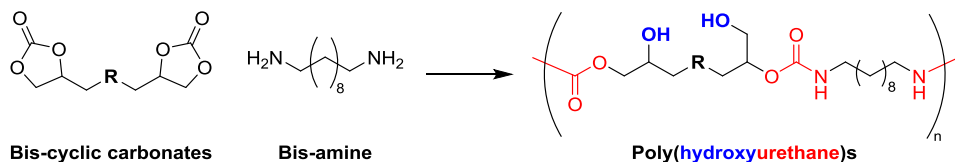


Figure 3. The four most studied synthetic pathways in obtaining polyurethanes without isocyanates.⁸

In the last decade, advances in this field have led to a number of isocyanate free processes^{8,10–13} The four most studied pathways towards NIPUs are: (1) step-growth polyaddition of bis-cyclic carbonates and amines⁸, (2) step-growth polycondensation of linear activated dicarbonates and diamines¹⁴, (3) step-growth polycondensation of linear activated carbamates and diols¹⁵, and (4) ROP of cyclic carbamates¹⁶ (Figure 3). Amongst these methods, polymerization with bis-cyclic carbonates and diamines is the most popular and promising synthetic pathway towards NIPUs (Scheme 1). With this method, the ring opening reaction with the amines generates hydroxyl groups, and as such, the polymers prepared in this manner are termed ‘poly(hydroxyurethane)s’ (PHUs). In addition, the hydroxyl functional groups can be modified at a later point in time, which can add more value to PHUs.



Scheme 1. Step-growth polyaddition of bis-cyclic carbonates and bis-amines to yield poly(hydroxyurethane)s or PHU's.

Among the family of cyclic carbonates, five and six membered bis-cyclic carbonates have been the most studied for the preparation of NIPUs.^{17–29} While six membered carbonates have shown to be more appropriate than five membered ones for polymerization due to their higher reactivity, their synthesis generally requires the use of toxic chlorinated carbonylating agents (i.e., phosgene or alkyl chloroformates).²⁸ On the other hand, five membered cyclic carbonates can be easily produced from the chemical insertion of CO₂ into naturally abundant epoxides.^{30,31}

The NIPUs prepared from five membered cyclic carbonates often require high temperatures, bulk conditions, and long reaction times to achieve high conversions and subsequently high molecular weight polymers. To improve this system, Caillol *et al.* recently found that the reactivity of these five membered cyclic carbonates could be activated by inserting heteroatoms near the cyclic carbonates.^{25,32} Another method to enhance the reactivity of five membered cyclic carbonates would be through the use of catalyst(s).¹⁹ For example, Andrioletti *et al.*³³ recently conducted a rational study of the aminolysis of five membered mono-cyclic carbonates using different organocatalysts. Their catalyst screening revealed that 1,5,7-triazabicyclo[4.4.0]dec-5-ene (TBD) and the cyclohexylphenyl thiourea were able to catalyze the aminolysis of the cyclic carbonates with cyclohexylamine, a low reactive amine, at room temperature. As far as we know, this rational has not been thoroughly explored and applied to PHUs and only few examples have been reported. For instance, Henderson *et*

al. showed that TBD could be an excellent catalyst for the preparation of PHUs from five membered cyclic carbonates.¹⁹

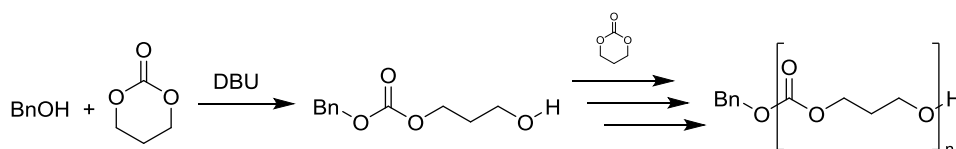
Another alternative to produce PHUs is through the use of larger cyclic carbonates. For example, Maisonneuve *et al.* reported using six membered cyclic carbonates that were 30 times more reactive than five membered ones.²⁹ However, many of these systems are still slow reacting and require high temperatures and long reaction times to obtain sufficient conversions and high molecular weight PHUs. Due to the harsh polymerization conditions needed, gelling has often been reported and this could arise from the pendant hydroxyl group reacting with the cyclic carbonates. Furthermore, due to the lack of reactivity of these cyclic carbonate substrates, explorations of NIPUs with lower reactive amines (i.e., aromatic diamines) have been typically avoided.

In summary, the preparation of poly(hydroxyurethane)s through the step growth polymerization of bis-cyclic carbonates and diamines is one the most promising pathways towards isocyanates free polyurethanes. To date, five and six membered cyclic carbonates have been thoroughly studied; however, harsh conditions (high temperatures and long reaction times) are necessary to obtain high monomer conversions. Due to their lack in reactivity, the PHU system is limited by the use of high temperatures that can lead to side reactions and the choice in amines. As such, the design of a more reactive cyclic carbonates for the preparation of PHUs is necessary.

1.3. Preparation of functional polycarbonates through the ring opening polymerization (ROP) of cyclic carbonates

Aliphatic polycarbonates are among one of the most promising biodegradable polymers and have received significant amount of attention.^{34,35} These materials are of great interest towards pharmaceutical applications because of their low

toxicity, biocompatibility, and biodegradability properties^{36,37}. For example, the use of aliphatic polycarbonates has already been studied for controlled drug delivery³⁸, tissue scaffolds, and antibacterial applications^{37,39-41}. In the literature, three main polymerization techniques have been investigated to synthesize polycarbonates: (i) polycondensation of dimethyl carbonate and diols⁴², (ii) copolymerization of epoxides and carbon dioxide^{43,44}, and (iii) ring opening polymerization (ROP) of cyclic carbonates.⁴⁵⁻⁴⁷ Among these methods, the ROP of cyclic carbonates has been of great interest to many. With the aid of organocatalysts, such as DBU, ROP of cyclic carbonates has shown high levels of control over the polymers' molecular weight, dispersity, and end-group fidelity (Scheme 2).⁴⁸



Scheme 2. Classic ROP of trimethylene carbonate using benzyl alcohol (BnOH, initiator) and DBU as a catalyst to yield aliphatic polycarbonates.

In order enable polycarbonates to interact with cells, pathogens, or organs for biomedical applications, one must be able to tailor the polymers' chemical structure with different functional groups. To date, cyclic carbonate pendant groups with functionalities such as alkyl⁴⁹, aryl⁵⁰, alkene³⁴, alkyne⁵¹, halides⁵², azides⁵³ and many others have all been realized and reported in the literature (Figure 4).⁵⁴⁻⁵⁶

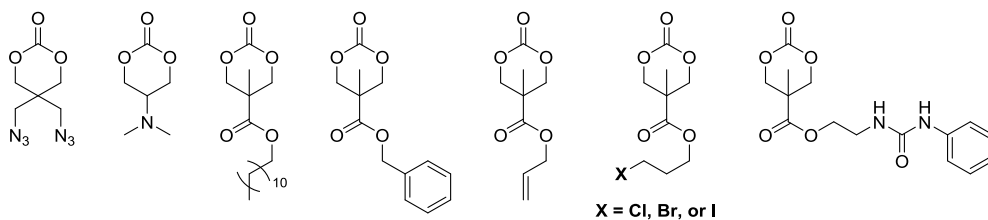
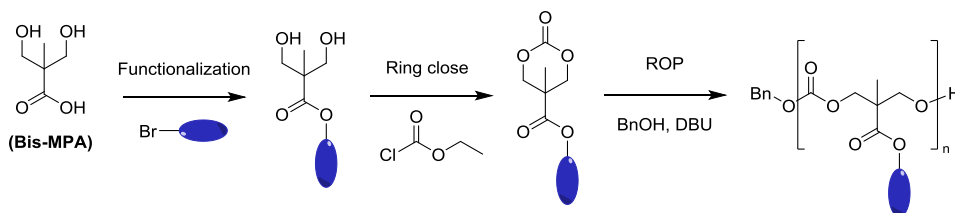


Figure 4. Here we show cyclic carbonates bearing a number of different functional pendant groups, including: azide, amine, alkyl, allyl, halide, etc. Aside from the first two cyclic carbonates (from the left), the rest of the cyclic carbonates were derived from bis-MPA.

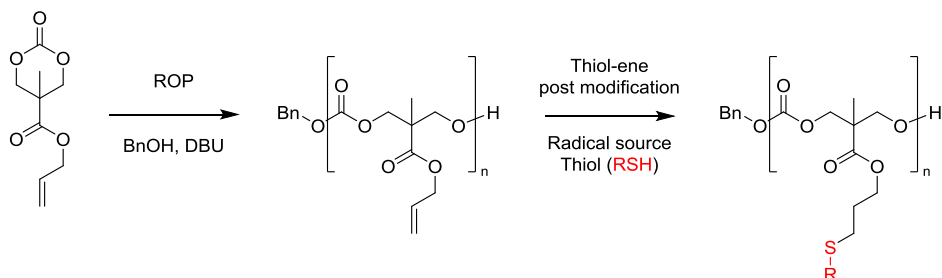
The most direct and facile way of incorporating functionalities into the final polymer product is by ROP cyclic carbonates already bearing the desired functional pendant groups. A popular and well-studied synthetic route for such functionalized cyclic carbonates is through the modification and ring-closure of 2,2-bis(hydroxymethyl)propionic acid (bis-MPA), a widely available and very inexpensive starting material (Scheme 3).^{46,51,54,57}



Scheme 3. Here we show the functionalization reaction of bis-MPA and the subsequent ring closing reaction with ethyl chloroformate to yield functionalized cyclic carbonate. Next, the ROP of the cyclic carbonate monomer yielded functionalized linear polycarbonates.³⁴

An alternative approach to prepare functionalized polycarbonates is through the incorporation of alkene pendant groups (i.e., allyl pendant groups) at the cyclic carbonate monomer level. This method is both elegant and highly advantageous, not only are alkene functionalities compatible with organocatalyzed (acidic or

basic) ROP conditions, but their double unsaturated bonds also allow for highly efficient and orthogonal reactions after the polymerization, such as radical thiol-ene addition⁵⁴, Michael addition⁵⁸, and free radical crosslinking⁵⁹ (Scheme 4). Another important advantage to having alkene pendant groups within the polycarbonate, is to allow for the incorporation of functional groups that are incompatible with organocatalyzed ROP conditions, such as alcohols and carboxylic acids.³⁴



Scheme 4. Cyclic carbonates bearing the allyl pendant groups can be ROP to form polycarbonates with allyl pendant groups, these groups can then be modified through thiol-ene reactions.³⁴

A significant number of publications related to ROP of cyclic carbonates have been devoted to six membered cyclic carbonates. This is most likely due to their: (i) inexpensive starting materials, (ii) facile functionalization and preparation, and (iii) facile ROP using a variety of commercially available catalysts. Nevertheless, in some particular cases, the polymerization of six membered cyclic carbonates can be limited. For instance, Dove *et al.* prepared allyl bearing polycarbonates from ROP of allyl bearing six membered cyclic carbonates.⁵⁴ However, long reaction times and large catalysts loadings were necessary to obtain high monomer conversions; such conditions would make it difficult to ensure end group fidelity. In addition, the poor reactivity of the monomer could also limit its potential to copolymerize with other common cyclic monomers (i.e., L-Lactide).

Preparing polycarbonates bearing tertiary or quaternary ammonium moieties is another limitation of cyclic carbonate systems. Such groups are highly desirable in preparing cationic polycarbonates suitable for gene therapy, drug delivery and antimicrobial applications.^{39,60,61} However, their preparation and purification requires many tedious steps which ultimately reduces the overall yield and scalability. Prior to this PhD work, very few examples existed in the literature regarding the ROP of cyclic carbonates bearing tertiary amine groups. For example, Wang *et al.* were able to prepare and ROP 16-membered cyclic dicarbonate. However, this process was limited by the yield in the monomer preparation (~25%).⁶² In another case, six-membered dimethylamine-functionalized cyclic carbonates were successfully prepared and polymerized using enzymatic catalysis by Zhang *et al.* However, this system was limited by the cost of serinol, one of the starting materials, and the moderate yield of the ring closing reaction. Although this system may be interesting from an academic point of view, it would be difficult to implement it at an industrial scale due to the cost of the starting material(s).⁶³

1.4. Motivations

In this PhD thesis, we explored the preparation and use of *N*-substituted eight membered cyclic carbonates to obtain PHUs and functional polycarbonates. These eight membered cyclic carbonates were prepared from diethanolamines that were inexpensive and easy to functionalize. By using these affordable starting materials, it would certainly help facilitate the implementation of *N*-substituted eight membered cyclic carbonates at an industrial scale. In the following paragraphs, we outlined the different chapters within this thesis regarding the investigation of new *N*-substituted eight membered cyclic carbonates for different purposes (Figure 5).

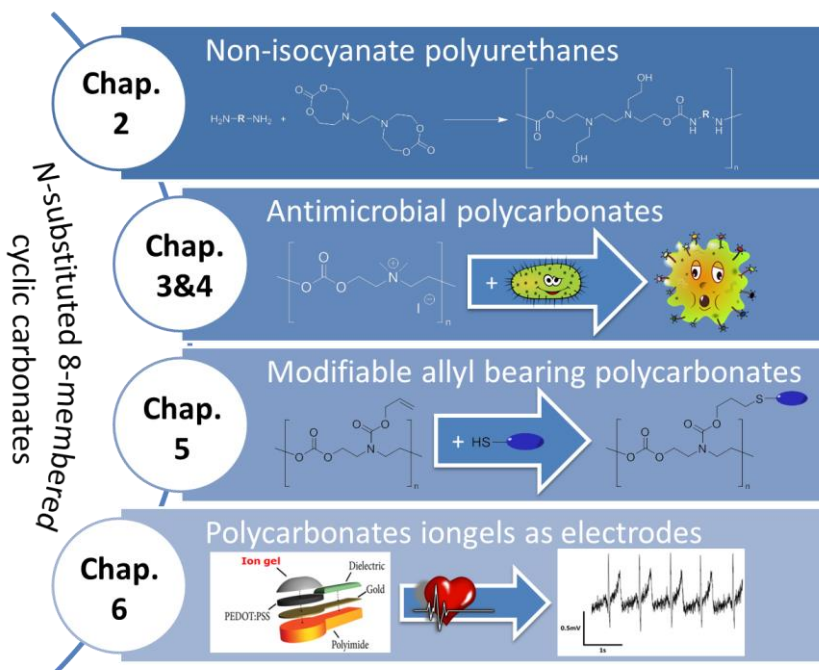


Figure 5. Visual representation of how the thesis was structured.

In **chapter 2**, we explored the potential of *N*-substituted bis-cyclic carbonates for synthesizing poly(hydroxyurethane)s, or PHUs. First, a kinetic study on the aminolysis of *N*-substituted eight membered carbonates with *n*-hexylamine was performed. The results from this work were later used to compare their reactivity to smaller five and six membered cyclic carbonates. A comprehensive computational study was also conducted to gain a deeper insight into the reactivity difference between the cyclic carbonate substrates. Finally, polymerizations towards NIPUs were carried out at room temperature with a variety of amines, including low reactive industrially relevant diamines.

In **chapter 3**, we studied the ring-opening polymerization (ROP) of *N*-substituted eight membered cyclic carbonates as an efficient way to obtain linear polycarbonates and hydrogels containing tertiary amines. First, we synthesized an eight membered aliphatic cyclic carbonate monomer using *N*-methyldiethanolamine, an inexpensive and readily available starting material. Subsequently, these monomers were polymerized with organocatalysts to afford linear polycarbonates and polycarbonate hydrogels. The nitrogen atoms in the polymers' backbone were then quaternized with iodomethane to yield cationic polymers. These charged polymers were then explored as potential antimicrobial agents towards clinically relevant microbes including *Staphylococcus aureus* (*S. aureus*) and *Escherichia coli* (*E. coli*). Polycarbonate hydrogels with such antimicrobial properties would be of great interest as biodegradable wound dressing materials.

In **chapter 4**, we also explored the ROP of charged *N*-substituted eight membered cyclic carbonates as a more efficient and direct way of obtaining polycarbonates containing quaternary amines. By quaternizing the tertiary amines of the cyclic carbonates beforehand, one can directly prepare charged polycarbonates without a need for a post-modification step and ensures better control of the quaternization of the polycarbonate. As in the previous case of chapter 3, hydrogels based on these charged monomers were prepared and also screened against bacteria to gauge their potential use as antimicrobial agents.

Afterwards, in **chapter 5**, we wanted to expand the *N*-substituted eight-membered cyclic carbonates platform by synthesizing and polymerizing of allyl functionalized monomers. In this chapter, we first synthesized a series of allyl bearing cyclic carbonate monomers based on diethanolamines, and we later investigated their ROP behaviors. Most importantly, we investigated the potential of the allyl pendant groups by functionalizing them with a variety of thiols using

thiol-ene 'click' chemistry. In addition, we explored the versatility of our monomers by preparing copolymers with commercially available cyclic monomers. By incorporating and modifying such allyl pendant groups, this helps to further extend the versatility of the cyclic carbonate platform to broader sets of functionalities and applications.

Next, in **chapter 6** we explored the feasibility of using *N*-substituted eight-membered cyclic carbonates as starting materials to prepare iongels electrolytes for bioelectronics. Iongels are soft-solid materials where ionic liquids (ILs) are immobilized inside a polymer matrix. Iongels generally have typical properties such as good chemical and electrochemical stability, low flammability, negligible vapor pressure, and high ionic conductivity.⁶⁴ For these properties, these materials can be used for the preparation of solid electrolytes for electrophysiology.⁶⁵ The combination of biodegradable polycarbonates polymer backbones and ionic moieties is a relatively unexplored field. In this chapter, we wanted to combine the promising features of ionic liquids and *N*-substituted eight membered cyclic carbonates to produce biodegradable iongels. The materials produced in this manner were mounted onto PEDOT:PSS based electrodes and used in the recording of heartbeats from the skin.

Finally in **chapter 7**, we highlighted and summarized the accomplishments and challenges of each part of this thesis.

Chapter 2



Non-isocyanate poly(hydroxyurethane)s

Chapter 2. Non-isocyanate poly(hydroxyurethane)s

2.1. Introduction

Polyurethanes (PUs) are considered as one of the most important and highly versatile class of polymeric materials. The demand for PUs is rising on average of 4.5% per year, and their production was estimated at 18 kilotons in 2016.^{8,9} Unfortunately, conventional polyurethane synthesis necessitates the use of isocyanate monomers that are known to be toxic^{33,66} and sensitive to moisture⁶⁷. With a possibility of European Union banning of the use of isocyanates, there is an emerging interest in finding environmentally friendlier approaches towards non-isocyanate polyurethanes (NIPUs).^{14,16} Synthetic research work on NIPUs has already been reported with the use of polyols^{68,69}, CO₂^{68,70,71}, and diamines¹⁰.

One of the more popular approaches to synthesize NIPUs is by the aminolysis of bis-cyclic carbonates with aliphatic diamines, which results in the formation of poly(hydroxyurethane)s. To date, NIPUs from five membered bis-cyclic carbonates prepared from CO₂ and epoxides systems have been extensively studied.^{67,69,72–81} These monomers are typically very stable and can be stored over long periods of time without degradation. However, their high chemical and thermal stability becomes a disadvantage during polymerizations. To achieve high molecular weight polymers with these monomers, the polymerization conditions often call for high temperatures, long reaction times, and the use of catalysts.

Few authors have reported the synthesis of NIPUs using cyclic carbonates with more than five members.^{7,82,83} For example, Cramail *et al.* synthesized six membered bis-cyclic carbonates from renewable sources, and found that they

were 30 times more reactive than the five membered bis-cyclic carbonates. However, the polymerizations were not well controlled and gels were often obtained at high conversions. In an another work, Endo *et al.* reported on the synthesis of seven membered bis-cyclic carbonates and the preparation of NIPUs derived from these monomers.^{7,84} The authors observed higher reactivity in the seven membered carbonate over the smaller five and six membered bis-cyclic carbonates. It is believed that the increased reactivity could be attributed to the greater ring strain of the seven membered cyclic carbonate ring versus the smaller cyclic carbonates.

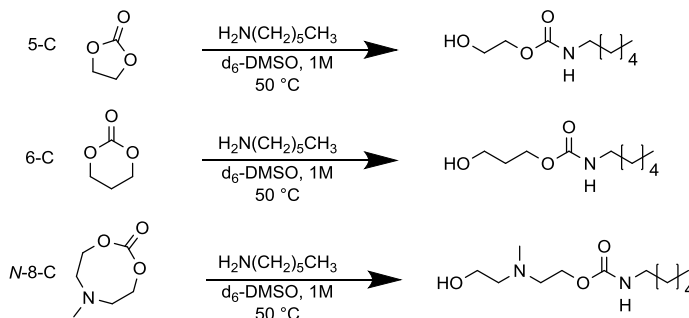
Recently, Hedrick *et al.* reported the synthesis of an *N*-substituted eight membered cyclic carbonates with tertiary amines in their structures.^{37,85} One of the main aspects which made the *N*-substituted eight membered cyclic carbonates attractive was its facile synthesis from diethanolamines, which are inexpensive and readily available starting materials derived from naturally abundant epoxides and aliphatic diamines.

In this chapter, *N*-substituted eight membered cyclic carbonates were explored as potential reagents for the synthesis of NIPUs. A kinetic study on ring opening of *N*-substituted eight membered carbonates with *n*-hexylamine demonstrated their high reactivity in comparison to the five and six membered cyclic carbonates. A comprehensive computational study was also conducted to gain a deeper insight into the reactivity of different cyclic carbonate sizes. Finally, different polymerizations towards NIPUs were carried out using different diamines, including low reactive industrially relevant diamines.

2.2. Results and discussion

2.2.1. Comparative study of different cyclic carbonates reactivity towards *n*-hexylamine

To understand the reactivity of the *N*-substituted eight membered cyclic carbonate (**N-8-C**), aminolysis reactions of different cyclic carbonates with *n*-hexylamine were carried out. The cyclic carbonates investigated included: ethylene carbonate (**5-C**, five membered cyclic carbonate), trimethylene carbonate (**6-C**, six membered cyclic carbonate), and 6-methyl-1,3,6-dioxocan-2-one (**N-8-C**, *N*-substituted eight membered cyclic carbonate). Reaction kinetics were followed by ^1H NMR in $\text{d}_6\text{-DMSO}$ at $50\text{ }^\circ\text{C}$ (Scheme 5).



Scheme 5. Aminolysis of cyclic carbonates with *n*-hexylamine.

As the cyclic carbonates reacted with the *n*-hexylamine, characteristic ^1H NMR signals of the methylene protons in the cyclic carbonates ($\text{CH}_2\text{-OCOO-}$) disappeared. The appearance of three new signals attributed to the formation of urethane was observed at 4.13 ppm ($\text{CH}_2\text{-OCONH}$), 3.57 ppm ($\text{CH}_2\text{-OH}$) and 3.12 ppm ($\text{CH}_2\text{-NHCOO}$); the conversions were determined by using relative peak integration values.

Overall, the reactions proceeded through second-order kinetics $-\text{d}[\text{M}]/\text{d}t = k[\text{M}]^2$, (where $[\text{M}] = [\text{cyclic carbonate}] = [\textit{n}\text{-hexylamine}]$), which was confirmed by the linear relationship between t and $1/(1-p)$, where t is time and p is the fraction of

monomer converted to urethane. Rate constants, k , were calculated for each of the cyclic carbonates (Figure 6). We found that the reaction kinetics were highly dependent on the size of the carbonate ring. Our findings were also congruent with the literature about **6-C** being more reactive than the **5-C**.⁸⁶ Astonishingly, we observed that **N-8-C** was five times more reactive than **6-C**. Even after 30 min of reaction time, we were able to obtain 71% conversion for the case of **N-8-C**.

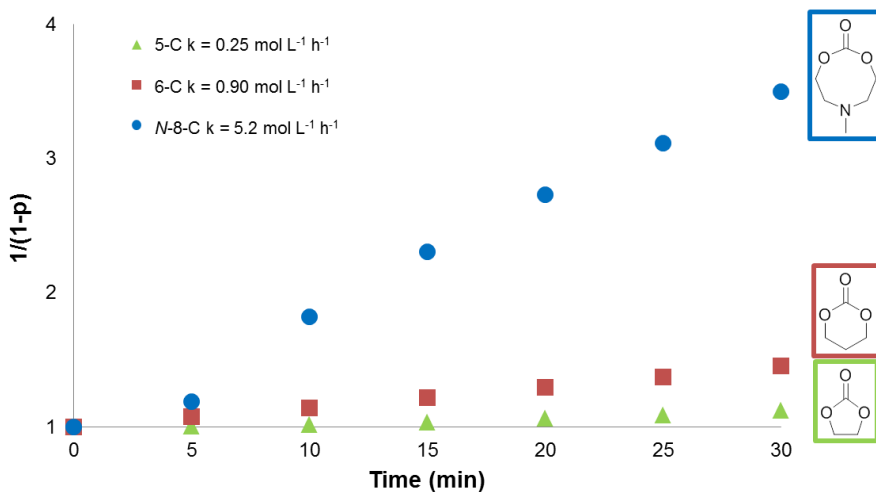


Figure 6. Kinetics plot from the aminolysis of various cyclic carbonates with *n*-hexylamine.

The kinetics of **N-8-C** with *n*-hexylamine was evaluated further at higher temperatures (65 and 80 °C). As expected, we found the reaction rate constant to increase with higher temperatures. For an initial concentration of 1 mol L⁻¹, the reaction rate constants at 50, 65, and 80 °C were 5.0, 10.1, and 17.6 mol L⁻¹ h⁻¹ respectively. Using these values, the activation energy (E_a) for **N-8-C** was estimated at 40 kJ mol⁻¹. This was twice the value obtained by Cramail *et al.* for their six membered bis-cyclic carbonates.⁸⁶ Furthermore, even at 80 °C, no side reactions were observed in any of these experiments. This work helped to

demonstrate the potential of using the *N*-substituted eight membered cyclic carbonate system for the synthesis of NIPUs.

2.2.2. Comparative study with low reactivity amines

We expanded our investigation of the reactivity of different sized cyclic carbonates towards amines of varying nucleophilicities, which included: *n*-hexylamine, cyclohexylamine, *N*-methylbutylamine, aniline, and monofunctional poly(ethylene glycol) amine (M_w 1000). Conversions were calculated from relative integral values from ^1H NMR spectroscopy; results are summarized in Figure 7.

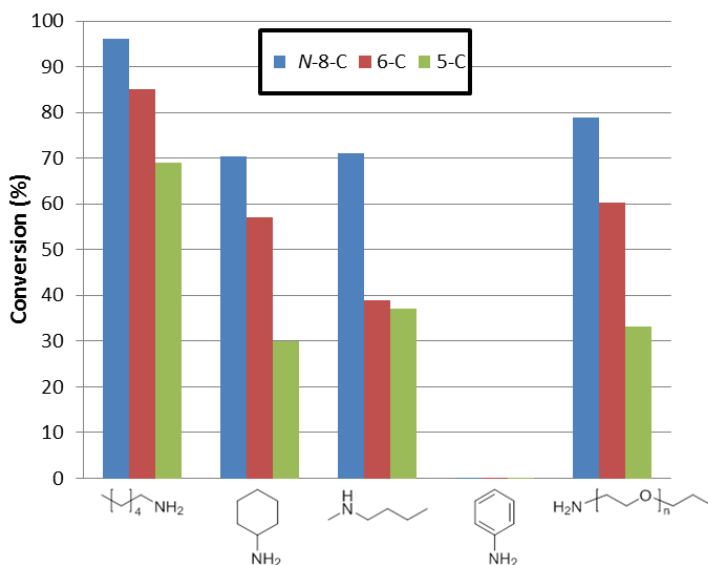


Figure 7. Conversions from reactions with *N*-8-C, 6-C, and 5-C with less reactive amines. Reactions were carried out at 50 °C for 6 hours.

Amongst the cyclic carbonates studied, the reaction conversions were higher whenever **N-8-C** was used. The only exception was for the case of aniline, where no reaction was observed for any of the tested cyclic carbonates. Amines such as cyclohexylamine and poly(ethylene glycol) amine were able to obtain higher

conversions when the size of the cyclic carbonate increased. We were also able to observe the aminolysis of the cyclic carbonates with *N*-methylbutylamine, a secondary amine. The enhanced reactivity of **N-8-C** with low reactive amines was congruent with the trends observed in the kinetic study; it also demonstrated its potential for the synthesis of NIPUs with various amines of different nucleophilicities.

2.2.3. Computational modeling

To further understand the reactivity differences across the three cyclic carbonates presented in the previous sections, we decided to conduct a few of our own computational studies. In the literature, two reaction mechanisms have been proposed for the aminolysis of five and six membered cyclic carbonates. The first mechanism, proposed by Tomita *et al.*, suggested a mechanism through an amphoteric tetrahedral intermediate⁸⁷. On the other hand, Zabalov *et al.* proposed that the formation of the hydroxyurethane from a five membered cyclic carbonate proceeds through a six centered ring intermediate with two amines present. In this sense, one of the amines behaves as a catalyst, and the other performs the nucleophilic attack.⁸⁸

Here in this work, we examined the reaction between **N-8-C** and methylamine through both mechanisms. We first examined the classical approach provided by Zabalov *et al.*, which consisted of a stepwise amine nucleophilic addition (TS1) and a subsequent ring opening process (TS2), see Figure 8. In another experiment, we tested the concerted amphoteric tetrahedral mechanism (TS3) provided by Tomita *et al.* As expected, the mechanism in TS3 presented a large activation energy of 33.3 kcal/mol, and it contained a four membered cyclic

transition state that was too strained to be plausible.¹ On the other hand, the computed energies for the stepwise approach were much lower; hence it was a more feasible pathway.

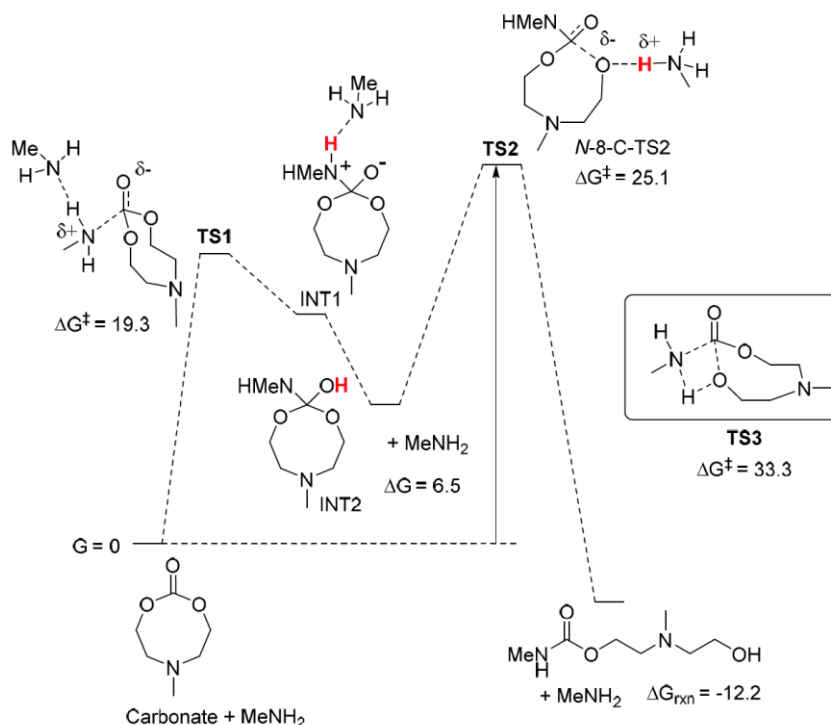


Figure 8. Reaction energy profile for *N*-8-C and its Gibbs Free energies computed at m062x/6-31+G(d,p) (pcm, solvent =DMSO) level.

Upon closer inspection, the initial amine addition transition state (TS1, Figure 8) presented an activation Gibbs Free energy of 19.3 kcal/mol. The following transition state (TS2) became the rate determining step with a barrier of 25.1 kcal/mol. It is important to note that a second methylamine molecule was included in these calculations, as it helped to stabilize the computed structures

¹ Even larger unattainable energies were computed for the related TS3 structures in the cases of 5-C (43.2 kcal mol⁻¹) and 6-C carbonates (42.2 kcal mol⁻¹).

and reduce the energy values. In fact, the non-stabilized transition states led to convergence problems and/or broke apart into the reactant structures during optimization. From a synthetic viewpoint, the stabilization and activation of the reaction with a second methylamine makes perfect sense.⁸⁹ In the experimental conditions, this stabilization could also be achieved by using a polar solvent, or by some small amount of water.

After the TS1, a high-in-energy zwitterionic intermediate was formed (INT1, ca. 17 kcal mol⁻¹). The intermediate then easily rearranges itself into a more stable uncharged INT2 (6.5 kcal/mol) via a simple proton shift. In fact, INT1 and INT2 represent two intermediates of a group of structures in equilibrium, where the proton can be shared by the different nitrogen and oxygen atoms (highlighted in red in Figure 8). At the end of the process, an energy difference of -12.2 kcal/mol between the final products and initial reagents was realized, which indicated an exergonic reaction.

Analogous reactions with **6-C** and **5-C** were also computed for using the approach provided by Zabalov *et al* (Figure 9). Interestingly, the energy barriers at the TS2 increased with decreasing cyclic carbonate sizes. Specifically, the TS2 values were realized from 25.1 kcal/mol in **N-8-C-TS2** to 32.0 kcal/mol in **5-C-TS2**. This trend was in agreement with the experimental observations from our kinetic studies.

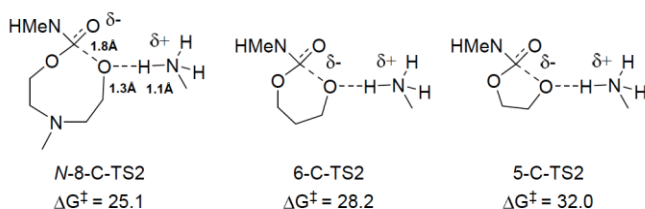
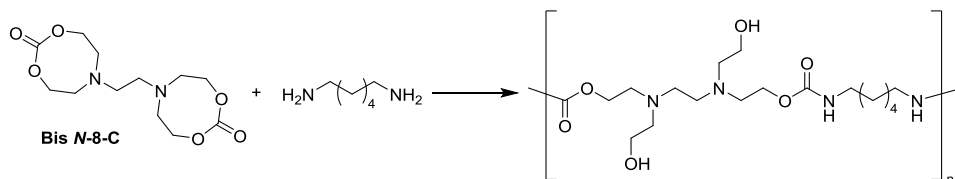


Figure 9. Comparison of the Free Gibbs activation energies for the ring opening process computed at m062x/6-31+G(d,p) (pcm, solvent =DMSO) level.

2.2.4. Synthesis of NIPUs based on bis *N*-8-C and diamines

With a better understanding of the urethane formation from ***N*-8-C**, we decided to investigate their potential for preparing NIPUs. For this, we first synthesized the bis-*N*-substituted eight membered cyclic carbonates (**bis *N*-8-C**). An additional kinetic experiment with *n*-hexylamine was performed with **bis *N*-8-C**, and a k value of $5.0 \text{ mol L}^{-1} \text{ h}^{-1}$ was obtained, and found to be similar to that of ***N*-8-C** ($5.2 \text{ mol L}^{-1} \text{ h}^{-1}$).



Scheme 6. Synthesis of NIPUs with the bis *N*-8-C with 1,6-hexamethylenediamine.

After confirming the similar reactivity profiles of **bis *N*-8-C** and ***N*-8-C**, we investigated the ability of **bis *N*-8-C** to synthesize NIPUs using the commercially available 1,6-hexamethylene diamine (Scheme 6). An initial polymerization was carried out at room temperature using d_6 -DMSO at 1 mol L^{-1} (NIPU1). The formation of NIPUs was confirmed by ^1H NMR spectroscopy, as shown in Figure 10. We observed the characteristic methylene proton signals of **bis *N*-8-C** at 4.08 and 2.76 ppm gradually disappear as new signals from the formation of poly(hydroxyurethane)s gradually appeared at 7.01, 3.95, 3.41, 2.93, 2.65, and 2.53 ppm. The polymerization reached a conversion of >95% after 24 h, which was more than twice the conversion value of Cramail's bis six membered cyclic carbonate with a similar diamine after 24 h $30 \text{ }^\circ\text{C}$.⁸⁶

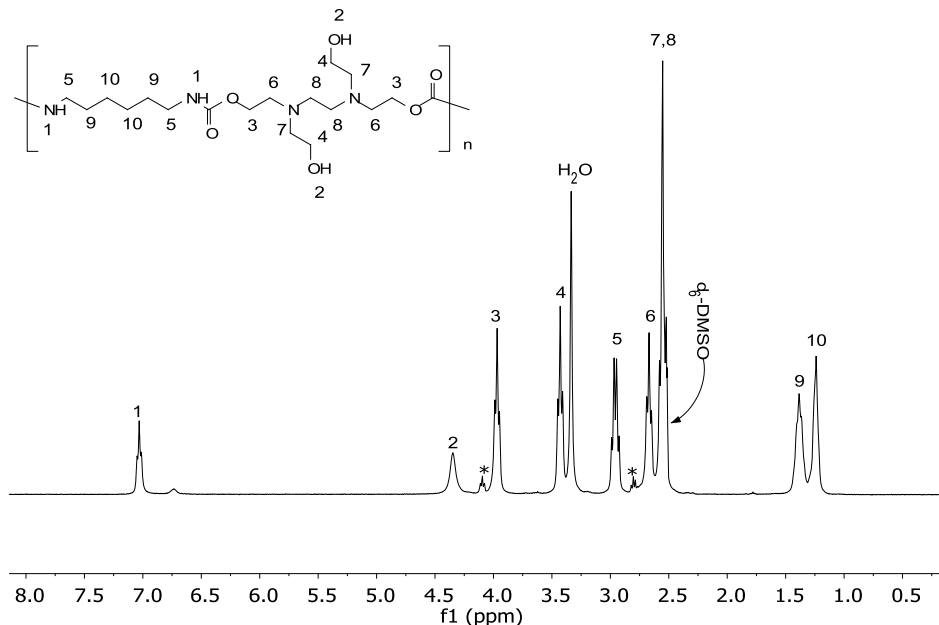


Figure 10. ^1H NMR of NIPU1 after 24 h at 25 °C. Proton signals attributed to the starting material bis *N-8-C* have been labeled with “*”.

To further verify the formation of NIPUs, FTIR spectroscopy was performed on the bis *N-8-C* monomer and the polymer. As the reaction proceeded, the complete disappearance of the cyclic carbonate ($\text{C}=\text{O}$) stretching band at 1725 cm^{-1} was observed. Two new bands which corresponded to the urethane linkage vibrations (amide I at 1688 cm^{-1} and amide II at 1529 cm^{-1}) appeared after the polymerization. In addition, a broad band centered around 3321 cm^{-1} was observed and identified as the N-H and O-H stretching vibrations. The collected data from ^1H NMR and FTIR were congruent with the reports in the literature regarding the formation of NIPUs via aminolysis of cyclic carbonates.^{69,86} Next, we conducted measurements with GPC and observed a M_n of $47,000\text{ g mol}^{-1}$ ($\text{Đ}:1.6$), see Table 1.

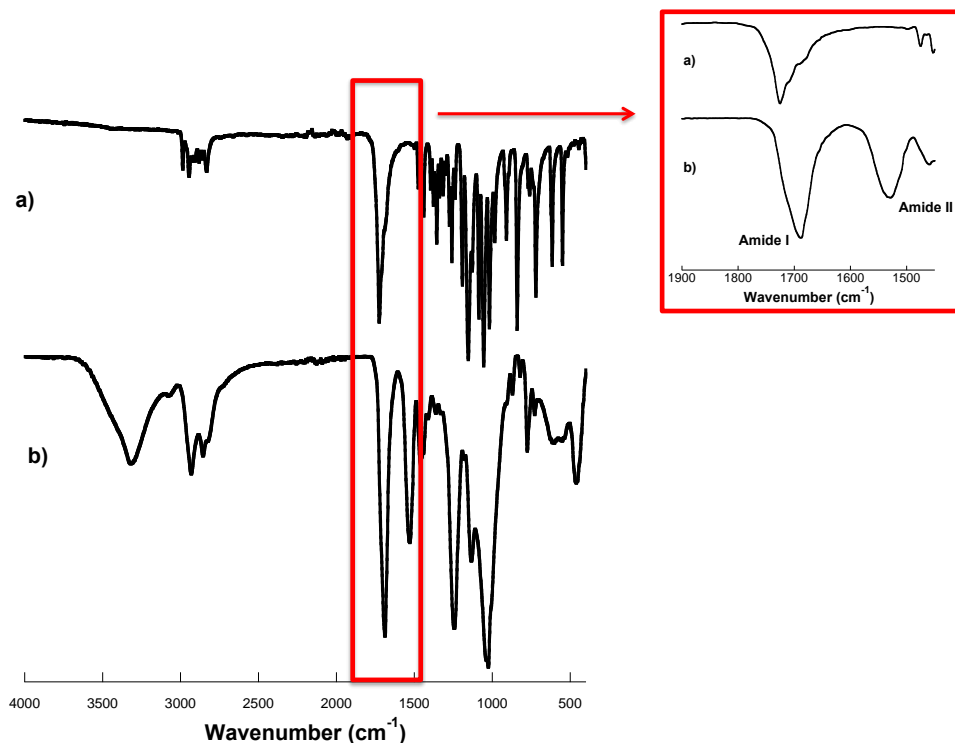


Figure 11. FTIR-ATR spectra of (a) bis *N*-8-C monomer and (b) lyophilized NIPU1.

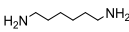
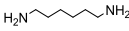
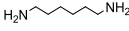
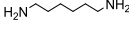

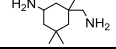
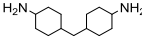
To expand on our preliminary investigations, higher reaction temperatures and other solvent conditions were examined (Entries 1 thru 4 of Table 1). For reactions that were carried out at 50 or 80 °C, gelation was observed during the polymerization process. In our opinion, the higher temperatures could induce some side reactions between the pendant hydroxyl group and the cyclic carbonate, as observed by Cramail et al.⁸⁶ When water was used as a solvent for the reaction, a solid white gel was obtained that could not be characterized by NMR spectroscopy or GPC. Nevertheless, the synthesized material was analyzed by FTIR spectroscopy and it had clear signals of urethane formation with peaks at 1680 cm⁻¹ (amide I) and 1535 cm⁻¹ (amide II). Interestingly, this suggested the possibility of performing this polymerization in aqueous media,

which is normally not possible with the traditional isocyanate chemistry. We believe that the water not only could act as reaction media, but also helps stabilize the transition state and facilitate the polymerization.

Because of the high reactivity of **bis N-8-C**, we wanted to expand the breadth of our NIPU synthesis to diamines less reactive than aliphatic primary amines (Table 1). In fact, one of the main limitations of PHUs is when the nucleophilicity of the amine is reduced, and in doing so, studies with less reactive amines are typically avoided.⁹⁰ Due to the high reactivity of our monomer, we wanted to see where its limits lied. For this, we considered two hindered primary diamines that are analogous to the two of the most industrially relevant aliphatic diisocyanates, which are isophorone diisocyanate and 4,4'-methylenebis(cyclohexyl isocyanate).⁶⁹ In addition, we also considered polymerizations with secondary diamines (*N,N'*-dimethyl-1,3-propanediamine).

We carried out polymerization reactions at room temperature for 24 hours in DMSO. With the *N,N'*-dimethyl-1,3-propanediamine, consisting of secondary diamines, we managed to obtain 85% conversion by ¹H NMR, see Entry 5 in Table 1. We were also unable to obtain a measureable weight value for this product by GPC. On the other hand, the two diamines analogous to industrially relevant isocyanates for PUs were tested and listed in Entries 6 and 7. The polymerizations were characterized by ¹H NMR spectroscopy and GPC, and in both cases managed to achieve high conversions and high molecular weights of around 20,000 g mol⁻¹. Altogether, these results confirmed that even with hindered amines, we were able to achieve high molecular weight NIPUs at room temperature.

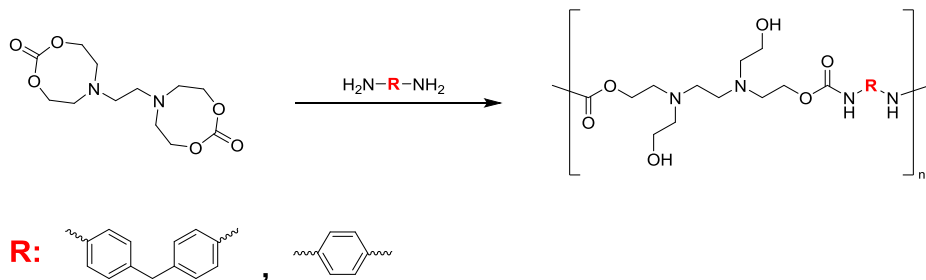
Table 1. Synthesis of NIPUs from bis *N*-8-C and diamines after 24 h.

NIPU	T (°C)	Diamine	Solvent	Conv. (%) ^a	M _n (g mol ⁻¹) ^b	Đ
1	25		DMSO	95	78,000	1.60
2	50		DMSO	89 ^c	38,200 ^c	1.66 ^c
3	80		DMSO	93 ^c	27,700 ^c	1.46 ^c
4	25		D ₂ O	- ^d	- ^d	- ^d
5	25		DMSO	85	- ^e	- ^e
6	25		DMSO	88	19,500	1.22
7	25		DMSO	95	22,700	1.26

Summary of NIPUs synthesized in this paper. ^a Conversions were calculated by ¹H NMR. ^b M_n values were obtained by GPC in DMF. ^c Partial gelation (less than 5 %) was observed in these cases. ^d Conversion and M_n values were unobtainable due to insolubility. ^e M_n values were below the detection limit of the GPC.

Due to the promising initial results with the **bis *N*-8-C** monomer, we were interested expanding our NIPU synthesis to low reactive aromatic diamines, which included 4,4'-diaminodiphenylmethane and *p*-phenylenediamine (Scheme 7). Because of their weak nucleophilicities, aromatic diamines are generally avoided for use in NIPU synthesis. In our testing, both diamines did not react with our **bis *N*-8-C** monomer at room temperature, despite using 2.5 mol% thiourea catalyst. Reactions were also tried at higher temperatures (50 °C to 120 °C) with a range of organocatalysts (thiourea, TBD, and DBU); however, none of the conditions were favorable. At high temperatures, even at 50 °C, we were able to observe the degradation of the **bis *N*-8-C** monomer after five hours. By ¹H NMR, it appeared that some of **bis *N*-8-C** monomer had reverted back its starting material. Due to the low reactivity of these aromatic amines and instability of our monomer at elevated temperatures, we decided not to continue in investigating

this any further. Perhaps the work here could be improved upon in the future by ensuring the purity of all materials, conducting the reactions in air-free environment, and the use of other catalysts.



Scheme 7. We were interested in preparing NIPUs with aromatic diamines, which included 4,4'-diaminodiphenylmethane (left) and *p*-phenylenediamine (right).

2.3. Conclusions

In conclusion, we demonstrated that the eight membered cyclic carbonate, such as the **bis N-8-C**, to be a good candidate for the synthesis of non-isocyanate poly(hydroxyurethane)s. Kinetic studies of the aminolysis of both **N-8-C** and **bis N-8-C** confirmed their extraordinary reactivity over the smaller cyclic carbonates. This was further supported with our computational study. Most importantly, high molecular weight NIPUs were formed via the polyaddition of **bis N-8-C** and 1,6-hexamethylenediamine. Gelling was observed at higher polymerization temperatures, and we suspected this was due to side reactions and the increased reactivity of the **bis N-8-C**. Finally, we also obtained NIPUs with hindered aliphatic diamines analogous to industrially relevant isocyanates. All of these results indicated the bis *N*-substituted eight membered cyclic carbonate to be an ideal candidate for sustainable synthesis of industrially relevant non-isocyanate poly(hydroxyurethane)s.

2.4. Experimental part

General information

^1H and ^{13}C NMR spectra were recorded with Bruker Avance DPX 300, Bruker Avance 400, or Bruker Avance 500 spectrometers. The NMR chemical shifts were reported as δ in parts per million (ppm) relative to the traces of non-deuterated solvent (eg. $\delta = 2.50$ ppm for $\text{d}_6\text{-DMSO}$ or $\delta = 7.26$ for CDCl_3). Data were reported as: chemical shift, multiplicity (s = singlet, d = doublet, t = triplet, m = multiplet, br = broad), coupling constants (J) given in Hertz (Hz), and integration. Fourier transform infrared - attenuated total reflection (FTIR-ATR) spectroscopy was performed with a Bruker Alpha. Gel permeation chromatography (GPC) was performed using an Agilent Technologies PL-GPC 50 Integrated GPC system, with a Shodex KD-806M column. For the GPC, *N,N*-Dimethylformamide with a 10mM concentration of LiBr at 50 °C was used as the solvent and toluene as a marker. Polystyrene of different molecular weights, ranging from 2,100 g mol^{-1} to 1,920,000 g mol^{-1} , were used for the calibration of the GPC.

Materials

1,3-Propanediol (98%), triethylamine ($\geq 99\%$), *N*-methyldiethanolamine ($\geq 99\%$), triphosgene (98%), *N,N,N',N'*-tetrakis(2-hydroxyethyl)ethylenediamine (technical grade), *n*-hexylamine (99%), ethylene carbonate (98%), cyclohexylamine ($\geq 99\%$), aniline (99%), *N*-butylmethylamine (96%), bis(pentafluorophenyl) carbonate (97%), 5-amino-1,3,3-trimethylcyclohexanemethylamine ($\geq 99\%$), 4,4'-methylenebis(cyclohexylamine) (97%), 1,6-hexamethylenediamine (96%), lithium bromide ($\geq 99\%$), DCM ($\geq 99.9\%$), and diethyl ether ($\geq 99.8\%$), were purchased and used as-is from Sigma Aldrich. Ethyl chloroformate (99%) and THF ($\geq 99\%$) were purchased and used as is from Acros. Acetone ($\geq 99.5\%$) and DMF (GPC grade) were purchased and used from Fisher. Methoxypolyethylene glycol amine (M_w 1,000) was purchased and used from Alfa Aesar. Deuterated solvents such as CDCl_3 , $\text{d}_6\text{-DMSO}$, and D_2O were purchased from Euro-top and used as is.

Synthesis of 1,3-dioxan-2-one (6-C)

Synthesis of 6-C was carried out in an adapted version of Toshiro et al.⁹¹ A 1 L single neck round bottom flask was charged with 1,3-propanediol (10 g, 0.131 mol, 1 equiv.), ethyl chloroformate (28.6 g, 0.264 mol, 2 equiv.), and 650 mL of anhydrous THF. The round bottom flask was kept in an ice bath and magnetically stirred. Triethylamine (28.1 g, 0.278 mol, 2.1 equiv.) added drip-wise into the reaction over 15 min with an additional funnel. After the addition of triethylamine, the reaction was taken out of the ice bath and stirred for an additional two hours at room temperature. The precipitated triethylamine hydrochloride salt was filtered away and discarded. The THF in the filtrate was evaporated and the remaining residue was recrystallized in diethyl ether. The final product consisted of white crystals (5.6 g, 42% yield). ¹H NMR (300 MHz, CDCl₃) δ 4.42 (t, J = 5.7 Hz, 4H), 2.12 (p, J = 5.7 Hz, 2H). ¹³C NMR (101 MHz, DMSO) δ 21.17, 39.52, 68.06, 148.13.

Synthesis of 6-methyl-1,3,5-dioxazocan-2-one (N-8-C)

Synthesis of N-8-C was carried out in an adapted version of Pascual et al.³⁷ A 1L single neck round bottom flask was charged with a stir bar, 5 g of N-methyldiethanolamine (42 mmol), 9.2 g of triethylamine (90.9 mmol), and 650 mL of anhydrous THF. An additional funnel was affixed to the round bottom flask and charged with 4.6 g of triphosgene (15.5 mmol) and 50 mL of anhydrous THF. The setup was then placed in a liquid nitrogen and acetone mixture. The triphosgene-THF mixture was dripped into round bottom flask and the triethylamine hydrochloride salt could be seen precipitating out of the reaction. After the addition of triphosgene, the reaction was stirred for an additional three hours. The precipitated triethylamine hydrochloride salt was filtered away and discarded. The filtrate was concentrated under reduced pressure and then treated with cold diethyl ether. The remaining triethylamine hydrochloride salt was then removed. The remaining filtrate, free of triethylamine hydrochloride salt,

was then concentrated under reduced pressure to give a pink colored liquid as the final product (4.47g, 73% yield). ^1H NMR (300 MHz, CDCl_3) δ 4.13 (t, J = 5.4 Hz, 4H), 2.71 (t, J = 5.3 Hz, 4H), 2.43 (s, 3H). ^{13}C NMR (75 MHz, CDCl_3) δ 156.11, 68.74, 56.14, 44.44. ^1H NMR (500 MHz, DMSO) δ 4.13 (t, J = 5.3 Hz, 4H), 2.73 (t, J = 5.3 Hz, 8H), 2.41 (s, 3H). ^{13}C NMR (101 MHz, DMSO) δ 155.36, 68.71, 55.64, 44.39, 39.52.

Synthesis of 6,6'-(ethane-1,2-diyl)bis(1,3,6-dioxazocan-2-one) (bis *N*-8-C)

Synthesis of bis *N*-8-C was mainly carried out in an adapted version of Pascual *et al.*³⁷ A 1 L single neck round bottom flask was charged with a stir bar, 5 g of *N,N,N',N'*-tetrakis(2-hydroxyethyl)ethylenediamine (21.16 mmol), 2.247 g of 1,8-bis(dimethylamino)naphthalene (10.48 mmol), and 400 mL of anhydrous THF. An additional funnel was affixed to the round bottom flask and charged with 18.4 g of bis(pentafluorophenyl) carbonate (46.69 mmol) and 50 mL of anhydrous THF. The bis(pentafluorophenyl) carbonate and THF mixture was then dripped into round bottom flask and stirred at room temperature for two hours. The reaction mixture was then concentrated under reduced pressure and then treated with excess ether. This mixture was then placed in the refrigerator overnight. The precipitated material was then collected and dried to give the 8-DC product (4.3 g, 71% yield). ^1H NMR (300 MHz, CDCl_3) δ 4.18 (t, J = 5.3 Hz, 8H), 2.82 (t, J = 5.3 Hz, 8H), 2.77 (s, 4H). ^1H NMR (300 MHz, DMSO) δ 4.08 (t, J = 5.3 Hz, 8H), 2.76 (t, J = 5.3 Hz, 8H), 2.62 (s, 4H). ^{13}C NMR (101 MHz, CDCl_3) δ 156.42, 69.27, 55.40, 54.95. ^{13}C NMR (75 MHz, DMSO) δ 53.50, 53.54, 68.89, 155.26.

We were also able to synthesize bis *N*-8-C by using the ring closing method with dimethyl carbonate, as reported by Meuldijk *et al.*⁹² However, the yield was much lower than the ring closing method with bis(pentafluorophenyl) carbonate.

General procedure for the kinetic study

In a typical procedure, carbonate (1 equiv.) was directly added into a NMR tube and dissolved in d_6 -DMSO to give a 1 M concentration. An amine (1 equiv.) was then added into the tube and then quickly inserted into the NMR. A spectrum was recorded every 5 min over a 30 min period.

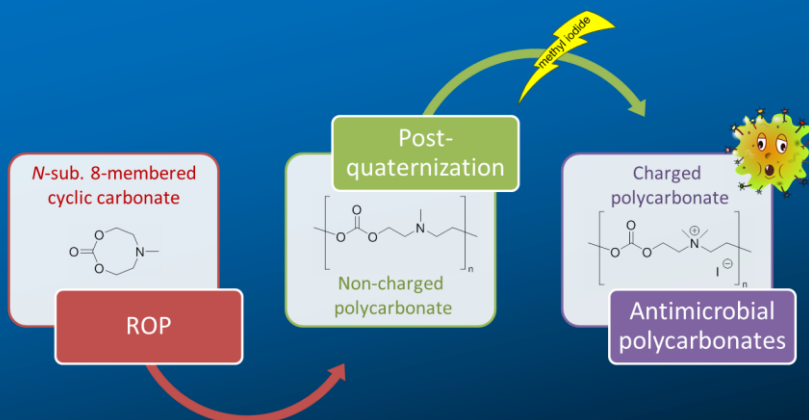
General procedure for the comparative study of low reactivity amines

In a typical procedure, carbonate (1 equiv.) was added into a vial and dissolved in d_6 -DMSO to give a 1 M concentration. An amine (1 equiv.) was then added into the vial. The reaction was then stirred for 6 h at 50 °C.

General procedure for polymerization

In a typical procedure, a vial was charged with bis *N*-8-C (100 mg, 347 μ mol, 1 equiv.), a diamine (1 equiv.), 347 μ L of d_6 -DMSO, and a stir bar. The reaction was stirred at room temperature for 1 d. The reaction was then characterized with ^1H NMR, FTIR-ATR, and GPC.

Chapter 3



**Antimicrobial polycarbonates
obtained by
post-functionalization**

Chapter 3. Antimicrobial polycarbonates obtained by post-functionalization

3.1. Introduction

The discovery and application of antibiotics, like penicillin, revolutionized healthcare treatment and greatly improved the quality of modern day life. However, the overuse of such antibiotics has ultimately led to the proliferation and more common outbreaks of antibiotic-resistant pathogens, such as: methicillin-resistant *Staphylococcus aureus* (MRSA). Biofilms consisting of these antibiotic-resistant bacteria is highly problematic for wound dressings and implants, where the bacteria can easily have a direct access and cause significant harm to a patient. The eradication of these hazardous bacteria is still an immense and unmet challenge, and the increase in these cases has raised many alarms in the healthcare services.⁴⁰

Efforts in developing new antimicrobials have been thwarted by the rapid evolution of drug resistance mechanisms of the microbes. Generally, such drug resistant microbes contain multiple drug deterrent mechanisms, which can include: the loss of pores in the membrane, increased outflow of material from the microbes through their pumps, and the ability to develop drug deactivating proteins. All of these mechanisms combined, makes it a formidable challenge to develop a long term solution in dealing with such resistant microbes.^{93–95} Indeed, a new methodology must be investigated and adopted in order to combat these microbes, and one of the promising solutions is through the use of macromolecular antimicrobials.⁴⁰

Macromolecular antimicrobial agents such as cationic polymers and peptides have recently been given increased attention because of their abilities to combat

multi-drug-resistant microbes. However, many of these antimicrobial peptides suffer from labor intensive and expensive synthetic procedures. For these reasons, attention has shifted to preparing synthetic polymers from cheap starting materials designed to mimic the facially amphiphilic structure of peptides. As such, these structures can form secondary structures upon interaction with the negatively charged microbial membranes. When designing these macromolecules, there are several key points that must be considered, which includes: (1) having sufficient contact with the microbes, (2) having sufficient cationic charges to promote adhesion to the microbial cell envelope, and (3) these materials must selectively target and kill microbes without harming mammalian cells. To expand on the later point, microbial membranes' surfaces are typically more negatively charged, or anionic, compared to mammalian cells. Unlike antibiotics, macromolecular antimicrobials do not seek out molecular targets (or proteins) specific to microbes.⁹⁶ Instead, they selectively target the microbials' membrane through the electrostatic attraction between the cationic groups of the polymers and the negatively charged bacterial membranes. To assess the compatibility of these antimicrobial agents with mammalian cells, hemolytic studies with red blood cells are typically performed.

To date, a number of different classes of polymers have emerged and exhibited characteristics that mimic antimicrobial peptides while addressing their drawbacks. Among these materials, polycarbonates derived from cyclic carbonates are one of the most promising for bio-applications, owing to their biodegradability, low toxicity and biocompatibility.³⁵ Six membered cyclic carbonates are the current dominating starting materials for ROP towards polycarbonates, and this is mainly due to their synthetic facility and versatility towards functional degradable polymers. Such flexibility of the six membered cyclic carbonate platforms has driven much interest into this area. However, the preparation of cationic polycarbonates from many of these monomers require

multi-step synthesis processes due to inherent incompatibility between tertiary amines and six membered cyclic carbonates. In a typical procedure to achieve antimicrobial polycarbonates bearing quaternary amine groups, cyclic carbonates bearing halogenated functionalities are first polymerized by ROP. In a follow up post-polymerization procedures, the halogenated functionalities are then modified using nucleophilic substitution methods with tertiary amines. A more simple and elegant method is to prepare cyclic carbonates already bearing tertiary functionalities. In the literature, only one example could be found regarding the ROP of six membered cyclic carbonate containing tertiary amine pendant groups. However, this monomer suffers from low synthetic yields and expensive starting materials.⁶³ Such drawbacks make it a difficult challenge to upscale this method and implement it at an industrial level.

In our previous chapter, we synthesized an innovative *N*-substituted eight membered aliphatic cyclic carbonate monomer using *N*-methyldiethanolamine, an inexpensive and readily available starting material. One of the main aspects which make the *N*-substituted eight membered cyclic carbonate an attractive platform was their simple synthesis from diethanolamines, which are derived from naturally abundant epoxides and aliphatic diamines. In addition, these monomers contain tertiary amines within their ring structure, which are also capable of subsequent quaternization with iodomethane to prepare cationic polycarbonates. Another promising feature of cyclic carbonates is that their ROP towards polycarbonates can be carried out with metal-free organocatalysts. One such benefit of organocatalysts over the more traditional metal based catalyst is the absence of metal contamination in the final polymer product. The presence of metals in polymers is a notable problem towards their implementation in biomedical applications because of their toxicities. Due to the challenges of deactivating and removing such metal-based catalysts, it is more advantageous to simply work with the more biocompatible organocatalysts.

For this study, charged polycarbonates with varying degrees of polymerization (DP) were prepared and investigated. Clinically relevant microbes including *Staphylococcus aureus* (*S. aureus*) and *Escherichia coli* (*E. coli*) were used to test the antimicrobial activity of the polymers. In order to expand the scope of this study, we explored the potential of *N*-substituted eight membered cyclic carbonates to form hydrogels exhibiting antimicrobial behaviors suitable for wound dressing applications. The treatment of wounds through the use of proper dressings (i.e., gauze pads) is essential for a patient's care. In the past decade, hydrogels have been studied as alternative materials in wound dressing applications.⁹⁷ Hydrogels have the ability to maintain wound occlusion by creating a more conducive environment for tissue regeneration than exposed wounds.⁹⁸⁻¹⁰⁰ The main problem with hydrogels is its high risk for infections, due to the moist environment the hydrogels provides. Therefore to design hydrogels that promotes cell proliferation while inhibiting the pathogen growth is essential and highly advantageous.

3.2. Results and discussion

3.2.1. Synthesis of the charged linear polycarbonate

First, we prepared our non-charged **N-8-C** monomer from the ring closure of *N*-methyldiethanolamine, as discussed in the previous chapter. What makes this monomer unique is its tertiary amine group within the cyclic carbonate structure, which ultimately becomes part of the polycarbonate backbone upon ROP of the monomer. Indeed, this amine group can be quaternized with iodomethane to afford charged polycarbonates with cationic groups within the backbone of the polymers (Figure 12). This synthetic pathway represented a dramatically simplified antimicrobial polycarbonate design where the charge(s) can be dispersed in the backbone of the polymer chain.

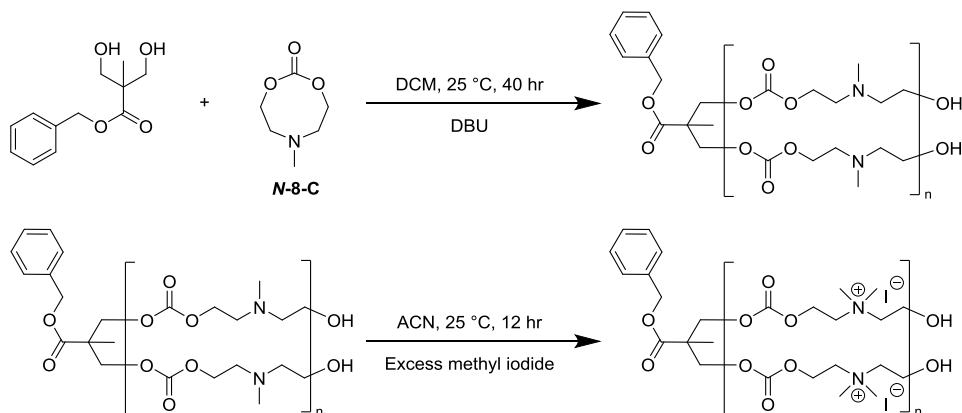


Figure 12. Polycarbonates were prepared via the ROP of *N*-8-C (top line) and later quaternized using iodomethane (bottom line).

With this approach, we first prepared organocatalyzed linear polymers targeting three different DPs (50, 100, and 200) with *N*-8-C and named them accordingly by their target DPs (**8M PDMEA 50**, **8M PDMEA 100**, and **8M PDMEA 200**), see Figure 12. The conversion of the polymerization was monitored by quantifying the disappearance of the signal assigned to the methyl group of cyclic carbonate centered at 2.51 ppm and the appearance of the new signal assigned to the methyl group of polycarbonate, centered at 2.36 ppm (Figure 13). Furthermore the methylene adjacent to the carbonyl shifted from 4.21 ppm to 4.19 ppm, and the methylene adjacent to the amine shifted from 2.78 ppm to 2.73 ppm. By ^{13}C NMR, we can observe the carbonyl of the carbonate shifting from 156.11 ppm to 155.24 ppm (Figure 14). Moreover, the methylene adjacent to the carbonyl shifted from 68.42 ppm to 65.65 ppm, and the methylene adjacent to the amine shifted from 56.14 ppm to 55.93 ppm. Lastly, the methyl pendant group shifted from 44.34 ppm to 42.83 ppm. The evidence for the formation of the polycarbonate was also confirmed by FTIR-ATR, where the C=O stretching from the carbonate shifted from 1743 cm^{-1} to 1737 cm^{-1} . A new and broad band at 1239 cm^{-1} was observed in the polymer's spectra, and was identified as the C-O stretching from the carbonate linkages (Figure 15).

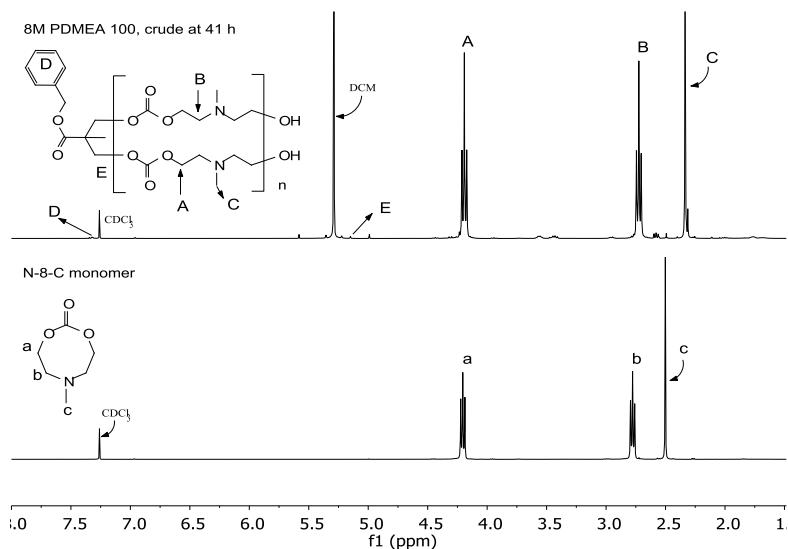


Figure 13. ^1H NMR of the monomer *N*-8-C (bottom) and the ROP of 8M PDMEA 100 (top) in its crude after 40 hours of reaction time in CDCl_3 . The conversion was followed by using the relative integral values of the methyl pendant groups.

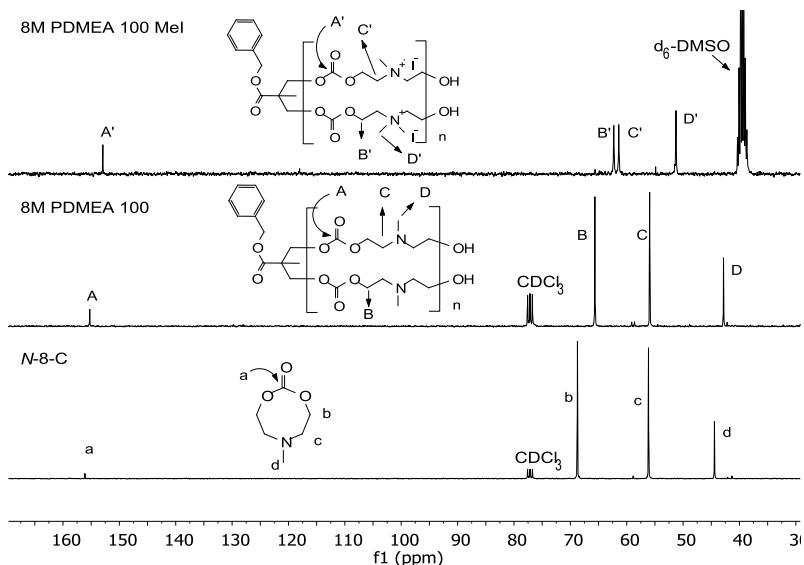


Figure 14. ^{13}C NMR of *N*-8-C (bottom), 8M PDMEA 100 (mid), and 8M PDMEA 100 MeI (top).

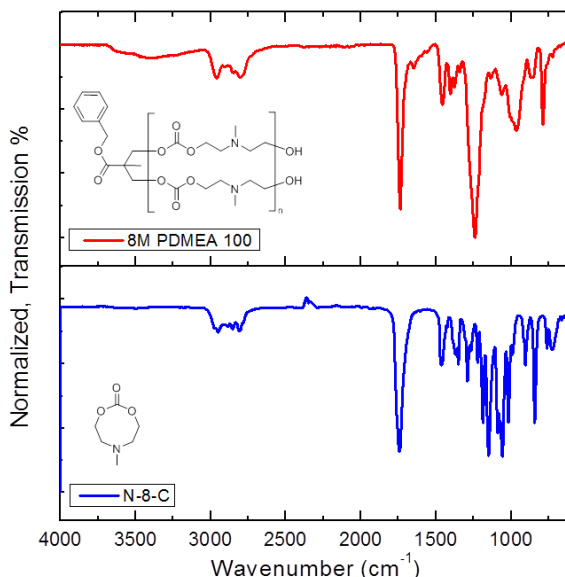


Figure 15. FTIR-ATR of the non-charged cyclic carbonate N-8-C (bottom) and the polymer 8M PDMEA 100 (top).

When the reaction was complete, benzoic acid was added to quench the reaction. The polymer was subjected to precipitation in cold diethyl ether, and later dried under high vacuum. Their molecular weights, M_n , and dispersities were also characterized and determined by SEC (Table 2). Molecular weights of 2,900 Da to 5,200 Da were realized, and we noticed the polymers' molecular weights would increase with DPs. However, they did not scale accordingly with the DP and were much lower than expected. Furthermore, the polydispersity (\mathcal{D}) values were quite high for ROPs, which could be result of water initiation and or other possible side reaction(s).

Table 2. Molecular weight measurements of linear non-charged polycarbonates

Name	M_n ($^1\text{H NMR}$) (kDa)	M_n (kDa) / \mathcal{D} (SEC)
8M PDMEA 50	4.1	2.9 / 1.4
8M PDMEA 100	12.8	4.7 / 1.4
8M PDMEA 200	16.9	5.2 / 1.4

Upon quaternizing these polymers with iodomethane, the samples were then renamed to: **8M PDMEA 50 MeI**, **8M PDMEA 100 MeI**, and **8M PDMEA 200 MeI**. The quaternized polymers were then studied by ^1H NMR in d_6 -DMSO due to their insolubility in CDCl_3 . The characteristic signal of the methylene protons adjacent to the carbonate moiety shifted to 4.59 ppm after quaternization. In addition, the signal attributed to the methyl protons shifted downfield to 3.24 ppm and the corresponding integration value doubled due to the presence of two methyl groups (Figure 17). With the cationic polymers, we were unable to characterize them with our SEC setup to determine if the quaternization procedure affected the molecular weights and distributions. However, we were still able to confirm the presence of polycarbonate linkages by detecting carbonyl signals from ^{13}C NMR at 152.93 ppm. Moreover, we also observed $\text{C}=\text{O}$ (1748 cm^{-1}) and $\text{C}-\text{O}$ (1244 cm^{-1}) stretching bands by FTIR-ATR (Figure 16).

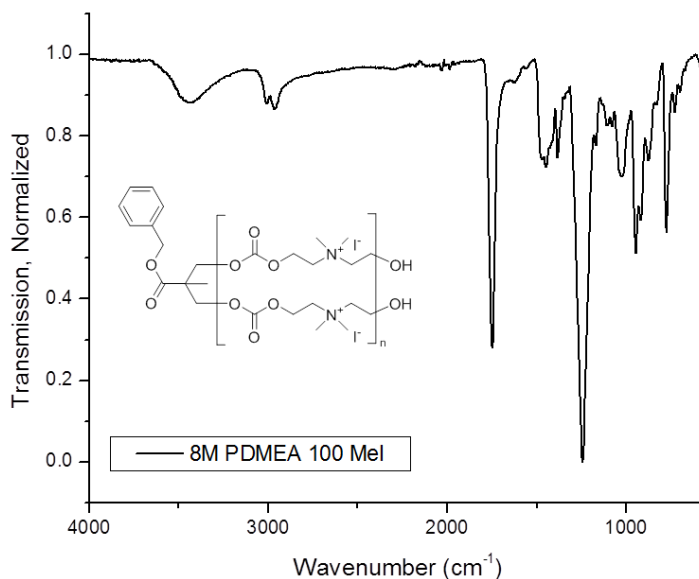


Figure 16. FTIR-ATR of 8M PDMEA 100 MeI after quaternization with iodomethane.

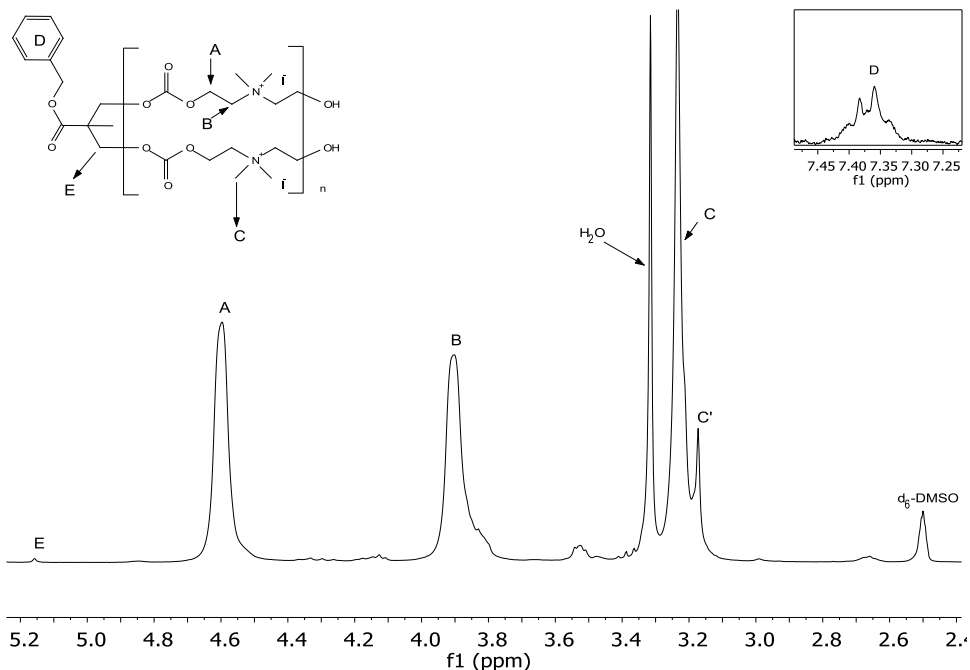


Figure 17. ^1H NMR in d_6 -DMSO of the polymer **8M PDMEA 100 MeI** after the quaternization with iodomethane.

In summary, ROP of the eight membered cyclic carbonate **N-8-C** were carried out to afford linear polycarbonates with differing amounts of DPs. Following the polymerization, the polymers were quaternized with iodomethane to form the cationic quaternary amine groups within the polymers' backbones with iodine anions. The polymerization and post-polymerization modifications were followed by NMR, FTIR, and SEC. Next, we investigated the preparation of charged polycarbonate hydrogels in a similar fashion.

3.2.2. Synthesis of the charged polycarbonate hydrogels

Upon the successful ROP of **N-8-C** to yield linear polycarbonates, we then turned our attention to preparing polycarbonate hydrogels. For this, we decided to utilize

our bis-cyclic carbonate monomer from our previous NIPU chapter, **bis N-8-C**, as a means to generate cross-linking points to form a three dimensional polymer networks (Figure 18). The hydrogels were synthesized by ROP of **N-8-C** and **bis N-8-C** initiated by PEG diols of different molecular weights (M_n 1500, 4000, and 8000 g mol^{-1}). Different amounts of **bis N-8-C** were surveyed at 4 to 20 mol%, and we determined that a minimum of 12 mol% was necessary to readily obtain gels. Next, the polycarbonate gels were treated with iodomethane to yield charged polycarbonate hydrogels.

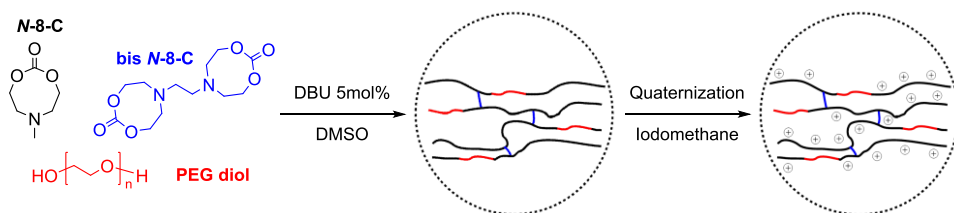


Figure 18. Cationic polycarbonate hydrogels were prepared using the non-charged N-8-C. An additional post-polymerization step with iodomethane was required to obtain the charged structures.

It is important to note, that these hydrogels are three dimensional in nature, and its network makes it a challenge to ensure complete quaternization of all the nitrogen atoms across the entirety of the hydrogels. And just as it is challenging for the quaternizing agents to penetrate into the network of the hydrogels, there is also the difficulty of removing any unreacted quaternizing agents from the hydrogels. In our case where we wanted to use this material in a wound dressing application, this was particularly important to keep in mind due to known toxicities of iodomethane. Thus, the gels were washed thoroughly with DCM and vacuum dried extensively to remove any unreacted iodomethane. Characterization of these charged polycarbonate gels by FTIR-ATR were conducted, we observed the formation and preservation of polycarbonate linkages throughout the entire process. Specifically, the quaternized gels had stretching bands associated with

C=O and C-O at 1740 cm^{-1} and 1250 cm^{-1} , respectively.³⁷ The rheological behavior of the non-quaternized and quaternized gels were investigated by measuring the elastic (G') and viscous (G'') moduli as a function of frequency at room temperature. In all cases, both types of gels (non-charged and charged) exhibited $G' > G''$ behaviors, which suggested that the materials were chemically cross-linked.³⁷

An important characteristic of hydrogels is its ability to hold water without losing their shapes or three dimensional networks. For this, water uptake studies were performed by submerging our polycarbonate gels in water and measuring their mass over time. Non-charged polycarbonate gels with 20 mol% **bis N-8-C** and were initiated with PEG₈₀₀₀, had swelling capabilities of ~100 wt%. Upon quaternizing these gels, the swelling ratio of the hydrogels increased to 705 wt%.³⁷ This dramatic increase in water uptake ability can be attributed to the cationic groups within the gels, which are hydrophilic and thus attracts and traps water within the gel easier.

In summary of this section, we successfully produced polycarbonates hydrogels using the non-charged **N-8-C** monomer. And afterwards, the materials were then treated with a quaternizing agent (i.e., iodomethane) to yield the cationic structures. Rheological studies were confirmed the presence of a three dimensional polymer network, and FTIR-ATR confirmed the presence of polycarbonate linkages. With the charged linear polycarbonate and charged polycarbonate hydrogels in hand, we then examined their potential use as antimicrobial agents.

3.2.3. Antimicrobial and hemolysis studies with linear polycarbonates

Linear polycarbonates bearing cationic quaternary ammonium groups derived from post-quaternization were studied for their antimicrobial properties. From this

work, the minimum inhibitory concentrations (MIC)² of **8M PDMEA 200 Mel** and **8M PDMEA 200** (its neutral analog) towards *S. aureus* were realized at 31 $\mu\text{g mL}^{-1}$ and $>1000 \mu\text{g mL}^{-1}$ respectively. This was to be expected, as the neutral analog does not have any cationic groups to target and disrupt the bacteria's membrane. Moreover, the smaller charged linear polycarbonates (**PDMEA 100 Mel** and **PDMEA 50 Mel**) exhibited similar antibacterial activity towards *S. aureus* as **PDMEA 200 Mel**.

Once the MIC values were established for *S. aureus*, we explored the antibacterial activity of the **8M PDMEA 200 Mel** with different concentrations (1x to 8x MIC), as shown in Figure 19. At concentrations of 1x MIC, we were able to observe the elimination of the bacteria within 30 min. At higher MICs, the gels exhibited even faster bactericidal activity and eliminated the bacteria in less than five minutes. The polymer **8M PDMEA 200 Mel** was also tested against *E. coli* and *C. albicans* and showed similar promising antibacterial activities.⁴⁰

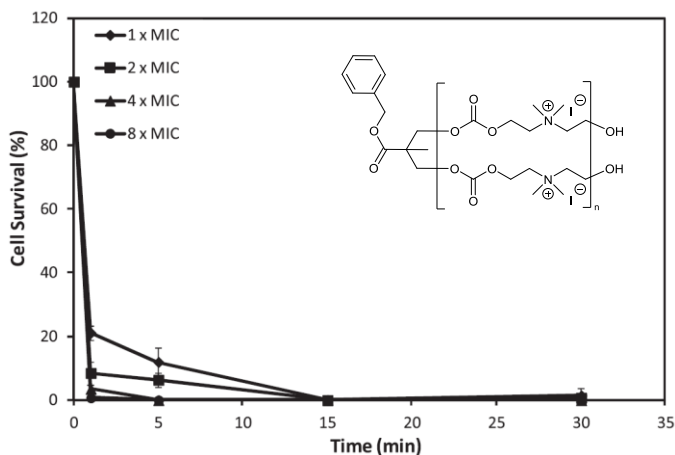


Figure 19. Antimicrobial studies of 8M PDMEA 200 Mel (inset) towards *S. aureus* were conducted using different minimum inhibitory concentrations (MIC) at 37 °C.

² Minimum inhibitory concentration, or MIC, is the minimum concentration of a material that prevents the growth of a bacterium

Survivability measurements of the bacteria were taken at different time intervals (1, 5, 15, and 30min).⁴⁰

For antimicrobial polymers to be qualified as suitable therapeutic agents, their selectivity for anionic microbial cell membrane over zwitterionic mammalian cell membrane should be considered. Charged linear polycarbonates (**8M PDMEA Mel 200**, **8M PDMEA Mel 100** and **8M PDMEA Mel 50**) showed no hemolysis against rat red blood cells (rRBCs) at concentrations of up to 1000 $\mu\text{g/mL}$ (Figure 20). The antimicrobial polymers were also tested for their cytotoxicity against human dermal fibroblast (HDF) and human embryonic kidney cell lines (HEK 293). Both cell lines showed $\sim 100\%$ cell viability for all the polymers tested up to 1000 $\mu\text{g/mL}$ after incubation with the polymers for up to 48 h at 37°C.

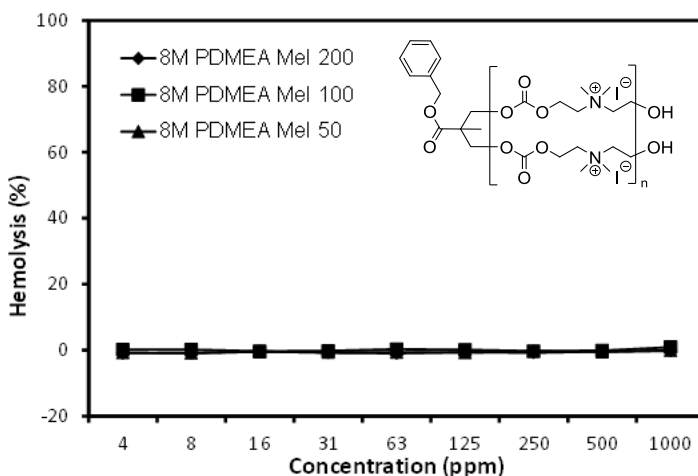


Figure 20. Charged linear polycarbonates showed no hemolysis activities regardless of DPs tested and concentrations up to 1000 $\mu\text{g/mL}$ after 1 hr of incubation at 37 °C.

In summary, linear polycarbonates bearing quaternary ammonium groups exhibited very fast and efficient bactericidal activity. It was also demonstrated that this antibacterial activity only occurs after the quaternization process, and

not beforehand. More importantly, the charged linear polycarbonates exhibited minimal hemolytic behavior, which is highly desirable for future bio-applications.

3.2.4. Antimicrobial and hemolysis studies with polycarbonate gels

After surveying the antibacterial activity of our linear polycarbonates, we next turned our attention towards the polycarbonate hydrogels that we prepared earlier. Just as in the case with our linear polycarbonates, the gels only exhibited antimicrobial activities after the post-quaternization procedure, and not before. From our antimicrobial results with the *S. aureus*, we observed a 10^8 CFU/mL reduction in colony count from an initial 10^{15} CFU/mL colony count after eight hours of treatment. Moreover, the antimicrobial activity appeared to be independent of the amount of cross linker (**bis N-8-C**) and the length of the PEG initiator used in the synthesis process. It is worth noting that the hydrogels exhibited bactericidal activity against other common pathogens (i.e., *E. coli*, *P. aeruginosa*, and *C. albicans*) with similar efficiencies.³⁷

The polycarbonate hydrogels' toxicities were evaluated with hemolysis assays with rat red blood cells, rRBC. The hydrogels in both their non-quaternized and quaternized states were shown to be non-hemolytic towards rRBC after an hour of incubation. Additionally, testing with HEK 293 cells also showed that both the non-quaternized and quaternized hydrogels were non-toxic toward the cells.

In summary, the charged polycarbonate hydrogels also displayed high and broad bactericidal activities with similar efficiencies as the linear charged polycarbonates. These hydrogels found to be nontoxic toward rRBC and HEK 293 cells. Such behaviors with low hemolytic behaviors and fast antimicrobial activities make these hydrogels a promising material for wound dressing applications.

3.3. Conclusion

Cationic linear polycarbonates and polycarbonate hydrogels were prepared using the ROP of *N*-substituted eight membered cyclic carbonates, and were subsequently post-quaternized with iodomethane to afford their cationic structures. All of these cationic materials in this chapter demonstrated high bactericidal activity against *E. coli* and *S. aureus* by disrupting the membrane of the bacteria. Furthermore, hemolysis testing showed that both the charged linear polycarbonates and hydrogels exhibited low hemolytic activity. These properties make these materials of interest in treating biofilms contaminated with pathogens or even possibly as wound dressings. Though these initial results looked promising, the process in obtaining these charged polycarbonates relied on a post-quaternization procedure, which can be difficult to ensure the complete quaternization of every amine in the polymer chain.

3.4. Experimental part

Materials and equipment

^1H and ^{13}C NMR spectra were recorded with Bruker Avance DPX 300, Bruker Avance 400, or Bruker Avance 500 spectrometers. The NMR chemical shifts were reported as δ in parts per million (ppm) relative to the traces of non-deuterated solvent (eg. $\delta = 2.50$ ppm for $\text{d}_6\text{-DMSO}$ or $\delta = 7.26$ for CDCl_3). Data were reported as: chemical shift, multiplicity (s = singlet, d = doublet, t = triplet, m = multiplet, br = broad), coupling constants (J) given in Hertz (Hz), and integration. Fourier transform infrared - attenuated total reflection (FTIR-ATR) spectroscopy was performed with a ThermoFisher Nicolet 6700. Gel permeation chromatographies (GPC-SEC) with the charged polycarbonates were performed using an Agilent Technologies PL-GPC 50 Integrated GPC system, with a Shodex KD-806M column.

Triethylamine ($\geq 99\%$), *N*-methyldiethanolamine ($\geq 99\%$), *N,N,N',N'*-tetrakis(2-hydroxyethyl)ethylenediamine (technical grade), polyethylene glycol (M_n 8000), and 1,8-diazabicyclo[5.4.0]undec-7-ene ($\geq 99\%$) were purchased from Sigma Aldrich and used as is. 1,8-Bis(dimethylamino)naphthalene (99%), iodomethane (99%), acetonitrile (extra dry), DCM ($\geq 99.9\%$), diethyl ether ($\geq 99.8\%$), acetone ($\geq 99.5\%$), and THF ($\geq 99\%$) were purchased and used as is from Fisher Scientific. Triphosgene was purchased from TCI and used as is. Bis(pentafluorophenyl) carbonate (97%) was purchased from Manchester Organics and was used as is. Deuterated solvents including $CDCl_3$ and d_6 -DMSO were purchased from Deutero and were used as is.

Typical eight-membered cyclic carbonate synthesis

6-Methyl-1,3,6-dioxazocan-2-one (Non-charged N-8-C): A 1L single neck round bottom flask was charged with *N*-methyldiethanolamine (10.0g, 83.9mmol), triethylamine (17.4g, 167.8 mmol), THF (600mL), and a large oval stir bar. The mixture was then allowed to stir and cooled to $-78^\circ C$ using a liquid nitrogen/acetone bath. This was then followed by a dripwise addition of triphosgene (8.3g, 28.8mmol) in THF (100mL). Once all of the triphosgene has been added, the reaction was taken out of the liquid nitrogen/acetone bath and allowed to stir for an additional two hours at room temperature. The reaction mixture was then filtered to remove the triethylammonium chloride salt and concentrated under vacuum. Cold diethyl ether (500mL) was then added to help precipitate the remaining salts, which were then filtered again. The remaining filtrate was concentrated under vacuum to give the final product as a yellow oil (9.24g, 76% yield). 1H NMR (500 MHz, DMSO): δ = 4.13 (t, CH₂, J = 5.3 Hz, 4H), 2.73 (t, CH₂, J = 5.3 Hz, 4H), 2.41 (s, CH₃, 3H). ^{13}C NMR (101 MHz, DMSO): δ = 155.36 (C=O), 68.71 (CH₂), 55.64 (CH₂), 44.39 (CH₃).

Synthesis of 6,6'-(ethane-1,2-diyl)bis(1,3,6-dioxazocan-2-one) (bis N-8-C)

Bis N-8-C: The same procedure was used and discussed in the previous chapter.

General procedure for charged linear polycarbonates (8M PDMEA 200 MeI)

To obtain the **8M PDMEA 200** non-charged polymer, a 12mL vial was charged with benzyl 2,2-Bis(hydroxymethyl)propionic acid (bis-MPA) diol (0.0039g, 0.0172mmol), *N*-8-C (0.5 g, 3.44 mmol), dichloromethane (1.5 g), and a stir bar in a N₂ filled glove box. The polymerization was catalyzed by the addition of DBU (0.013 g, 0.086 mmol). After complete monomer conversion (~24 h) the reaction mixture was quenched with benzoic acid and precipitated with diethyl ether. The precipitated polymer was then isolated and dried under vacuum.

To obtain the **8M PDMEA 200 MeI** charged polycarbonates, the previously collected polymers were dissolved in acetonitrile and treated with excess iodomethane. After 12 hr at RT, a pale yellow precipitate was observed, collected, and dried under vacuum.

General procedure for gel preparation with non-charged cyclic carbonates

A 12mL vial was charged with a stirbar, **N-8-C** (0.310g, 2.2mmol), **bis N-8-C** (0.120g, 0.42mmol), and PEG₁₅₀₀ end capped diol (0.030g) were dissolved in 2mL of DCM. Next, DBU (0.018g, 0.11mmol) was added, and the reaction was stirred at 25 °C for 8 hr. The stir bar was then removed, and the DCM was allowed to evaporate overnight at RT. The DBU was quenched with excess benzoic acid in DCM. The resulting hydrogels were washed with DCM to remove the catalysts and any soluble fractions. To quaternize the gels, the gels were immersed with excess iodomethane for 2 d at RT under N₂ and washed again with DCM and dried under vacuum.

Rheology

Rheology measurements on the gels were conducted on Anton Paar Physica MCR 101 rheometer using oscillatory tests with parallel plate geometry. Angular frequency sweeps from 0.0628 s^{-1} to 314 s^{-1} at constant strain amplitude ($\gamma = 1\%$) were applied at $25\text{ }^{\circ}\text{C}$. Later, G' and G'' values were plotted versus frequency.

Antibacterial assays (for linear polycarbonates)⁴⁰

The polymers' antimicrobial effectiveness was tested against five clinically relevant microbes: *S. epidermidis* (ATCC 12228), *S. aureus* (ATCC 29737), *E. coli* (ATCC 25922), *P. aeruginosa* (ATCC 9027) and *C. albicans* (ATCC 10231). MIC for the polymers was evaluated through a broth microdilution method. Polymer was incubated with bacteria or fungi for 18 h ($37\text{ }^{\circ}\text{C}$) or 42 h ($25\text{ }^{\circ}\text{C}$) respectively. Killing efficiency of the polymer against different microbes was conducted using the agar plating assay. Bacteria and fungi were pretreated with the polymer according to the MIC measurement protocol before the microbes were streaked onto agar plates. The agar plates after being streaked with bacteria or fungi were nurtured for 18 h ($37\text{ }^{\circ}\text{C}$) and 42 h ($25\text{ }^{\circ}\text{C}$) respectively. Killing kinetics of the polymer was studied by incubating the polymer with the microbes at different time points before the microbes were plated onto agar plates and incubated as stated previously. Details for all the experiments were described in a previous publication.¹⁰¹

Antibacterial assays (for polycarbonate hydrogels)³⁷

Escherichia coli (ATCC 25922), *Pseudomonas aeruginosa* (ATCC 9027), and *Staphylococcus aureus* (ATCC 29737) were reconstituted from their lyophilized forms according to the manufacturer's protocol and cultured in tryptic soy broth (TSB) at $37\text{ }^{\circ}\text{C}$ under constant shaking of 300 rpm, while *Candida albicans* (ATCC 10231) was cultured in yeast media broth (YMB) at room temperature under constant shaking of 50 rpm. Prior to treatment, the microbes were first inoculated overnight to enter into log growth phase. The quaternized hydrogel

was cut into a 5 mm × 5 mm square and placed into a 1.7 mL microcentrifuge tube. TSB or YMB (100 µL) was added into the tube before an equal volume of microbe suspension (3×10^5 CFU/mL) was added. Prior to this, the concentration of microbe solution was adjusted to give an initial optical density (O.D.) reading of approximately 0.07 at 600 nm wavelength on a microplate reader (TECAN, Switzerland), which corresponds to the concentration of McFarland 1 solution (3×10^8 CFU/mL). The tube was kept either at 37 °C for bacterial samples or room temperature for *C. albicans* under constant shaking (300 and 50 rpm for bacteria and fungi, respectively) for 24 and 42 h, respectively. After the hydrogel treatment, the samples were taken for a series of 10-fold dilution and plated onto agar plates. The plates were incubated for 24 h at 37 °C for bacterial samples or 42 h at room temperature for *C. albicans* before the number of colony-forming units (CFU) was counted. Microbes treated with hydrogel without cationic polycarbonates were used as negative control, and each test was carried out in three replicates.

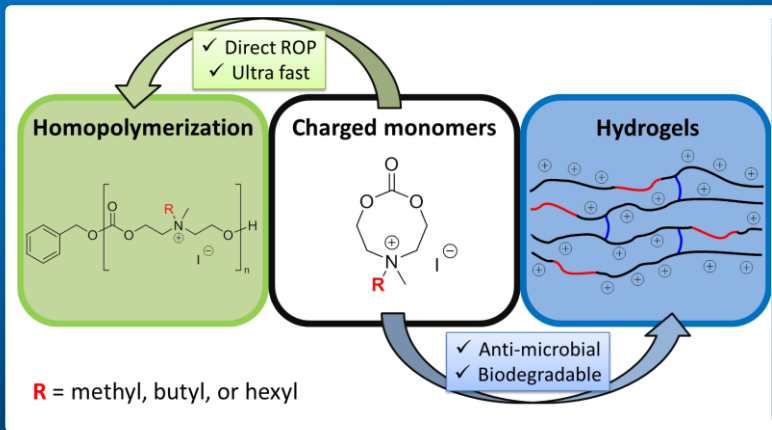
Hemolysis assay^{37,40}

Hemolysis of the polymers was evaluated using freshly drawn rat red blood cells (rRBCs), after obtaining approval by Animal Handling Unit of Biomedical Research Center, Singapore. The rRBCs were subjected to a 25× volumetric dilution in PBS to achieve a 4% blood content. The diluted rRBCs were added to hydrogels and incubated in 37 °C. After incubation, the samples were pelleted under 3000 g for 5 min. The supernatant (100µL) was transferred to a 96-well plate, and hemoglobin release was analyzed spectrophotometrically by measuring absorbance at 576 nm using a microplate reader (TECAN, Switzerland). Two control groups were used in this assay: untreated RBC suspended in PBS (negative control) and RBC treated with 0.1% Triton-X (positive control). Percentage hemolysis was calculated as follows:

Hemolysis (%)

$$= \left[\frac{O.D._{576 \text{ nm}} \text{ of treated sample} - O.D._{576 \text{ nm}} \text{ of negative control}}{O.D._{576 \text{ nm}} \text{ of positive control} - O.D._{576 \text{ nm}} \text{ of negative control}} \right] \times 100\%$$

Chapter 4



Antimicrobial polycarbonates obtained by ROP of ionic monomers

Chapter 4. Antimicrobial polycarbonates obtained by ROP of ionic monomers

4.1. Introduction

In the previous chapter, we established that **N-8-C** can be used to prepare cationic polycarbonates with antimicrobial properties by post-quaternization. Polycations or cationic polymers are commonly employed nowadays in many different applications such as household products (e.g., soaps and shampoos)¹⁰² or flocculants for water purification¹⁰³. Over the past decade, a considerable amount of attention in the scientific community has been given to the synthesis of cationic polymers with hydrolyzable polymer backbones. The main reason for this is to develop cationic polymers which can undergo biodegradation during and/or after its usage, whether it's outside or inside a living body.

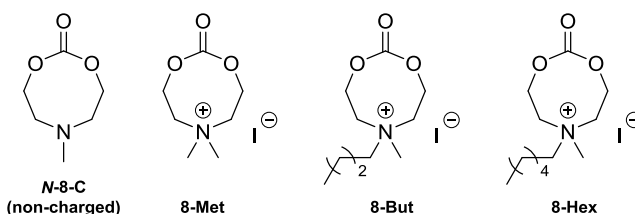
In the previous chapter, the process in obtaining these charged polycarbonates relied on a post-quaternization procedure. Such a method can be difficult to ensure the complete quaternization of every amine in the polymer chain. This holds particularly true for quaternizing hydrogel, as well as, removing the toxic unreacted quaternizing agents due to the three dimensional network of polymer chains. In this chapter, we report the preparation of charged polycarbonates by means of quaternizing the tertiary amines at the monomer level. By quaternizing the tertiary amines beforehand, one can directly prepare charged polycarbonates without a need for the post-modification step. Furthermore, this method allows for better control of the degree of quaternization within the polymer chains. Herein, we report the synthesis of cationic monomers and examined them with homopolymerizations and computational studies. Hydrogels based on these charged monomers were also prepared and characterized. Finally, these

hydrogels were screened against both gram positive and gram negative bacteria to gauge their potential use as antimicrobial agents.

4.2. Results and discussion

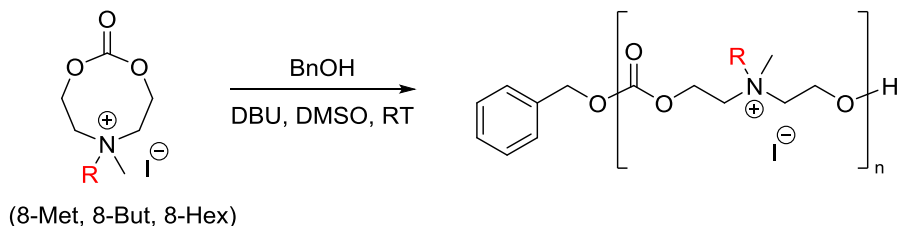
4.2.1. Synthesis and polymerization of charged monomers

First, non-charged *N*-substituted eight membered cyclic carbonates were synthesized using the previously reported ring closure process of diethanolamines with triphosgene.^{37,85,104} Three non-charged cyclic monomers with different alkyl chains were prepared. Subsequently, these monomers were treated with iodomethane to afford their quaternized versions (i.e. **8-Met**, **8-But** and **8-Hex**) in excellent isolated yields of ~93% (Scheme 8). The monomers' structures were confirmed by ¹H and ¹³C NMR and FTIR-ATR spectroscopy.³⁹



Scheme 8. Charged aliphatic *N*-substituted eight-membered cyclic carbonates used in the direct preparation of cationic polycarbonates.

Next, the ROP behavior of the quaternized monomer in the presence of DBU was then evaluated (Scheme 9). The DBU organocatalyst was used based on past successful ROP of eight membered cyclic carbonates.¹⁰⁴ The monomer **8-Met** was found to be insoluble in many organic solvents except for DMSO. Despite DMSO not being the most suitable solvent for ROP, a series of homopolymerizations were carried out with **8-Met** at three different DPs (i.e. 50, 100 and 200), see Table 1 (Entries 3, 4, and 5).



Scheme 9. Representative scheme to obtain linear homopolymers via ROP of monomer **8-Met**, **8-But** and **8-Hex**.

Table 3. Exploration of homopolymerization of charged eight-membered cyclic monomers via ROP in DMSO.

Entry	Monomer	Target DP	DBU amt	Time	% conv.	M_n by ^1H NMR
1	<i>N</i> -8-C	50	5.00 mol%	1 week	34 %	-
2	8-Met	50	(none)	1d	>97%	14,200
3			0.33 mol%	1min	>97%	14,900
4		100	0.33 mol%	1min	>97%	20,600
5		200	0.33 mol%	1min	>97%	39,300
6		8-But	200	1.00 mol%	1min	>97%
7	8-Hex	200	1.00 mol%	1min	>97%	71,200

After screening reaction conditions with different catalyst loadings, we found that 0.33 mol% of DBU was optimum for the **8-Met** monomer. With ^1H NMR, we followed the polymerizations and noted the shifting of **8-Met**'s methylene protons adjacent to the carbonate at 4.62 ppm to 4.59 ppm (Figure 21). Monomer conversion was determined using relative peak integrations values. Polymerization was also evidenced by the shifting of the carbonyl in the ^{13}C NMR from 153.26 ppm to 152.92 ppm. Further characterization by FTIR-ATR provided additional evidence of the formation of polycarbonate by the disappearance of the monomer's C=O stretching band at 1758 cm^{-1} and the appearance of a

polycarbonate C=O band at 1751 cm^{-1} . A large new peak at 1247 cm^{-1} was also observed and identified as the C-O from the polycarbonate (Figure 22).

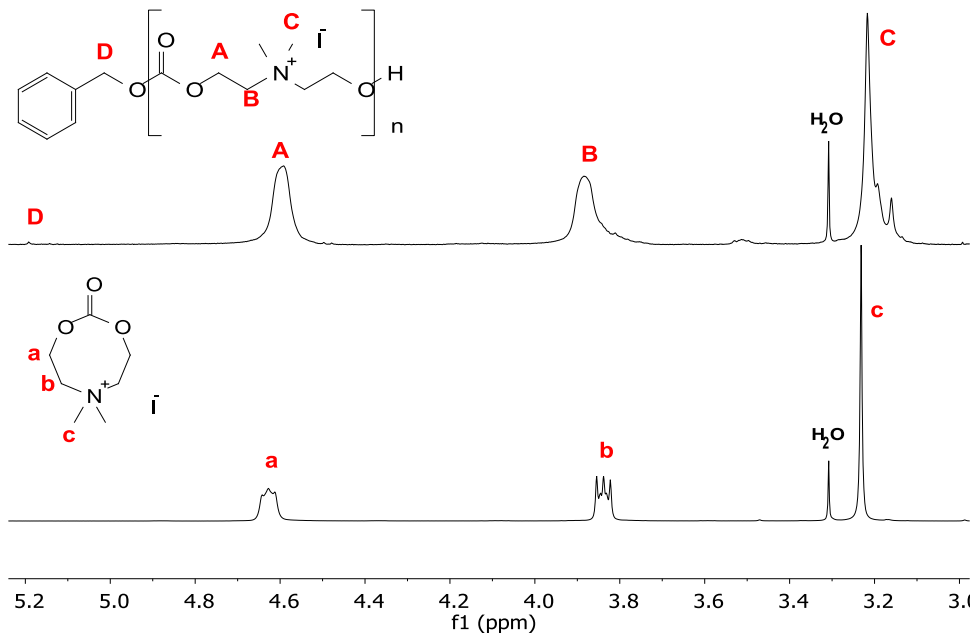


Figure 21. Homopolymerizations of 8-Met (DP: 50) were carried out and characterized with ^1H NMR in d_6 -DMSO. Depicted above is of the homopolymer, and below is the monomer 8-Met.

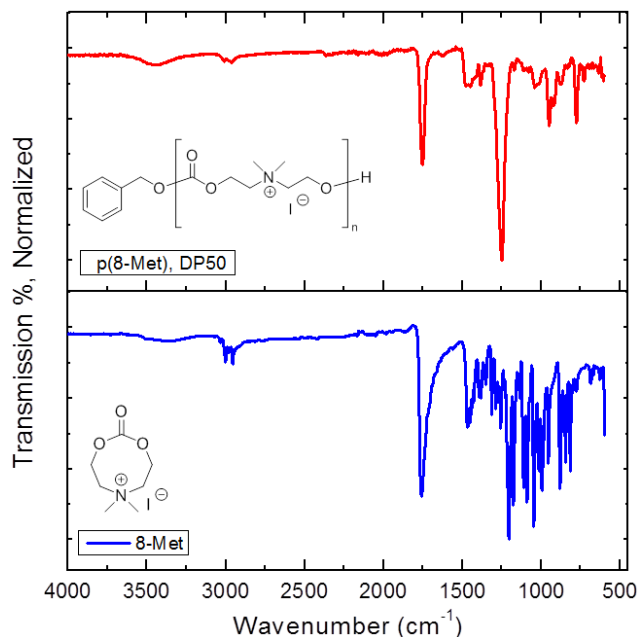


Figure 22. FTIR-ATR of **8-Met** (bottom) and its homopolymer at DP50 (top).

All polymerizations with the charged monomers listed in Table 3 at different DPs reached full conversion incredibly fast in comparison to the non-charged monomer. For the analogous non-charged **N-8-C** monomer, we were only able to observe 34% monomer conversion despite using much more catalyst (DBU) and a longer reaction time. Moreover, we observed that **8-Met** was reactive enough to polymerize by itself within 24 hours without the presence of a catalyst. We attempted to characterize the charged polymers by GPC in various solvents including DMF, THF, and H₂O, but we were unable to obtain any data. We suspect that the polymers had either (1) degraded into smaller chains or (2) adhered to the columns in the GPC. We also attempted an anion exchange procedure with LiTFSI in H₂O; however, we were also unable to obtain any readings with our GPC-SEC setup.

Polymerizations with **8-But** and **8-Hex** were carried out in a similar fashion as mentioned previously. At first, 0.33 mol% DBU was applied to each of the polymerizations, and we observed a decrease in reactivity with increasing length of the alkane pendant group. As a solution, DBU content was increased to 1 mol%, and we were again able to realize full monomer conversions of **8-But** and **8-But** within one minute reaction time. Like before, the polymerizations were confirmed by ^1H and ^{13}C NMR, but we were unable to obtain any data by SEC despite trying different combinations of solvents (THF and DMF), salts (LiBr and LiTFSI), and salt concentrations (5 and 10mM).

The solubility of the cationic polycarbonates was surveyed in a range of organic solvents. The polymers were consistently insoluble in solvents such as DCM, ACN, THF, and acetone. However, all synthesized polycarbonates were soluble in polar aprotic solvents such as DMF and DMSO. We found the polymers' solubility in water to be influenced by the alkyl chain length. All polymers derived from **8-Met** were soluble in H_2O , however the polymers loses its solubility in water as the pendant group extended to **8-But** and **8-Hex**.

To summarize this section, we observed quite an extraordinary reactivity of the **8-Met** and the other charged monomers in our homopolymerization studies. We observed that **8-Met** was reactive enough to polymerize by itself within 24 hours without the presence of a catalyst. Under the conditions used, complete monomer conversion of the non-charged **8-Met** analog could not be obtained even when more DBU was used. A tremendous difference in reactivity was found between the charged and non-charged monomers, despite having the same ring size. Therefore, we decided next to examine this difference further with a computational study.

4.2.2. Computational modeling of charged monomers

To gain a deeper insight into the reactivity differences between the non-charged monomers and their charged analogs, DFT calculations were carried out³. The calculations were performed at the M062X/6-311+G(d,p) level with DMSO as the solvent (IEFPCM). Ammonium species **A-1** with a chloride anion served as a model for the **8-Met**, see Figure 23.

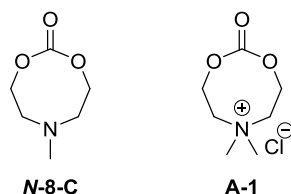


Figure 23. Depicted here are the substrates used in the computational study, neutral amine monomer (**N-8-C**, left) and the ammonium species (**A-1**, right).

The two substrates (**A-1** and **N-8-C**) were taken at their ground states ($G=0$) respective to their energy profiles. Similarly to our previous mechanistic study with NIPUs in Chapter 2, the ring opening reactions for both substrates followed a stepwise process (Figure 24). In the computational study for **A-1**, the initial nucleophilic addition of methanol to **A-1** via **TS1** led to the formation of the quaternized intermediate (**INT1**). This then proceeded through a ring opening process (**TS2**) to arrive at the open-chain monomeric product. For **A-1**, the Gibbs free energies of both transition steps were low (**TS1**, $\Delta G^\ddagger = 21.0$ kcal/mol, **TS2**, $\Delta G^\ddagger = 20.7$ kcal/mol), and their similar values indicated that they would both contribute almost equally to the reaction rate.

³ The reported energy values correspond to Free energies (G) and are given in kcal/mol. For further computational details, see Supporting Information.

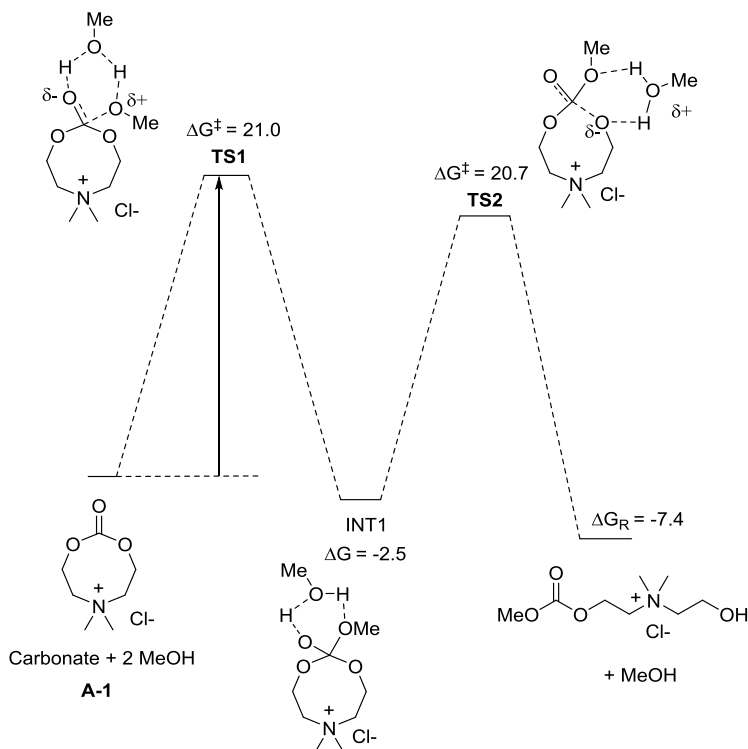


Figure 24. Reaction energy profile for substrate **A-1** and its Gibbs Free energies computed at M062X/6-311+G(d,p) (iefpcm, solvent =DMSO) level.

As with our previous computational study in Chapter 2, the computed activation energies were exceedingly high ($\Delta G^\ddagger = 41.7$ kcal/mol) when a single explicit molecule of methanol was present. However, the activation barrier was largely reduced when a second molecule of methanol was incorporated into the studies (**TS1**, $\Delta G^\ddagger = 21.0$ kcal/mol).

Calculations were also performed in a similar manner for the neutral **N-8-C**, and the energy values for both substrates can be found in Table 4. When comparing these two substrates, **A-1** has energy values 5-6 kcal/mol lower than the **N-8-C**. This energy difference theoretically corresponds to a 10^4 times faster reaction

rate, which is in fair agreement with the observed experimental rate. These findings suggest that the positive charge on nitrogen exerts a strong inductive effect through the carbon chain which makes the remote carbonyl group highly electrophilic and more susceptible to ring opening.

In addition, calculations with DBU were also examined, and we found that its presence reduces the activation energy by ca. 10 kcal/mol. In this case, the DBU would bind and activate the incoming molecule of methanol, thus increase its nucleophilicity during the initial attack at **TS1**. This drop in activation energy would help to accelerate the reactions and is what we observed experimentally.

Table 4. Comparison of the Gibbs Free energy values for the three different substrates, computed at M062X/6-311+G(d,p) (iefpcm, solvent =DMSO) level.

Name	A-1	N-8-C
TS1	$\Delta G^\ddagger = 21.0$ kcal/mol	$\Delta G^\ddagger = 26.6$ kcal/mol
INT1	$\Delta G = -2.5$ kcal/mol	$\Delta G = 3.1$ kcal/mol
TS2	$\Delta G^\ddagger = 20.7$ kcal/mol	$\Delta G^\ddagger = 23.5$ kcal/mol
Product	$\Delta G = -7.4$ kcal/mol	$\Delta G = -5.7$ kcal/mol

4.2.3. Charged polycarbonate hydrogels derived from charged monomers

In order to prepare polycarbonate hydrogels, charged mono-functional eight-membered cyclic carbonates were directly co-polymerized in DMSO with eight-membered bis-cyclic carbonate (**bis N-8-C**) and PEG-diol. Again, DBU was used to catalyze the ROP reactions (Figure 25). The resulting hydrogels were named according to the charged eight-membered cyclic carbonate monomer used in the synthesis (i.e. **Gel-8-Met**, **Gel-8-But**, and **Gel-8-Hex**).

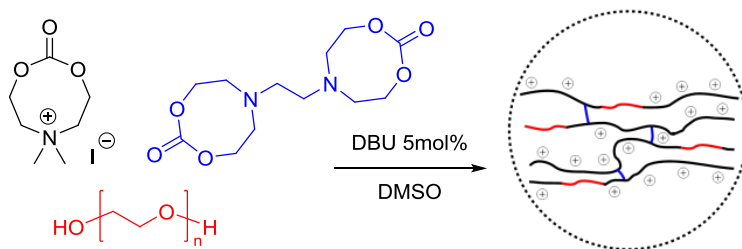


Figure 25. A representative scheme used to create the polycarbonate ion gels using the 8-Met (black, monomer), bis N-8-C (blue, crosslinker), and PEG (red, initiator).

The reaction was confirmed by FTIR-ATR after the removal of DMSO from the gels. Evidence of the formation of the polycarbonate structure was noted by the disappearance of the monomers' C=O stretching band at 1758 cm^{-1} and the appearance of a new C=O band at 1744 cm^{-1} . Furthermore, a large new peak at 1244 cm^{-1} was identified as the C-O from the polymer (Figure 27).

To further confirm the formation three-dimensional cross-linked network, the rheological behaviors of the gels were studied using oscillatory tests at room temperature. We were able to realize the elastic modulus (G') to be greater than the loss modulus (G'') for all the hydrogels. This $G' > G''$ behavior suggests that the gels that we obtained were covalently crosslinked. Furthermore, we continued to observe this trend when DMSO was removed from one of the gels and replaced with water (100 wt%), see Figure 26.

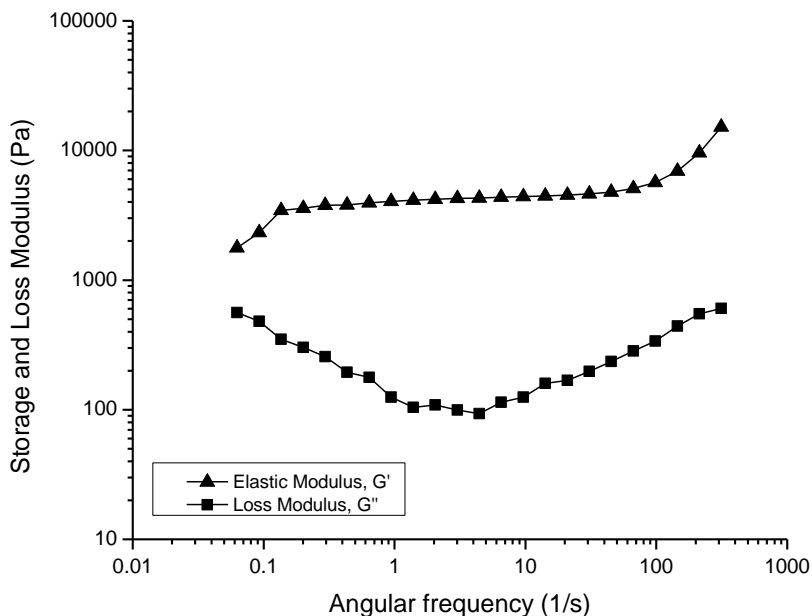


Figure 26. Rheological studies using oscillatory tests were performed on Gel-8-Met re-swollen with water. Here we have plotted the elastic modulus (G' , \blacktriangle) and the loss modulus (G'' , \blacksquare). The $G' > G''$ trend indicates that we have a three dimensionally covalently bonded network throughout the gel.

4.2.4. Assessing the swelling and degradation behavior of the charged polycarbonate gels

A particular characteristic of cationic hydrogels is their ability to swell in water without losing their three-dimensional structure. The level of swelling, responsiveness, and degradability are important features that should be taken into account when designing these hydrogels. Here, the swelling behaviors of the gels were studied by submerging dried pieces of gels in water. As expected, the swelling behaviors of the gels were influenced by the length of the pendant groups of the polycarbonate within the hydrogels. By using longer alkyl chains (from methyl to hexyl), we observed increased hydrophobicity of the gels, and

ability to swell water was reduced from 600 wt% to 55 wt% (Table 5). On the other hand, the “time to degradation” for the gels was significantly delayed from 8 h to 5 days by using monomers with longer alkane chains, (methyl < butyl << hexyl). The reasoning for this could be that the water would have a more difficult time penetrating into gels exhibiting higher hydrophobicities. This would ultimately delay the water from entering the hydrogels and initiate the degradation of the carbonate linkages.

Table 5. Summary of different compositions used to prepare the gels and their swelling behaviors in H₂O

Entry	Gel name	S _t (1hr, wt%) ^a	Time to degradation ^b
1	Gel-8-Met	600	8 hr
2	Gel-8-But	108	11 hr
3	Gel-8-Hex	55	5 d

^aSwelling degree of the gels after being immersed in H₂O for one hour at room temperature. ^bThe amount of time it took for the gels to dissolve completely into the H₂O during the swelling tests.

The degradation of **Gel-8-Met** was followed by FTIR-ATR and compared to its pristine initial state, shown in Figure 27. Upon degradation, the signals pertaining to the carbonate linkages decreased in intensity, whereas the carboxylic acid signal (C=O stretch, 1702 cm⁻¹) grew.³⁷ By using these results, we can expect to engineer new gels with a blend of the available monomers to achieve specific swelling properties and longevity in water.

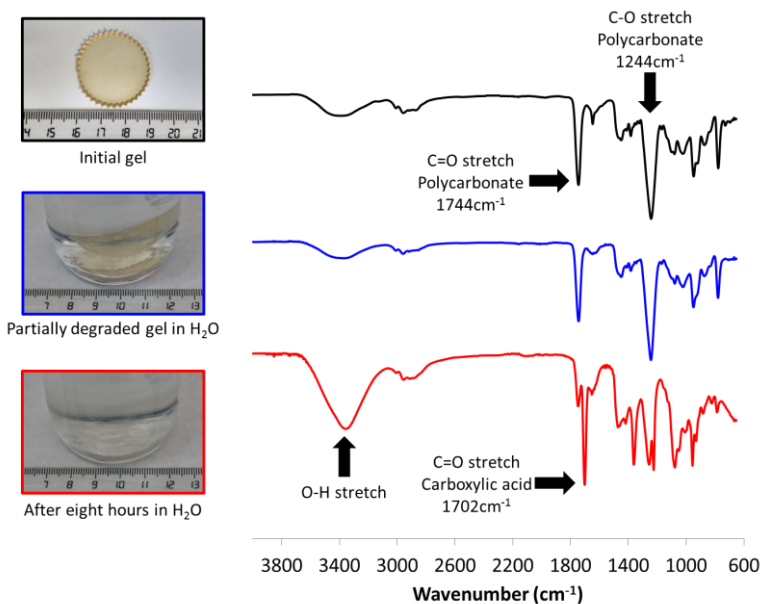


Figure 27. We used FTIR-ATR to characterize the Gel-8-Met in its initial state (black) and after leaving the gel in water after eight hours at room temperature (red); an additional intermediary scan was also performed (blue). Polycarbonate signals at 1744 and 1244 cm⁻¹ decreased with time in water, and carboxylic acid signal at 1702 cm⁻¹ was observed upon the degradation of the polycarbonate.

4.2.5. Antimicrobial studies

The antimicrobial properties of **Gel-8-Met**, **Gel-8-But** and **Gel-8-Hex** hydrogels prepared from the direct polymerization of charged cyclic carbonates were assessed against two frequent pathogens: *Escherichia coli* (E. coli, Gram-negative) and *Staphylococcus aureus* (S. aureus, Gram-positive). These microbes are common pathogens that often manifest on dermal wounds and are typically treated by topical application of antibiotics.

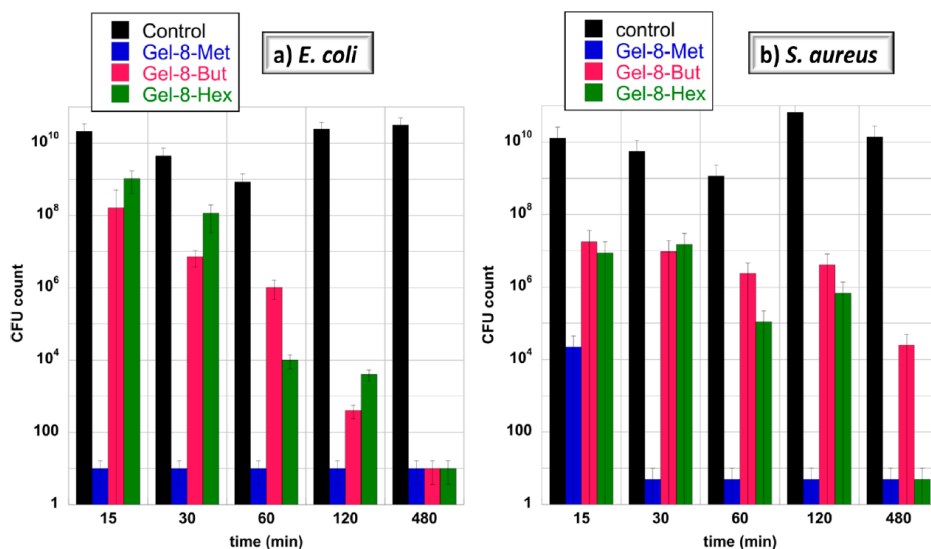


Figure 28. Antibacterial efficacy of the hydrogels measured at different times (15 min, 30 min, 1 hr, 2 hrs, and 8 hrs) against *E. coli* (left) and *S. aureus* (right). The CFU/mL values were calculated from counting the number of colonies on agar plates when different dilutions were plated.

All hydrogels in the study significantly reduced the bacteria population after one hour of treatment (Figure 28). The sample showing the least antibacterial activity against *E. coli*, **Gel-8-But**, was still able to reduce the number of bacteria by two orders of magnitude (from 10^8 to 10^6 CFU/ml) within one hour. **Gel-8-Hex** showed stronger bactericidal activity towards *E. coli*, with a reduction of approximately five orders of magnitude (from 10^9 to 10^4 CFU/ml). **Gel-8-Met** displayed the strongest antibacterial activity against *E. coli* of the three hydrogels, and was able to kill all the bacteria in the solution within 15 min. After eight hours of incubation with each type of hydrogel, no bacterial growth of *E. coli* was detected. The hydrogels also displayed bactericidal activity against *S. aureus*, but to a lesser degree compared to *E. coli*. Similarly, the **Gel-8-Met** displayed the strongest antibacterial activity, followed by **Gel-8-Hex** and then **Gel-8-But**. The most promising candidate, **Gel-8-Met**, reduced the bacteria count

from 10^4 to ~ 10 CFU/ml after 30min of incubation. The least active antibacterial gel, **Gel-8-But**, was able to reduce the *S. aureus* amount by about one order of magnitude within one hour. This gel was able to further reduce the bacteria count by another two orders of magnitude after eight hours. Control experiments were also performed for both bacteria without the presence of hydrogels, and the results showed that the bacteria population did not diminish over time.

When comparing the hydrogels from the previous chapter to the ones shown here, the materials prepared with the post-quaternization methodology exhibited less antimicrobial activities. For example, the hydrogels prepared using the post-quaternization method, were unable to completely eliminate *S. aureus* after an incubation period of 18 hours. On the other hand, the **Gel-8-Met** from this chapter successfully suppressed both bacteria (*S. aureus* and *E. coli*) within 30 minutes to <100 CFU/mL. Perhaps this perceived higher antimicrobial activity could be due to a possible difference in dispersion or quantity of quaternary amines present throughout the gels.

Some studies in the past have shown the killing efficiency increases with the longer alkyl chains. However, in our case here, the shorter the alkyl-chain displayed the highest antibacterial activity.¹⁰⁵ In our opinion, the higher antibacterial efficiency of **Gel-8-Met** could be due to higher solubility in aqueous media. This can then facilitate faster contact between the gels and bacteria, and thus enhances its antimicrobial efficiency.

In order to obtain another perspective on the antimicrobial mechanism, scanning electron microscopy (SEM) images were taken before and after treating the *E. coli* with the hydrogels. As shown in Figure 29, the surfaces of *E. coli* cells were highly distorted, which suggested that bacteria were killed via membrane disruption, or lysis.

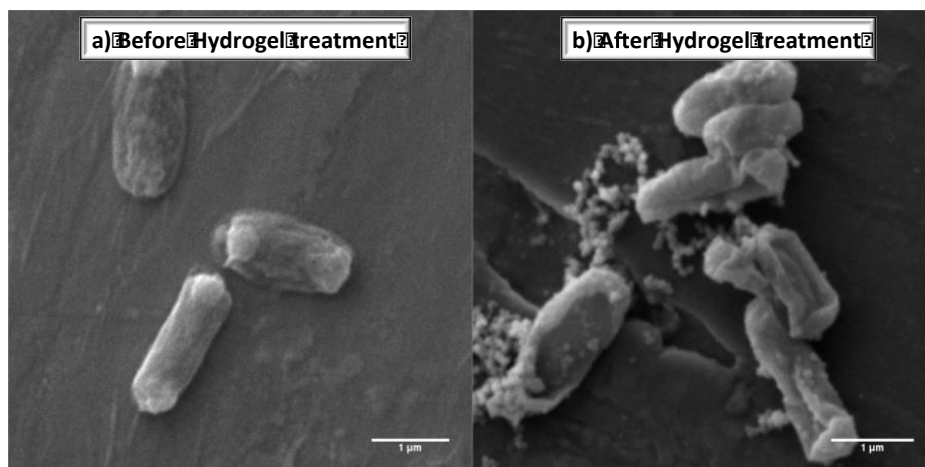


Figure 29. Scanning electron microscopy (SEM) images of *E. coli* were taken before (left) and after (right) eight hours of treatment with Gel-8-Met; scale bars corresponds to 1 µm. The micrograph after the hydrogel treatment suggests that the bacteria underwent membrane disruption.

In summary, polycarbonates bearing quaternary ammonium groups exhibited bactericidal activity towards *S. aureus* and *E. Coli*. The polycarbonate hydrogels derived from charged monomers showed very fast bactericidal activity and were able to eliminate much of the bacteria within eight hours of exposure. However, for these antimicrobial polymers to be useful, they must be selective in disrupting microbial cells over mammalian cells.

4.2.6. Hemolysis studies

Hemolysis studies were carried for the hydrogels (**Gel-8-Met**, **Gel-8-But** and **Gel-8-Hex**) and approximately 80 - 95% of the red blood cells underwent lysis within one hour of treatment. Clearly, the hydrogels prepared with the charged monomers exhibited much higher hemolysis than those prepared with the post-quaternization strategy. We believe the difference was due to the higher amounts

of quaternized ammonium functional groups present within the gels. This could then lead poorer selectivity and overall higher bactericidal and hemolysis activities. As a possible way to address the high hemolytic activity, we propose that new hydrogels could be prepared by using a mixture of both charged and non-charged monomers to reduce the amount of quaternary ammonium groups.

4.3. Conclusion

In this chapter, we report the synthesis and the ROP of cationic aliphatic cyclic carbonates with three different alkane pendant groups (*N*-methyl, *N*-butyl, and *N*-hexyl). The charged monomers showed very high reactivity rates and were even polymerizable in DMSO and catalyst free conditions that are generally unfavorable for ROP. Complete monomer conversions could be realized within a minute upon adding small amounts of DBU catalyst. A computational study showed that the cationic cyclic monomers were indeed orders of magnitude more reactive than their non-charged analogs, and this was in line with the observations from our experimental studies. Polycarbonate gels were also prepared from the aforementioned monomers, and their swelling and the biodegradability behaviors appeared to be highly dependent on the nature of the monomers' pendant group. Rheological measurements were also conducted and confirmed the successful crosslinking within the hydrogels. These hydrogels also demonstrated bactericidal activity against *E. coli* and *S. aureus* by disrupting the membrane of the bacteria. With further tailoring of the gel's composition, new hydrogels based on this system could be prepared for future works in biodegradable broad-spectrum antimicrobial research activities and applications.

4.4 Experimental part

Materials and equipment

^1H and ^{13}C NMR spectra were recorded with Bruker Avance DPX 300, Bruker Avance 400, or Bruker Avance 500 spectrometers. The NMR chemical shifts were reported as δ in parts per million (ppm) relative to the traces of non-deuterated solvent (eg. $\delta = 2.50$ ppm for d_6 -DMSO or $\delta = 7.26$ for CDCl_3). Data were reported as: chemical shift, multiplicity (s = singlet, d = doublet, t = triplet, m = multiplet, br = broad), coupling constants (J) given in Hertz (Hz), and integration. Fourier transform infrared - attenuated total reflection (FTIR-ATR) spectroscopy was performed with a ThermoFisher Nicolet 6700. Gel permeation chromatographies (GPC-SEC) with the charged polycarbonates were performed using an Agilent Technologies PL-GPC 50 Integrated GPC system, with a Shodex KD-806M column.

Triethylamine ($\geq 99\%$), benzyl alcohol (99.8%), *N*-methyldiethanolamine ($\geq 99\%$), *N*-butyldiethanolamine ($\geq 99\%$), diethanolamine ($\geq 98.5\%$), *N,N,N',N'*-tetrakis(2-hydroxyethyl)ethylenediamine (technical grade), and 1,8-diazabicyclo[5.4.0]undec-7-ene ($\geq 99\%$) were purchased from Sigma Aldrich and used as is. 1,8-Bis(dimethylamino)naphthalene (99%), 1-Bromohexane ($\geq 99\%$), potassium carbonate (ACS grade, anhydrous), sodium iodide ($\geq 99\%$), magnesium sulfate (97%), iodomethane (99%), acetonitrile (extra dry), DCM ($\geq 99.9\%$), and diethyl ether ($\geq 99.8\%$), acetone ($\geq 99.5\%$) THF ($\geq 99\%$), DMSO, and DMF (GPC grade) were purchased and used as is from Fisher Scientific. Triphosgene was purchased from TCI and used as is. Bis(pentafluorophenyl) carbonate (97%) was purchased from Manchester Organics and was used as is. Deuterated solvents including CDCl_3 and d_6 -DMSO were purchased from Deutero and were used as is.

Synthesis of *N*-Hexyldiethanolamine

N-Hexyldiethanolamine: A 500mL single neck round bottom flask was charged with 1-bromohexane (9.9g), diethanolamine (9.6g), potassium carbonate

(17.12g), sodium iodide (2g), acetonitrile (160mL), and a stir bar. The mixture was heated to reflux under N₂ for 18hrs. Afterwards, the mixture was filtered and concentrated under vacuum. The remaining material was dissolved in DCM (120mL) and then washed with deionized H₂O (3x120mL). The organic portion was then dried over MgSO₄, filtered, and concentrated under vacuum to give the product as a colorless oil (9.3g, 53% yield). ¹H NMR (400 MHz, CDCl₃) δ 3.63 (broad s, 2H), 3.55 (t, *J* = 5.2 Hz, 4H), 2.59 (t, *J* = 5.4 Hz, 4H), 2.46 (t, *J* = 7.6 Hz, 2H), 1.46 – 1.33 (m, 2H), 1.33 – 1.11 (m, 6H), 0.83 (t, *J* = 6.5 Hz, 3H). ¹³C NMR (101 MHz, CDCl₃) δ 59.58, 56.14, 54.88, 31.78, 27.07, 26.75, 22.65, 14.05.

Typical eight-membered cyclic carbonate synthesis

6-Methyl-1,3,6-dioxazocan-2-one (Non-charged N-8-C): A 1L single neck round bottom flask was charged with *N*-methyldiethanolamine (10.0g, 83.9mmol), triethylamine (17.4g, 167.8 mmol), THF (600mL), and a large oval stir bar. The mixture was then allowed to stir and cooled to -78°C using a liquid nitrogen/acetone bath. This was then followed by a dripwise addition of triphosgene (8.3g, 28.8mmol) in THF (100mL). Once all of the triphosgene has been added, the reaction was taken out of the liquid nitrogen/acetone bath and allowed to stir for an additional two hours at room temperature. The reaction mixture was then filtered to remove the triethylammonium chloride salt and concentrated under vacuum. Cold diethyl ether (500mL) was then added to help precipitate the remaining salts, which were then filtered again. The remaining filtrate was concentrated under vacuum to give the final product as a yellow oil (9.24g, 76% yield). ¹H NMR (500 MHz, DMSO): δ = 4.13 (t, CH₂, *J* = 5.3 Hz, 4H), 2.73 (t, CH₂, *J* = 5.3 Hz, 4H), 2.41 (s, CH₃, 3H). ¹³C NMR (101 MHz, DMSO): δ = 155.36 (C=O), 68.71 (CH₂), 55.64 (CH₂), 44.39 (CH₃).

6-Butyl-1,3,6-dioxazocan-2-one (Non-charged 8-But): Reddish yellow oil (13.8g, 88% yield). ¹H NMR (300 MHz, DMSO) δ 4.09 (t, *J* = 5.2 Hz, 4H), 2.73 (t, *J* = 5.3

Hz, 4H), 2.54 (t, $J = 7.1$ Hz, 4H), 1.43 – 1.30 (m, 2H), 1.30 – 1.15 (m, 2H), 0.86 (t, $J = 7.2$ Hz, 3H). ^{13}C NMR (101 MHz, DMSO) δ 155.32, 69.02, 56.15, 53.55, 29.19, 19.64, 13.84.

6-Hexyl-1,3,6-dioxazocan-2-one (Non-charged 8-Hex): Brownish oil (15.5g, 86% yield). ^1H NMR (300 MHz, DMSO) δ 4.08 (t, $J = 5.3$ Hz, 4H), 2.72 (t, $J = 5.3$ Hz, 4H), 2.58 – 2.44 (m, 2H), 1.36 (s, 2H), 1.23 (s, 6H), 0.86 (t, $J = 6.9$ Hz, 3H). ^{13}C NMR (101 MHz, DMSO) δ 155.29, 69.00, 56.45, 53.55, 31.21, 26.94, 26.11, 22.08, 13.84.

Quaternization of cyclic carbonates with iodomethane

6,6-Dimethyl-2-oxo-1,3,6-dioxazocan-6-ium iodide (8-Met): A 16mL vial was charged with 6-Methyl-1,3,6-dioxazocan-2-one (0.5g, 3.44mmol), ACN (2mL), and a stir bar. Iodomethane (0.585g, 4.134mmol) was then added dripwise and the reaction continued to stir for two hours at room temperature. The products were precipitated with ether and dried under vacuum. A fine white powdered product was collected (0.92g, 93% yield). ^1H NMR (300 MHz, DMSO) δ 4.62 (t, $J = 4.5$ Hz, 2H), 3.90 – 3.81 (m, 4H), 3.25 (s, 6H). ^{13}C NMR (75 MHz, DMSO) δ 153.26, 65.47, 64.72, 51.75.

6-Butyl-6-methyl-2-oxo-1,3,6-dioxazocan-6-ium iodide (8-But): Yellow solid (0.81g, 93% yield). ^1H NMR (400 MHz, DMSO) δ 4.62 (s, 4H), 3.91 – 3.77 (m, 4H), 3.54 – 3.47 (m, 2H), 3.19 (s, 3H), 1.76 – 1.65 (m, 2H), 1.33 (h, $J = 7.3$ Hz, 2H), 0.93 (t, $J = 7.3$ Hz, 3H). ^{13}C NMR (101 MHz, DMSO) δ 153.18, 64.62, 63.73, 63.53, 48.11, 23.50, 19.17, 13.44.

6-Hexyl-6-methyl-2-oxo-1,3,6-dioxazocan-6-ium iodide (8-Hex): Dark yellow solid (0.78g, 94% yield). ^1H NMR (400 MHz, DMSO) δ 4.73 – 4.54 (m, 4H), 3.93 – 3.77 (m, 4H), 3.56 – 3.46 (m, 2H), 3.19 (s, 3H), 1.79 – 1.62 (m, 2H), 1.35 – 1.21 (m,

6H), 0.86 (t, $J = 6.4$ Hz, 3H). ^{13}C NMR (101 MHz, DMSO) δ 153.17, 64.61, 63.89, 63.68, 30.52, 25.35, 21.76, 21.46, 13.76.

Synthesis of 6,6'-(ethane-1,2-diyl)bis(1,3,6-dioxazocan-2-one) (bis *N*-8-C)

Bis *N*-8-C: The same procedure was used and discussed in the previous chapter.

General procedure for homopolymerizing with charged cyclic carbonates

Monomer **8-Met** (574mg, 2mmol, 50 equiv.) and benzyl alcohol (4.33mg, 0.04mmol, 1 equiv.) were first dissolved in dried DMSO (1.5mL). Later, DBU (3.04mg, 0.02mmol) was added to the reaction. A ^1H NMR sample was made after one minute to confirm the complete conversion of the monomer to product. The crude polymer solution was precipitated in excess DCM and dried under vacuum to give a white powder (Yield: 0.41g, 71%).

General procedure for gel preparation with charged cyclic carbonates

A 12mL vial was charged with a stirbar, **8-Met** (0.632g, 2.2mmol), bis *N*-8-C (0.120g, 0.42mmol), and PEG₁₅₀₀ end capped diol (0.030g) were dissolved in 1mL of DMSO. Next, DBU (0.018g, 0.11mmol) was added into the reaction which was then heated to 50 °C for 10min. The contents of the vial was then poured out into silicone molds and allowed to cool to room temperature in N₂ atmosphere overnight. To remove the DMSO and catalysts, the gel was immersed in excess DCM for 1d at room temperature. Lastly, the gels were dried under vacuum to give a white opaque gel.

Rheology

Rheology measurements on the gels were conducted on Anton Paar Physica MCR 101 rheometer using oscillatory tests with parallel plate geometry. Angular

frequency sweeps from 0.0628 s^{-1} to 314 s^{-1} at constant strain amplitude ($\gamma = 1\%$) were applied at $25 \text{ }^\circ\text{C}$. Later, G' and G'' values were plotted versus frequency.

Swelling test

Dried pieces of gels ($\sim 100 \text{ mg}$) were immersed in deionized H_2O at room temperature. After a certain time, the gels were removed from the water and the excess water was gently removed from surface of the gel with a paper towel. The increase in mass was followed gravimetrically. The swelling degree (S_t) was calculated using the following formula:

$$S_t (\%) = \frac{m_t - m_0}{m_0} * 100$$

Where ' m_t ' is the mass of the gel after time t and ' m_0 ' is the initial mass of the dried gel.

Antibacterial assays.

Escherichia coli cells from C41 strain were grown overnight in Luria-Bertani (LB) media at 37°C and constant shaking of 200 rpm. Dry hydrogels were cut into 5 mm^2 squares, weighted to ensure the same amount of material for all the samples, and placed in 1.5 ml centrifuge tubes. The concentration of bacteria solution was adjusted with LB media to an O.D.=1 at 600 nm (Corresponding to approximately $2.4 \times 10^9 \text{ CFU/ml}$) in a Nanodrop One (ThermoScientific). Then 1 ml of bacteria solution was added to the tubes containing hydrogels and to a negative control tube without hydrogel. All tubes were incubated at room temperature with slow shaking (20 rpm), under those conditions no significant bacterial growth will occur during the experiment. At each time measured, $100 \text{ }\mu\text{l}$ samples were collected and serial dilutions were prepared with LB media before being plated on LB-agar plates. After overnight incubation at 37°C , the colony-forming units (CFU) on the plates of different dilutions were counted. The CFU/ml

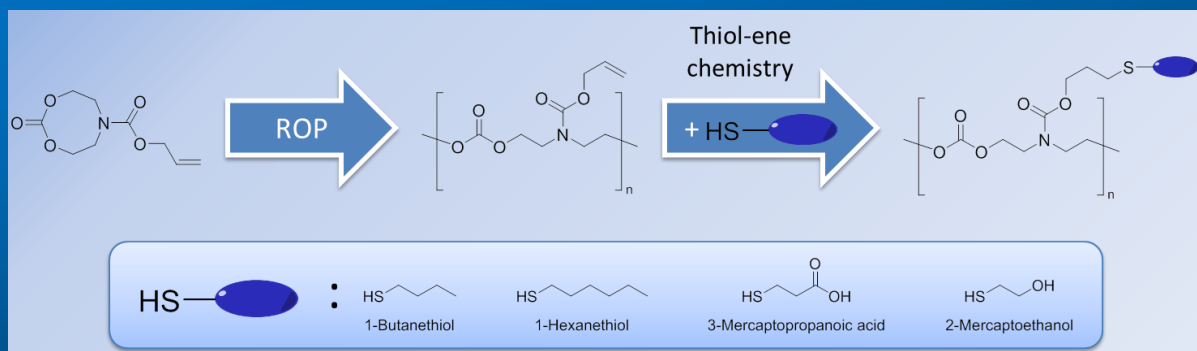
of the samples in the presence of the hydrogels were calculated from the CFU at different dilutions. Each test was carried out in three replicates.

In order to observe bacteria damage by SEM, *E. coli* bacterial cells control or treated with **Gel-8-Met** as described above were washed with PBS twice, and fixed with glutaraldehyde (GA) 2.5% (v/v in PBS) for two hours. After the samples were washed twice with PBS and re-suspended in water. The samples were diluted 10 times and a final volume of 2 μ l of each sample was deposited over a metallic cylinder for the metallization process with an Au-Pd alloy (60% Au, 40% Pd). Images were acquired using a JSM-6490LV SEM (JEOL, Japan) at 5kV.

Hemolysis assay

The hemolytic activity of the hydrogels over red blood cells was tested using rat red blood cells (rRBC) collected from the Animal Facility Unit of CIC BiomaGUNE (Spain). Red cells were washed four times in PBS by centrifugation at 2000 g for 10 minutes. The RBC solution was diluted in PBS to give a standardized absorbance value of 0.6 at 412 nm when diluted 1:100. Dry hydrogels were cut into 5 mm² squares, weighted to ensure the same amount of material for all the samples, and placed in 1.5 ml centrifuge tubes. 1.5 ml of rRBC solution was added to each tube, and at each incubation time 200 μ l of sample was collected. All samples were centrifuged 10 minutes at 2000 g and the supernatants were diluted 1:10 in PBS to measure the absorbance at 412 nm. As a positive control, using the same standard concentration, a 100 % hemolysis rRBC solution was lysed in water. As a negative control, a rRBC solution was treated without the hydrogels. The data was normalized using the positive control as 100% hemolysis.

Chapter 5



Synthesis, polymerization, and post-modification of allyl functional monomers

Chapter 5. Synthesis, polymerization, and post-modification of allyl functional monomers

5.1. Introduction

The success of applying polycarbonates in nanomedicine has been largely attributed to the facility of introducing desired functionalities along the polymers' backbone. This can easily be achieved by incorporating various functionalities at the cyclic carbonate monomer level before the ROP process. In this regard, significant advances in this manner have been developed and adopted. For example, preparation and polymerization of a broad selection of six membered cyclic carbonates have been extensively studied. A vast amount of these monomers are derivatives of 2,2-bis(hydroxymethyl)propionic acid (bis-MPA), which can be purchased very cheaply from many commercial resources and can be easily functionalized via its carboxylic acid group with alkyl halides.^{106–108}

However, it is important to note that not all pendant functional groups, such as alcohols and carboxylic acids, are compatible with organocatalyzed ROP conditions. In these cases, the functionalities must be incorporated into the polymer chain using highly efficient post-modification approaches.¹⁰⁹ A solution to this would be to first polymerize a monomer bearing a modifiable yet robust pendant group that can then be modified in a post-polymerization step. One such method to prepare functional polycarbonates using post-polymerization process was reported by Hedrick *et al.*¹⁰⁸ In their case, they utilized cyclic monomers with pentafluorophenyl activated ester pendant groups. These activated pendant groups would remain untouched during the acid catalyzed polymerization, but then were easily modified with amines and alcohols in high yields in a post-polymerization step. This approach however was limited by the monetary cost of bis(pentafluorophenyl) carbonate intermediate. Another approach is by preparing

and polymerizing cyclic carbonates bearing allyl pendant groups that could be readily modified with thiol-ene 'click' chemistry, as reported by Dove *et al.*¹⁰⁶ This particular approach remains one of the more dominant method of obtaining functional polycarbonates owing to its high conversions, selectivity, easiness to prepare, and fast reaction rates.¹¹⁰ In the works of Tempelaar *et al.*, they demonstrated allyl bearing polycarbonates could be readily prepared from ROP cyclic carbonates and later modified with a host of thiols.³⁴ In addition, amino acids (i.e., L-cysteine⁵⁸ and dopamine¹¹¹) have been successfully incorporated in a same manner onto polycarbonates for bio-applications.

To date, a significant number of publications related to ROP of cyclic carbonates have been devoted to six membered cyclic carbonates. In our previous works, we demonstrated the potential use of *N*-substituted eight membered cyclic carbonate monomers to obtain polyurethanes and antimicrobial polycarbonates. One of the key advantages of using the larger ring size is their enhanced reactivity over the smaller cyclic carbonates.¹¹² Similarly to bis-MPA starting material for the six membered cyclic carbonates, diethanolamines can be purchased in bulk at low costs and used as starting materials to prepare *N*-substituted eight membered cyclic carbonates. Moreover, they can also be easily modified with alkyl halides as shown by Venkataraman *et al.*⁸⁵ However, unlike the six membered cyclic carbonates, *N*-substituted eight membered cyclic carbonates bearing allyl functionalities enabling efficient thiol-ene post-polymerization modifications remains unexplored.^{39,40,113}

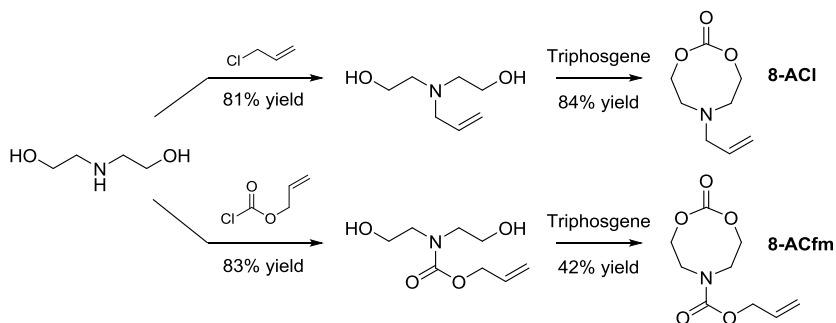
Our motivation for this chapter stems from the curiosity of bridging two ideas: (i) *N*-substituted eight membered cyclic carbonates and (ii) allyl functionalities and their modifications through thiol-ene chemistry. Our objectives were to synthesize a series of allyl bearing monomers based on diethanolamines, and then polymerize them via ROP facilitated by organocatalysts. In addition, we wanted

to assess the versatility of our monomers by preparing copolymers with other cyclic monomers. And most importantly, we wanted to perform thiol-ene reactions with a variety of thiols to functionalize the allyl pendant groups. The results from this work would help to expand the versatility of the polycarbonate platform.

5.2. Results and Discussion

5.2.1. Monomer preparation

Herein, we envisioned a simple two-step approach to obtain different allyl bearing *N*-substituted eight membered cyclic carbonates (Scheme 10). Previously, Venkataraman and Waymouth *et al.*⁸⁵ observed a considerable increase in reactivity of cyclic carbonates whenever they bore a carbamate pendant groups. With this in mind, two allyl bearing *N*-substituted eight membered cyclic carbonates were prepared, one with carbamate pendant groups and the other without. In the first step, we reacted diethanolamine with allyl chloride and allyl chloroformate to afford allyl bearing diols in excellent yields of ~80%. In the second step, the previously prepared diols were ring closed with triphosgene in the presence of triethylamine to afford two allyl bearing cyclic carbonates, **8-ACI** and **8-ACfm**, in yields of 84 and 42% respectively. We suspect that the difference in yield was attributed to the large reactivity difference between these two cyclic carbonates, which will be expanded upon in the following section.



Scheme 10. Two-step synthesis approach to obtain allyl bearing eight membered cyclic carbonates.

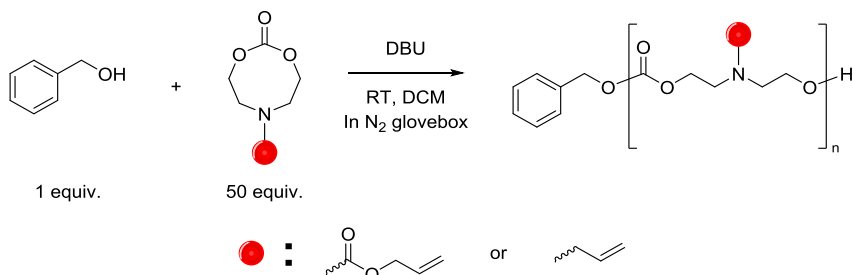
The reactions towards **8-ACl** and **8-ACfm** were followed with NMR (^1H and ^{13}C) and FTIR-ATR spectroscopy. In the case of **8-ACl**, the methylene protons between the amine and alcohols shifted from 2.50 ppm (N-CH₂-) and 3.42 ppm (-CH₂-OH) to 2.75 ppm and 4.10 ppm respectively. The protons associated with the allyl group were situated at 5.15 ppm (=CH₂) and 5.78 ppm (CH=C), and did not shift after the ring closure procedure. By ^{13}C NMR, we could clearly observe the formation of the carbonate by the carbonyl signal at 155.48 ppm. Furthermore, we followed the methylene carbons which shifted from 59.17 ppm (N-CH₂-) and 56.14 ppm (-CH₂-OH) to 53.07 ppm and 68.91 ppm respectively. By FTIR-ATR, we were able to realize the formation of the carbonate group at 1741 cm⁻¹ (C=O, stretch), and the presence of the allyl group at 3076 cm⁻¹ (=C-H, stretch) and 1648 cm⁻¹ (C=C, stretch).

For **8-ACfm**, the methylene protons between the amine and alcohols shifted from 3.29 ppm (N-CH₂-) and 3.49 ppm (-CH₂-OH) to 2.76 ppm and 4.09 ppm respectively. The protons associated with the allyl were situated at 5.00 ppm (=CH₂) and 5.78 ppm (CH=C) and did not shift after the ring closure procedure, as with the case of **8-ACl**. By ^{13}C NMR, we could clearly observe the formation of the carbonate by the carbonyl signal at 155.54 ppm and the carbamate at 155.01 ppm. Furthermore, we followed the methylene carbons which shifted from 50.25

ppm (N-CH_2 -) and 59.11 ppm ($-\text{CH}_2\text{-OH}$) to 47.91 ppm and 68.50 ppm respectively. By FTIR-ATR, we were able to realize the formation of the carbonate at 1752 cm^{-1} (C=O , stretch), the carbamate at 1695 cm^{-1} (C=O , stretch), and the allyl at 3076 cm^{-1} ($=\text{C-H}$, stretch) and 1648 cm^{-1} (C=C , stretch).

5.2.2. Model polymerizations with allyl bearing monomers.

For our model polymerizations with **8-ACI** and **8-ACfm**, we elected to use the organocatalyst 1,8-diazabicyclo[5.4.0]undec-7-ene (DBU) because of previously reported efficacy in polymerizing *N*-substituted eight membered cyclic carbonates. A brief kinetics study was conducted with both monomers to assess their ROP behaviors. For each monomer, polymerization was targeted for a degree of polymerization (DP) of 50 from the monomer to initiator (benzyl alcohol, BnOH) ratio in DCM, as shown in Scheme 11.



Scheme 11. Typical ROP of allyl bearing eight membered cyclic carbonates, targeting a degree of polymerization of 50.

Initially, both monomers were treated with 10 mol% of DBU and we followed the monomer conversions by using relative integral values from ^1H NMR spectroscopy. The polymerization and conversion of **8-ACfm** was monitored by following the methylene protons ($-\text{CH}_2$ -) adjacent to the carbonyl of the carbonate. In this sense, the triplet at 4.33 ppm (monomer) disappeared as the

reaction progressed, and a new broader triplet at 4.17 ppm (polymer) appeared.⁴ Most notably, we observed a large difference in reactivity between monomers **8-ACI** and **8-ACfm**, where **8-ACfm** was able to achieve 97% conversion in only 10 minutes. On the other hand, **8-ACI** only achieved 14% conversion after one hour reaction time (Figure 30).

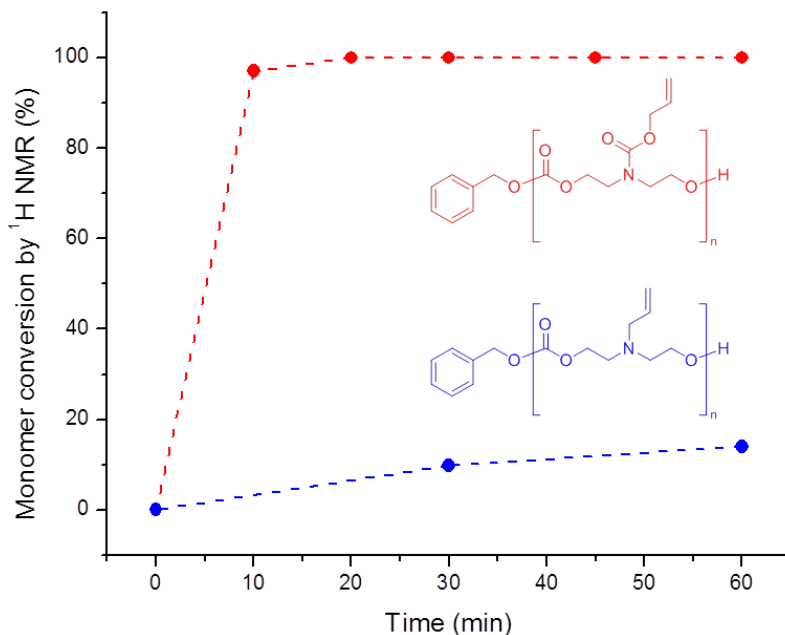


Figure 30. Model polymerizations were carried out with monomers **8-ACfm** (red) and **8-ACI** (blue) with DBU (10 mol%) at room temperature. The monomer **8-ACfm** was able to reach full conversion within 10 minutes, whereas **8-ACI** only achieved 14% conversion after one hour.

We believe that this large discrepancy in reactivity is related with the *N*-substituent pendant group of the cyclic carbonate. Previously, Venkataraman *et al.*⁸⁵ synthesized and polymerized numerous *N*-substituted eight membered cyclic carbonates based on diethanolamines with different pendant groups. In

⁴ ¹H NMR was performed in and referenced to d₆-DMSO.

fact, the monomers with carbamate pendant groups reacted much faster than the others without it. In our previous work, charged eight membered cyclic carbonates were synthesized by quaternizing the tertiary amine within the cyclic carbonate with iodomethane. We believe that the positively charged nitrogen would exert a strong inductive effect across the carbon chain, and thereby making the carbonates' carbonyl group highly electrophilic. As a result, the monomers were shown to be much more susceptible to ring opening and the charged monomers were estimated to be 10^4 more reactive than their non-charged analogs.³⁹ We suspect that the high reactivity of **8-ACfm** can be reasoned for in a similar manner as the charged cyclic carbonates. In the case of **8-ACfm**, the carbonyl of the carbamate could function as an electron sink, and thereby pulling the lone pair electrons away from the nitrogen and making it more positively charged. Perhaps in this way, the slightly positive nitrogen could have an inductive effect across the cyclic carbonate and make the carbonates' carbonyl group more electrophilic and easier to ring open.

In summary, we successfully polymerized allyl bearing eight membered cyclic carbonates using organocatalysts. Although the reactions yields for the preparation of **8-ACfm** were less favorable than **8-ACI**, this monomer was more suitable for ROP because of its high reactivity.

5.2.3. Exploration of the polymerization conditions with **8-ACfm**.

The ROP behavior of **8-ACfm** was explored further in a systematic fashion by reducing the catalyst loading by a factor of four (DBU, 2.5 mol%). In doing so, we were still able to observe high monomer conversions ($\geq 97\%$) after one hour of reaction time at room temperature (Table 6). The high reactivity of **8-ACfm** was quite exceptional, in particular when compared to the well-studied allyl bearing six membered cyclic carbonate, 5-methyl-5-allyloxycarbonyl-1,3-dioxan-2-one (MAC). For example, Tempelaar *et al.* reported 90% monomer conversion after

four hours when polymerizing MAC with 5 mol% DBU at room temperature.³⁴ Also worth mentioning, the resulting polymer was quite dispersed (ρ : 1.8) and the use of a dual organocatalyst system was implemented to yield more monodisperse polymers (ρ : 1.12). However, with the dual catalyst method, they had to use much more catalyst and longer reaction times (up to 768 hours) to obtain appreciable monomer conversion (>90%).

Initiator versatility was investigated by initiating the polymerization with the commonly used macroinitiator polyethylene glycol (PEG_{8k}, M_n : 8,000 Da). The reaction reached full conversion within an hour and was precipitated in THF. The resulting polymer was characterized by SEC, and showed a M_n value of 14,400 Da (ρ : 1.2). As a reference, the SEC of the macroinitiator PEG_{8k} showed a M_n of 11,500 Da (ρ : 1.1). Based on this, we can confirm the addition of polycarbonate linkages onto the PEG_{8k} macroinitiator.

Additional polymerizations were carried out with the monomer **8-ACfm** using range of DPs (10, 50, 100, and 200), see Table 6. Between DP10 and DP50, we observed a logical and expected increase of M_n (1,700 to 6,100 Da) while maintaining low dispersities (ρ : 1.1 to 1.2). However, as polymerizations exceeded DP50, the observed molecular weights with SEC and our anticipated values were largely inconsistent with each other. Moreover, these molecular weights were much lower than those calculated by end group analysis ($M_{n,NMR}$). This data suggested that there are competitive pathways for enchainment, which became more evident as we increased the DP. It appears that in our system, the DBU catalyst can mediate the ring-opening polymerization by two competitive mechanisms to afford a mixture of linear and cyclic polymer chains. The low molecular weights (M_n) observed by SEC were consistent with the formation of a mixture of linear and cyclic chains. In this case, the ¹H NMR end group analysis would overestimate the molecular weights ($M_{n,NMR}$) because only a fraction of the

chains are linear with benzyl alcohol end groups. This phenomenon prompted us to use MALDI-ToF, an alternative polymerization characterization technique, to help us to confirm the presence of cyclic structures. As expected, MALDI-ToF characterization of polymer **2** showed a mixture of linear and cyclic chains (Figure 31). For the cyclic polymers, their lack of propagating ends prevents further addition of monomers, thus stunting the growth of the polymer chain. We believe that the polymerization initially proceeds through the benzyl alcohol initiator to afford linear polycarbonate chains. The cyclic polymer structure shouldn't come as a complete surprise, in fact, cyclic polycarbonates have been intentionally prepared by Chang *et al.*¹¹⁴ via zwitterionic ROP of *N*-substituted eight membered cyclic carbonates.

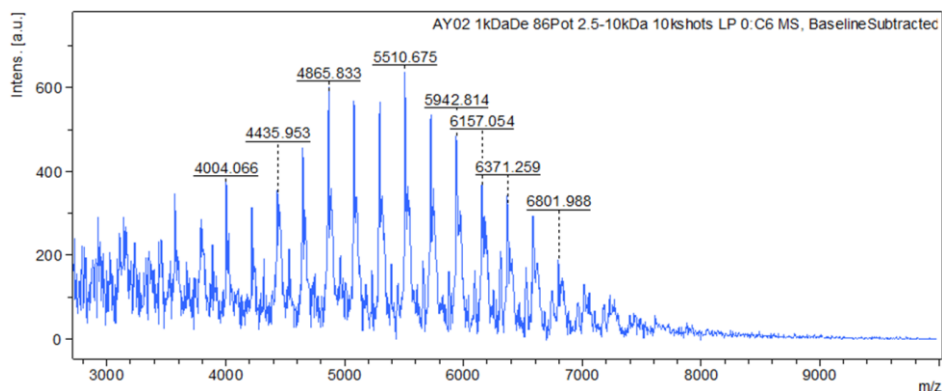


Figure 31. MALDI-TOF of the ROP of Polymer **2** (DP50). Here we observed signals that corresponded to both linear and cyclic polycarbonates.

Table 6. Polymerization conditions and SEC results from ROP of 8-ACfm and 8-ACI

Polym.	Initiator (I)	Monomer (M)	Catalyst (C)	[I] ₀ : [M] ₀ : [C]	Time	% Conv. ^a	M _{n,NMR} (Da) ^a	M _{n,SEC} (Da) ^b	Đ ^b
1	BnOH	8-ACfm	DBU	1:10:1	1 h	≥ 97	2,430	1,700	1.2
2	BnOH	8-ACfm	DBU	1:50:5	1 h	≥ 97	8,770	6,100	1.1
3	BnOH	8-ACfm	DBU	1:100:10	1 h	≥ 97	15,140	6,000	1.2
4	BnOH	8-ACfm	DBU	1:200:20	1 h	≥ 97	37,290	7,000	1.2
5	PEG _{8k}	8-ACfm	DBU	1:50:5	1 h	≥ 97	18,760	14,400	1.2
6	BnOH	8-ACI	DBU	1:50:5	2 w	81	6,390	2,600	1.3

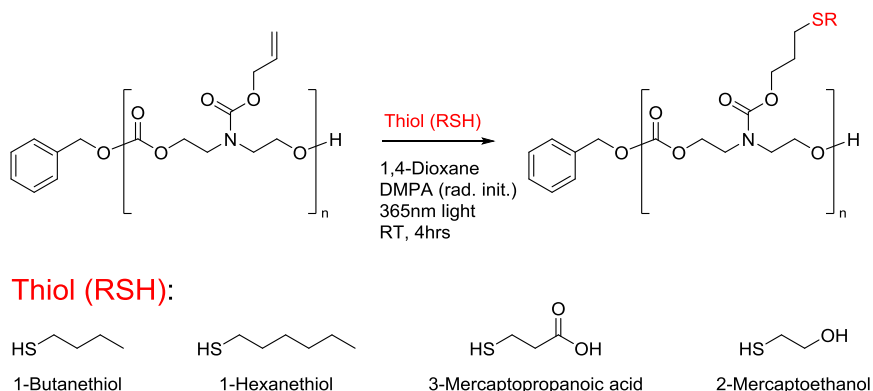
All reactions were conducted in DCM at room temperature inside a N₂ filled glovebox. ^aConversion was determined by ¹H NMR spectroscopy. ^bMolecular weight (M_n) and polydispersity (Đ) were characterized using size exclusion chromatography SEC in THF, the reported numbers are in reference to polystyrene standards.

Here we report the polymerization of **8-ACfm**, and we observed the plateau of M_n with increasing DP. We attributed this phenomenon to the formation cyclic polycarbonates during the ROP process. It appeared that we were unable to selectively produce linear polycarbonates, and we believe this can be mediated through a more selective catalyst system, such as the one reported by Waymouth *et al.*^{115,116}

5.2.4. Photo-induced thiol-ene reactions with allyl bearing polycarbonates

Although the polymerizations were giving a mixture of linear and cyclic structures, the main objective of this paper was to assess the polymerizability of the monomers while maintaining its allyl functionality for post-polymerization functionalization via thiol-ene chemistry. In this sense, we first obtained the allyl bearing polymer **2**, and we were interested in modifying this polymer with four different thiols (i.e., 1-butanethiol, 1-hexanethiol, 3-mercaptopropionic acid, and

2-mercaptoethanol), as seen in Scheme 12. The thiol-ene reactions were carried out at room temperature in 1,4-dioxane and with 2,2-dimethoxy-2-phenylacetophenone (DMPA), a commercially available UV activated radical initiator. An excess ratio of 10 equivalence of thiol per allyl group was used to minimize the cross-linking between allyl groups; in doing so, this will help to preserve the monomodal and narrow SEC distribution traces.³⁴



Scheme 12. Radical addition of thiols onto polycarbonate based on 8-ACfm.

As we performed the thiol-ene reactions with 1-butanethiol, we were able to follow the reactions with ¹H NMR. Initially, we observed multiplets attributed to CH_{allyl} and CH_{2,allyl} at 6.02-5.83 ppm and 5.36-5.16 ppm respectively. As the reactions proceeded, we would observe their disappearances and the appearance of several new peaks (Figure 32). Most notably, the methylene protons between the carbamate and allyl shifted from 4.59 ppm (double triplet) to 4.18 ppm (triplet). Also, peaks attributed to the reacted 1-butanethiol could be observed at 2.51, 1.56, 1.41, and 0.92 ppm. Likewise in ¹³CNMR, we observed the disappearance of CH_{allyl} and CH_{2,allyl} at 132.72 and 117.90 ppm and the appearance of peaks at 31.85, 31.70, 22.02, and 13.74 ppm, which indicated the successful addition of 1-butanethiol. By FTIR-ATR, we noted the absence of C=C stretching at 1648 cm⁻¹ after thiol-ene reaction, which helped to confirm the consumption of the allyl groups. Similar trends were observed for all the thiols: 1-

hexanethiol (**2b**), 3-mercaptopropanoic acid (**2c**), and 2-mercaptoethanol (**2d**). Yield of modifications were calculated by relative integral values from ^1H NMR of the polycarbonate backbone to the added functional groups, and we observed high efficiency of functionalization ($\geq 90\%$) for all cases (Table 7). Also to note, the successful addition of alcohol and carboxylic acid functional groups was achieved, and this could not be obtained by standard ROP of cyclic carbonates bearing these functionalities.

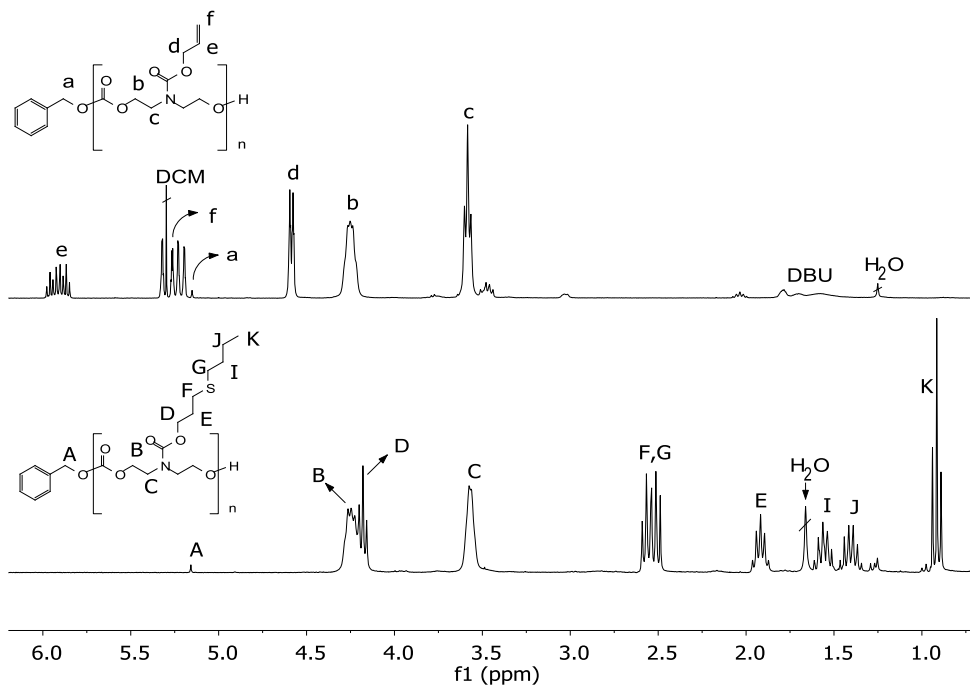


Figure 32. ^1H NMR in CDCl_3 of polymer 2 in its crude (above) and after the radical thiol-ene functionalization with 1-butanethiol (below).

Size exclusion chromatography was also performed for each of the thiol-modified polymers (Table 7), and we observed an increase in M_n compared to the 'virgin' polymer (**2**) in each case. Regarding the polymers modified with 1-butanethiol (**2a**) and 1-hexanethiol (**2b**), we expected and observed an increase in M_n as the

alkyl chain extended from butyl to hexyl. Lastly, polydispersity values remained relatively low and similar to the starting polymer; this can be interpreted as an absence or minimal cross linking amongst allyl groups.

Table 7. Post-polymerization radical thiol-ene functionalization of polycarbonates.

Polymer	Thiol	Yield of modification	$M_{n,SEC}$ (Da)	\bar{D}
2	(none)	-	6,100	1.1
2a	1-butanethiol	95%	8,300	1.2
2b	1-hexanethiol	92%	13,000	1.1
2c	3-mercaptopropionic acid	≥97%	7,800	1.1
2d	2-mercaptoethanol	≥97%	6,500	1.2

The functionalization of allyl bearing polycarbonates using thiol-ene chemistry was demonstrated using a variety of thiols, including ones that bearing alcohol and carboxylic acid groups that are known to be incompatible with standard ROP conditions. The success in selectively adding these thiols were reflected in increased M_n and significant shifts in the ^1H and ^{13}C NMR. Although we worked with the photoinitiator DMPA, we are optimistic that the same results could be achieved using AIBN, a thermal initiator. Next, we then turned our attention to producing copolymers with our allyl bearing cyclic carbonate monomer.

5.2.5. Exploration of copolymerization

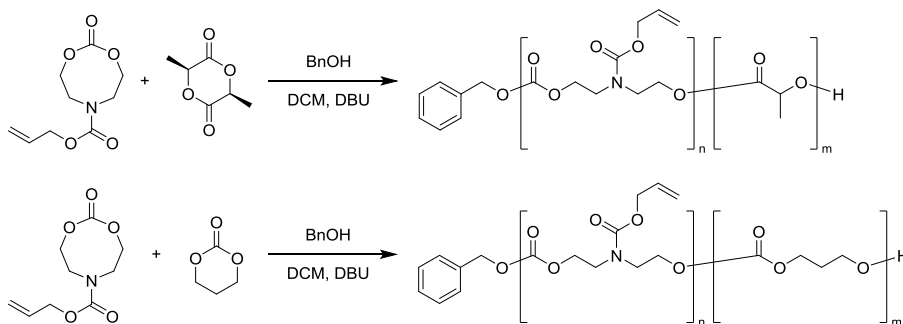
One of the main advantages of **8-ACfm** in comparison to the six membered cyclic carbonates, is its superior polymerization kinetics which will allow for the copolymerization with other cyclic monomers in a reasonable amount of time. In order to investigate the versatility of **8-ACfm**, the *N*-substituted monomer was copolymerized with the commercially available L-Lactide and the well-studied TMC under similar ROP conditions used previously (Table 8, Figure 33, and Scheme 13). In each of the cases, the **8-ACfm** monomer obtained conversions of ≥97% within one hour. The monomer L-Lactide in polymer **7** displayed similar

fast reactivity rates and also obtained high conversions after one hour. For trimethylene carbonate, or TMC, in polymer **8** we anticipated longer reaction times would be necessary to achieve similar conversions based on the previous study we performed.¹¹² As expected, a reaction time of 24 hours was necessary to obtain ~90% conversion of the TMC monomer. Monomodal distributions were observed for polymers **7** and **8** by SEC with M_n values of 14,400 Da (δ : 1.4) and 5,100 Da (δ : 1.3), respectively.

Table 8. Copolymerization of with 8-ACfm to access functional copolymers

Polym.	Mon. (M1)	Mon. (M2)	[I] ₀ : [M1] ₀ : [M2] ₀ : [C]	Time	Conv. % ^a (M1)	Conv. % (M2) ^a	M_n (Da) ^b	δ ^b
7	8-ACfm	L-Lactide	1:25:25:5	1 h	≥97	≥97	11,200	1.4
8	8-ACfm	TMC	1:25:25:5	1 d	≥97	93	5,100	1.3

Both polymerizations utilized BnOH as an initiator (I) and DBU as the catalyst (C).



Scheme 13. Here we show the copolymerization of 8-ACfm with L-Lactide (above) and TMC (below).

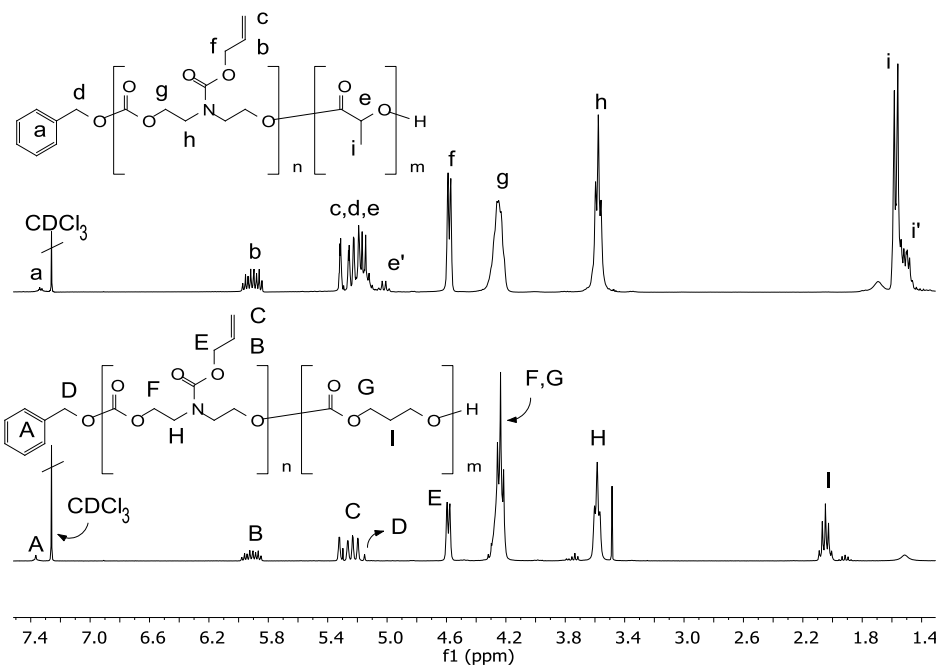


Figure 33. Here we show the ^1H NMRs of the two copolymers in CDCl_3 and their corresponding proton assignments; the copolymers with L-Lactide (above, polymer 7) and TMC (below, polymer 8).

To assess the fidelity of the allyl pendant groups for the prepared copolymers, thiol-ene reactions with 1-butanethiol were performed for polymers 7 and 8 to yield polymers 7a and 8a (Table 9). Reactions were carried in a similar fashion as previously reported, and an excess of thiol to allyl (10:1) ratio was used. Characterization by SEC showed each of the copolymers shifting to higher M_n upon the addition of 1-butanethiol. Furthermore, the modified copolymers maintained similar polydispersity values prior to the thiol-ene reactions. The successful addition of thiols was also evident by peak shifts in the ^1H NMRs (Figure 34).

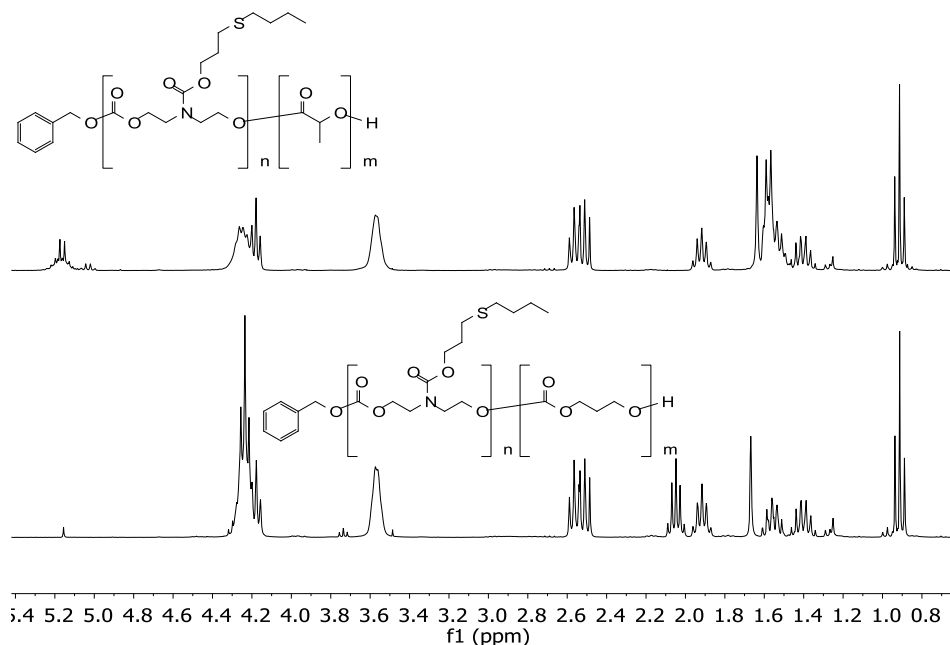


Figure 34. ^1H NMR of Polymer 7a (top) and 8a (bottom) in CDCl_3 after thiol-ene modification with 1-butanethiol.

Table 9. Post-polymerization radical thiol-ene functionalization with 1-butanethiol of copolymers

Polymer	Thiol	$M_{n,SEC}$ (Da)	\bar{D}
7	(none)	11,200	1.4
7a	1-butanethiol	13,400	1.6
8	(none)	5,100	1.3
8a	1-butanethiol	7,200	1.4

The extraordinary reactivity of **8-ACfm** was indeed observed in both copolymerizations, and this can be highly advantageous to produce randomly dispersed allyl functionalities throughout the polymer chains. Indeed, this will allow for the incorporation of various functionalities in conventional polymers, such as: poly(lactide) or poly(trimethylenecarbonate). In doing so, this could

enable the engineering and preparation of new polymers to suit various applications.

5.3. Conclusions

In conclusion, we report the preparation of two allyl functionalized eight membered cyclic carbonates based on diethanolamines. Our kinetic studies revealed the superior reactivity of **8-ACfm** over **8-ACI**, and it was able to obtain high conversions after one hour despite the low organocatalyst loading of 2.5 mol%. Homopolymers with **8-ACfm** were also prepared and a MALDI-ToF characterization confirmed the presence of linear and cyclic polycarbonates. Such information could to explain the difficulty in obtaining M_n beyond ~6000 Da. Nonetheless, we successfully functionalized our homopolymers with four different thiols and tracked their changes with NMR, SEC, and FTIR. Finally, **8-ACfm** was copolymerized via ROP along with L-Lactide and TMC, the resulting copolymers were functionalized with thiol-ene chemistry with similar success. The facile and versatility of the *N*-substituted eight membered cyclic carbonate provides an attractive platform to produce tailorable biodegradable metal-free aliphatic polycarbonates, which could be of great interest to the biomedical field.

5.4. Experimental section

Materials and equipment

^1H and ^{13}C NMR spectra were recorded with Bruker Avance DPX 300, Bruker FourierTM 300, and Bruker Avance 400 spectrometers. The NMR chemical shifts were reported as δ in parts per million (ppm) relative to the traces of non-deuterated solvent (eg. $\delta = 2.50$ ppm for d_6 -DMSO or $\delta = 7.26$ for CDCl_3). Fourier transform infrared - attenuated total reflection (FTIR-ATR) spectroscopy was performed with a Bruker Alpha. Gel permeation chromatography size exclusion chromatography (SEC) was performed on a system consisting of a Shimadzu

LC-20A pump, Waters 717 autosampler, Waters 2410 differential refractometer, and three columns in series (Styragel HR2, HR4 and HR6). The SEC system ran on THF (HPLC grade) at 35 °C using a flow rate of 1 ml.min⁻¹ and was calibrated using polystyrene standards ranging from 595 to 3.95x10⁶ Da. All SEC samples were diluted to 5mg/mL, filtered with 0.45 micron PTFE filter, and lastly toluene was added as a flow marker.

Triethylamine (≥99%), allyl chloride (98%), benzyl alcohol (99.8%), benzoic acid (>99.5%), diethanolamine (≥98.5%), 2,2'-azobis(2-methylpropionitrile) (98%), 2,2-dimethoxy-2-phenylacetophenone (99%), 1,5,7-triazabicyclo[4.4.0]dec-5-ene (98%), and 1,8-diazabicyclo[5.4.0]undec-7-ene (≥99%) were purchased from Sigma Aldrich and used as is. Allyl chloroformate (97%), potassium carbonate (ACS grade, anhydrous), potassium iodide (≥99%), 1-butanethiol (>99%), 3-mercaptopropionic acid (99%), and sodium sulfate (97%) were purchased and used as is from Fisher Scientific. Triphosgene (>98%), 1-hexanethiol (>96%), and 2-mercaptoethanol (>98%) were purchased from TCI and used as is. Analytical grade solvents were purchased and used as is from Fisher Scientific. For solvents used within the glovebox, extra dried solvents were purchased from Fisher Scientific and stored over molecular sieves. Deuterated solvents were purchased from Deutero and were used as is.

Methods and procedures

Synthesis of Allyl bis(2-hydroxyethyl)carbamate (DEA-AllylCfm)

A 1 L round-bottom flask was charged with a magnetic stir bar, diethanolamine (1.1 equiv., 0.11 mol, 11.6 g), potassium carbonate (2.1 equiv. 0.21 mol, 29 g), deionized water (260 mL), and THF (140 mL). The reaction mixture was stirred for 30 min in an ice bath. Afterwards, allyl chloroformate (1 equiv., 0.1 mol, 10.6 mL) was added in one-shot directly into the reaction mixture. The reaction was kept in the ice bath for two hours stirring, and then taken out to stir at room

temperature overnight. The product was extracted in ethyl acetate (3x300 mL) and the organic fraction was dried over NaSO₄ and later concentrated under vacuum. The product was a colorless viscous liquid (15.7 g, 83% yield). ¹H NMR (300 MHz, CDCl₃) δ 5.93 (ddt, *J* = 17.2, 10.9, 5.6 Hz, 1H), 5.38 – 5.14 (m, 2H), 4.60 (dt, *J* = 5.6, 1.4 Hz, 2H), 3.83 (broad s, 4H), 3.50 (t, *J* = 4.9 Hz, 4H). ¹H NMR (300 MHz, DMSO) δ 5.91 (ddt, *J* = 17.3, 10.4, 5.1 Hz, 1H), 5.34 – 5.13 (m, 2H), 4.72 (dt, *J* = 11.2, 5.4 Hz, 2H), 4.50 (dt, *J* = 5.1, 1.6 Hz, 2H), 3.49 (q, *J* = 6.0 Hz, 4H), 3.29 (s, 4H). ¹³C NMR (101 MHz, DMSO) δ 155.20, 133.60, 116.67, 64.94, 59.11 (d, *J* = 43.2 Hz), 50.25 (d, *J* = 51.0 Hz). FTIR-ATR: 3376cm⁻¹ (O-H, stretch), 1671cm⁻¹ (C=O, stretch), 1648cm⁻¹ (C=C, stretch).

Synthesis of 2,2'-(Allylazanediyl)bis(ethan-1-ol) (DEA-AllylCl)

A 500 mL round-bottom flask was charged with a magnetic stir bar, diethanolamine (1.6 equiv., 0.183 mol, 19.2 g), potassium carbonate (2.2 equiv. 0.248 mol, 34.24 g), potassium iodide (4 g), allyl chloride (1 equiv., 0.113 mol, 8.65 g), and ACN (320 mL). The reaction mixture was heated and stirred for 20 hr in an oil bath at 40 °C. Afterwards, the stir bar was removed and the reaction was concentrated under vacuum. The residues were dissolved in 100mL of brine and washed with chloroform (3x300 mL). The organic portion was collected and dried over NaSO₄. The mixture was filtered and then concentrated under vacuum to give the final product as a yellowish viscous liquid (13.29 g, 81% yield). ¹H NMR (300 MHz, DMSO) δ 5.82 (ddt, *J* = 17.3, 10.1, 6.3 Hz, 1H), 5.23 – 5.04 (m, 2H), 4.32 (t, *J* = 5.5 Hz, 2H), 3.42 (td, *J* = 6.3, 5.4 Hz, 4H), 3.12 (dt, *J* = 6.4, 1.4 Hz, 2H), 2.50 (t, *J* = 6.4 Hz, 4H). ¹³C NMR (101 MHz, DMSO) δ 136.33, 116.83, 59.17, 57.74, 56.14, 39.52. FTIR-ATR: 3337cm⁻¹ (O-H, stretch), 3075 (=C-H, stretch), 1642cm⁻¹ (C=C, stretch).

Synthesis of Allyl 2-oxo-1,3,6-dioxazocane-6-carboxylate (8-ACfm)

A 1 L round-bottom flask was charged with a stir bar, DEA-AllylCfm (1 equiv., 41.96 mmol, 7.94 g), triethylamine (2.6 equiv. 108 mmol, 15 mL), and 300mL of THF. An additional funnel was affixed to the round bottom flask and charged with a solution of triphosgene (0.42 equiv., 17.5 mmol, 5.19 g) in 50mL of THF. The setup was then placed in a liquid nitrogen and acetone bath, and the triphosgene solution was added dropwise. A white precipitate (triethylamine hydrochloride) was immediately formed upon the addition of the triphosgene. After the addition of triphosgene was completed, the reaction mixture was taken out of its liquid nitrogen-acetone bath and allowed to stir at room temperature for an additional two hours. The precipitated triethylamine hydrochloride salt was filtered away and the remaining solution was concentrated under vacuum to afford a reddish oil. This oil was then purified via flash chromatography over silica gel in an eluent consisting of DCM:EtOAc (7:3, v/v) to give the final product as a pale yellow oil (3.76 g, 42% yield). ^1H NMR (300 MHz, DMSO) δ 5.90 (ddt, $J = 17.3, 10.4, 5.1$ Hz, 1H), 5.36 – 5.13 (m, 2H), 4.54 (dt, $J = 5.1, 1.6$ Hz, 2H), 4.33 (t, $J = 4.4$ Hz, 4H), 3.58 (t, $J = 4.5$ Hz, 4H). ^{13}C NMR (101 MHz, DMSO) δ 155.54 , 155.01 , 133.04 , 116.98 , 68.50 (d, $J = 98.9$ Hz), 65.68 , 47.91 (d, $J = 20.6$ Hz). FTIR-ATR: 3076 (=C-H, stretch), 1752 cm^{-1} (C=O_{carbonate}, stretch), 1695 cm^{-1} (C=O_{carbamate}, stretch), 1648 cm^{-1} (C=C, stretch).

Synthesis of 6-Allyl-1,3,6-dioxazocan-2-one (8-ACI)

A 1 L round-bottom flask was charged with a stir bar, DEA-AllylCl (1 equiv., 41.96 mmol, 6.09 g), triethylamine (2 equiv. 83.9 mmol, 12 mL), and 300mL of THF. An additional funnel was affixed to the round bottom flask and charged with a solution of triphosgene (0.33 equiv., 14 mmol, 4.15 g) in 50mL of THF. The setup was then placed in a liquid nitrogen and acetone bath, and the triphosgene solution was added dropwise. A white precipitate (triethylamine hydrochloride) was immediately formed upon the addition of the triphosgene. After the addition of triphosgene was completed, the reaction mixture was taken out of its liquid

nitrogen-acetone bath and allowed to stir at room temperature for an additional two hours. The precipitated triethylamine hydrochloride salt was filtered away and the remaining solution was concentrated under vacuum to afford a pinkish oil. This oil was then purified via flash chromatography over silica gel in an eluent consisting of DCM:EtOAc (1:1, v/v) to give the final product as a pale yellow oil (6.07 g, 84.5% yield). ^1H NMR (300 MHz, DMSO) δ 5.78 (ddt, $J = 16.6, 11.2, 6.2$ Hz, 1H), 5.26 – 5.04 (m, 2H), 4.10 (t, $J = 5.2$ Hz, 4H), 3.19 (d, $J = 6.1$ Hz, 2H), 2.75 (t, $J = 5.2$ Hz, 4H). ^{13}C NMR (101 MHz, DMSO) δ 155.48, 135.26, 117.46, 68.91, 58.94, 53.07, 39.52. FTIR-ATR: 3076 (=C-H, stretch), 1741 cm^{-1} (C=O, stretch), 1648 cm^{-1} (C=C, stretch).

Homopolymerization of 8-ACfm (polymer **2**)

All polymerizations were carried out in a nitrogen filled glovebox at 25°C and the starting materials were dried under vacuum overnight. A 16mL vial was charged with a stir bar, 8-ACfm (0.5197g, 2.415mmol), benzyl alcohol (BnOH), and dried DCM (4 mL). The amount of BnOH was scaled accordingly as we targeted different degrees of polymerizations, DP's. As the solution was stirring, DBU catalyst (36.1 μL , 0.2415mmol, 10 mol % of monomer) was added in one shot. Once the reaction was complete, the catalyst was quenched by adding benzoic acid (~40mg). The polymer was purified by dissolving and precipitating in DCM and cold ether, respectively. ^1H NMR (300 MHz, CDCl_3) δ 7.36 (s, OBn-ArH), 6.02 – 5.83 (m, CH_{allyl}), 5.36 – 5.16 (m, $\text{CH}_{2\text{-allyl}}$), 5.15 (s, OBn- CH_2), 4.59 (d, $J = 5.5$ Hz, NC(O)OCH_2), 4.25 (m, $\text{OCH}_2\text{CH}_2\text{N}$), 3.58 (t, $J = 5.5$ Hz, $\text{OCH}_2\text{CH}_2\text{N}$). ^{13}C NMR (101 MHz, CDCl_3) δ 155.83 (OC(O)O), 154.93 (NC(O)O), 137.49 (ArC), 132.72 (CH_{allyl}), 117.90 ($\text{CH}_{2\text{-allyl}}$), 66.55 ($\text{OCH}_2\text{CH}_2\text{N}$), 66.17 (NC(O)OCH_2), 47.34 (d, $J = 51.1$ Hz, $\text{OCH}_2\text{CH}_2\text{N}$). FTIR-ATR: 1744 cm^{-1} (C=O_{carbonate}, stretch), 1694 cm^{-1} (C=O_{carbamate}, stretch), 1648 cm^{-1} (C=C, stretch), 1227 cm^{-1} (C-O_{carbonate}, stretch).

Polymerization of 8-ACfm using PEG8k as macroinitiator (polymer 5)

A 16mL vial was charged with a stir bar, 8-ACfm (0.5197g, 2.415mmol, 50 equiv.), poly(ethylene oxide) diol (M_n : 8,000 g mol⁻¹) (0.3864g), and dried DCM (2 mL). The PEG diol in this case would serve as the initiator for the ROP. As the solution was stirring, DBU catalyst (36.1μL, 0.2415mmol, 10 mol % of monomers) was added in one shot. After 2 hr stirring at room temperature in the glovebox, excess benzoic acid was added to quench the reaction. The polymer was then precipitated in cold THF. ¹H NMR (300 MHz, CDCl₃) δ 6.01 – 5.83 (m, CH_{allyl}), 5.35 – 5.17 (m, CH_{2-allyl}), 4.59 (dt, $J = 5.6, 1.4$ Hz, NC(O)OCH₂), 4.33 – 4.19 (m, OCH₂CH₂N), 3.64 (s, OCH₂CH₂), 3.58 (t, $J = 5.6$ Hz, OCH₂CH₂N). FTIR-ATR: 1745cm⁻¹ (C=O_{carbonate}, stretch), 1696cm⁻¹ (C=O_{carbamate}, stretch), 1649cm⁻¹ (C=C, stretch), 1230cm⁻¹ (C-O, stretch).

Homopolymerization of 8-ACI (polymer 6)

The polymerization was prepared using the same approach as the above-mentioned procedure. A 16mL vial was charged with a stir bar, 8-ACI (0.4135g, 2.415mmol, 50 equiv.), benzyl alcohol (BnOH, 5μL, 1 equiv.), and dried DCM (4 mL). As the solution was stirring, DBU catalyst (36.1μL, 0.2415mmol, 10 mol % of monomer) was added in one shot. After two weeks of stirring at room temperature, the reaction was quenched with excess benzoic acid. The polymer was then precipitated in cold petroleum ether. ¹H NMR (300 MHz, CDCl₃) δ 7.36 (s, OBn-ArH), 5.93 – 5.70 (m, CH_{allyl}), 5.25 – 5.09 (m, CH_{2-allyl} and OBn-CH₂), 4.17 (t, $J = 6.1$ Hz, OCH₂CH₂N), 3.21 (d, $J = 6.4$ Hz, NCH₂CH), 2.82 (t, $J = 6.1$ Hz, OCH₂CH₂N). FTIR-ATR: 3493cm⁻¹ (O-H, stretch), 1741cm⁻¹ (C=O_{carbonate}, stretch), 1645cm⁻¹ (C=C, stretch), 1241cm⁻¹ (C-O_{carbonate}, stretch).

Synthesis of co-polymers

Polymer 7. A 16mL vial was charged with a stir bar, 8-ACfm (0.2599g, 1.2075mmol, 25 equiv.), L-Lactide (0.174g, 1.2075mmol, 25 equiv.), benzyl

alcohol (5 μ L, 1 equiv.), and dried DCM (2 mL). As the solution was stirring, DBU catalyst (36.1 μ L, 0.2415mmol, 10 mol % of monomers) was added in one shot. After 2 hr stirring at room temperature in the glovebox, excess benzoic acid was added to quench the reaction. The polymer was then precipitated in cold methanol. ^1H NMR (300 MHz, CDCl_3) δ 7.33 (s, OBn-ArH), 6.00 – 5.82 (m, CH_{allyl}), 5.36 – 4.97 (m, PLA-CH, OBn- CH_2 , and $\text{CH}_{2\text{-allyl}}$), 4.58 (dt, $J = 5.5, 1.5$ Hz, $\text{NC}(\text{O})\text{OCH}_2$), 4.34 – 4.17 (m, $\text{OCH}_2\text{CH}_2\text{N}$), 3.58 (t, $J = 5.6$ Hz, $\text{OCH}_2\text{CH}_2\text{N}$), 1.62 – 1.45 (m, PLA- CH_3). FTIR-ATR: 3515cm^{-1} (O-H, stretch), 1744cm^{-1} ($\text{C}=\text{O}_{\text{carbonate, ester}}$, stretch), 1698cm^{-1} ($\text{C}=\text{O}_{\text{carbamate}}$, stretch), 1648cm^{-1} (C=C, stretch), 1231cm^{-1} (C-O, stretch).

Polymer 8. A 16mL vial was charged with a stir bar, 8-ACfm (0.2599g, 1.2075mmol, 25 equiv.), TMC (0.1233g, 1.2075mmol, 25 equiv.), benzyl alcohol (5 μ L, 1 equiv.), and dried DCM (2 mL). As the solution was stirring, DBU catalyst (36.1 μ L, 0.2415mmol, 10 mol % of monomers) was added in one shot. After 24 hr stirring at room temperature in the glovebox, excess benzoic acid was added to quench the reaction. The polymer was then precipitated in cold methanol. ^1H NMR (300 MHz, CDCl_3) δ 7.37 (s, OBn-ArH), 6.01 – 5.81 (m, CH_{allyl}), 5.36 – 5.17 (m, $\text{CH}_{2\text{-allyl}}$), 5.15 (s, OBn- CH_2), 4.59 (dt, $J = 5.5, 1.4$ Hz, $\text{NC}(\text{O})\text{OCH}_2$), 4.37 – 4.12 (m, $\text{OCH}_2\text{CH}_2\text{N}$, PTMC- OCH_2), 3.58 (t, $J = 5.5$ Hz, $\text{OCH}_2\text{CH}_2\text{N}$), 2.05 (p, $J = 6.3$ Hz, PTMC- OCH_2CH_2). FTIR-ATR: 3493cm^{-1} (O-H, stretch), 1741cm^{-1} ($\text{C}=\text{O}_{\text{carbonate}}$, stretch), 1697cm^{-1} ($\text{C}=\text{O}_{\text{carbamate}}$, stretch), 1649cm^{-1} (C=C, stretch), 1225cm^{-1} (C-O, stretch).

Thiol-ene reaction with DMPA

A solution containing the polymer (100mg/mL) was prepared in DCM. A 27mL vial was charged with a stir bar, 1mL of the polymer containing solution, 1-butanethiol (1.48 mL), and DMPA (11.9mg). As the solution was stirring at room temperature, the reaction medium was illuminated (365nm light) at a distance of

5cm with a from a Spectroline® ENF-240C/FE. The reaction was left for four hours stirring at room temperature, and the resulting product was precipitated in cold methanol.

Polymer 2a. ^1H NMR (300 MHz, CDCl_3) δ 7.37 (s, OBn-ArH), 5.16 (s, OBn- CH_2), 4.31 – 4.21 (m, $\text{OCH}_2\text{CH}_2\text{N}$), 4.18 (t, $J = 6.4$ Hz, NC(O)OCH_2), 3.57 (m, $\text{OCH}_2\text{CH}_2\text{N}$), 2.57 (t, $J = 7.1$ Hz, $\text{O(CH}_2)_2\text{CH}_2\text{S}$), 2.51 (t, $J = 7.2$ Hz, $\text{O(CH}_2)_3\text{SCH}_2$), 1.92 (p, $J = 6.7$ Hz, $\text{OCH}_2\text{CH}_2\text{CH}_2\text{S}$), 1.56 (p, $J = 8.0, 7.0, 6.6$ Hz, $\text{SCH}_2\text{CH}_2\text{CH}_2\text{CH}_3$), 1.41 (h, $J = 7.9, 7.5, 7.1, 7.0$ Hz, $\text{SCH}_2\text{CH}_2\text{CH}_2\text{CH}_3$), 0.92 (t, $J = 7.3$ Hz, CH_3). ^{13}C NMR (101 MHz, CDCl_3) δ 155.91 (OC(O)O), 154.81 (NC(O)O), 128.64 (ArC), 69.26 (ArCH_2O), 66.02 ($\text{OCH}_2\text{CH}_2\text{N}$), 64.64 ($\text{OCH}_2(\text{CH}_2)_2\text{S}$), 47.18 (d, $J = 46.8$ Hz, $\text{OCH}_2\text{CH}_2\text{N}$), 31.85 ($\text{SCH}_2(\text{CH}_2)_2\text{CH}_3$), 31.70 ($\text{SCH}_2\text{CH}_2\text{CH}_2\text{CH}_3$), 29.11 ($\text{O(CH}_2)_2\text{CH}_2\text{S}$), 28.53 ($\text{OCH}_2\text{CH}_2\text{CH}_2\text{S}$), 22.02 ($\text{S(CH}_2)_2\text{CH}_2\text{CH}_3$), 13.74 (CH_3). FTIR-ATR: $\sim 3500\text{cm}^{-1}$ (O-H, stretch), 1746cm^{-1} ($\text{C=O}_{\text{carbonate}}$, stretch), 1697cm^{-1} ($\text{C=O}_{\text{carbamate}}$, stretch), 1228cm^{-1} (C-O, stretch).

Polymer 2b. ^1H NMR (300 MHz, CDCl_3) δ 7.37 (s, OBn-ArH), 5.16 (s, OBn- CH_2), 4.30 – 4.21 (m, $\text{OCH}_2\text{CH}_2\text{N}$), 4.18 (t, $J = 6.4$ Hz, NC(O)OCH_2), 3.67 – 3.49 (m, $\text{OCH}_2\text{CH}_2\text{N}$), 2.56 (t, $J = 7.3$ Hz, $\text{O(CH}_2)_2\text{CH}_2\text{S}$), 2.51 (t, $J = 7.6$ Hz, $\text{O(CH}_2)_3\text{SCH}_2$), 1.92 (p, $J = 6.6$ Hz, $\text{OCH}_2\text{CH}_2\text{CH}_2\text{S}$), 1.57 (p, $J = 7.0$ Hz, $\text{SCH}_2\text{CH}_2(\text{CH}_2)_3\text{CH}_3$), 1.44 – 1.20 (m, $\text{S(CH}_2)_2(\text{CH}_2)_3\text{CH}_3$), 0.89 (t, $J = 6.8$ Hz, CH_3). ^{13}C NMR (101 MHz, CDCl_3) δ 155.91 (OC(O)O), 154.82 (NC(O)O), 128.64 (ArC), 69.27 (ArCH_2O), 66.02 ($\text{OCH}_2\text{CH}_2\text{N}$), 64.65 ($\text{OCH}_2(\text{CH}_2)_2\text{S}$), 47.19 (d, $J = 47.1$ Hz, $\text{OCH}_2\text{CH}_2\text{N}$), 32.21 ($\text{SCH}_2(\text{CH}_2)_4\text{CH}_3$), 31.48 ($\text{CH}_2\text{CH}_2\text{CH}_3$), 29.60 ($\text{O(CH}_2)_2\text{CH}_2\text{S}$), 29.12 ($\text{CH}_2(\text{CH}_2)_3\text{CH}_3$), 28.63 ($\text{CH}_2(\text{CH}_2)_2\text{CH}_3$), 28.55 ($\text{OCH}_2\text{CH}_2\text{CH}_2\text{S}$), 22.60 (CH_2CH_3), 14.09 (CH_3). FTIR-ATR: $\sim 3500\text{cm}^{-1}$ (O-H, stretch), 1747cm^{-1} ($\text{C=O}_{\text{carbonate}}$, stretch), 1698cm^{-1} ($\text{C=O}_{\text{carbamate}}$, stretch), 1230cm^{-1} (C-O, stretch).

Polymer 2c. ^1H NMR (300 MHz, DMSO) δ 7.37 (s, OBn-ArH), 5.13 (s, OBn-CH₂), 4.17 (m, OCH₂CH₂N), 4.03 (t, $J = 6.1$ Hz, NC(O)OCH₂), 3.48 (s, OCH₂CH₂N), 2.66 (t, $J = 7.1$ Hz, SCH₂CH₂C(O)OH), 2.55 (t, $J = 7.2$ Hz, CH₂C(O)OH), 2.47 (t, $J = 7.2$, 6.8 Hz, O(CH₂)₂CH₂S), 1.80 (p, $J = 6.5$ Hz, OCH₂CH₂CH₂S). ^{13}C NMR (101 MHz, DMSO) δ 173.14 (C(O)OH), 155.43 (OC(O)O), 154.33 (NC(O)O), 128.48 (ArC), 68.48 (ArCH₂O), 65.27 (d, $J = 26.9$ Hz, OCH₂CH₂N), 63.82 (OCH₂(CH₂)₂S), 45.92 (d, $J = 24.8$ Hz, OCH₂CH₂N), 34.68 (CH₂C(O)OH), 28.56 (O(CH₂)₂CH₂S), 27.49 (SCH₂CH₂C(O)OH), 26.39 (OCH₂CH₂CH₂S). FTIR-ATR: ~ 3500 to $\sim 2500\text{cm}^{-1}$ (O-H_{end group, carboxylic acid, stretch}), 1741cm^{-1} (C=O_{carbonate, stretch}), 1693cm^{-1} (C=O_{carbamate, stretch}), 1230cm^{-1} (C-O_{carbonate, carboxylic acid, stretch}).

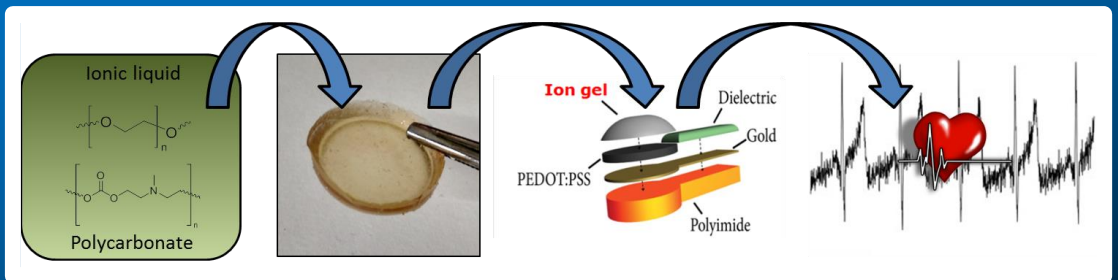
Polymer 2d. ^1H NMR (300 MHz, CDCl₃) δ 7.37 (s, OBn-ArH), 5.16 (s, OBn-CH₂), 4.32 – 4.22 (m, OCH₂CH₂N), 4.19 (t, $J = 6.2$ Hz, NC(O)OCH₂), 3.73 (t, $J = 6.2$ Hz, SCH₂CH₂OH), 3.64 – 3.52 (m, OCH₂CH₂N), 2.72 (t, $J = 6.2$ Hz, SCH₂CH₂OH), 2.62 (t, $J = 7.2$ Hz, O(CH₂)₂CH₂S), 1.93 (p, $J = 6.5$ Hz, OCH₂CH₂CH₂S). ^{13}C NMR (101 MHz, CDCl₃) δ 156.05 (OC(O)O), 154.86 (NC(O)O), 128.71 (ArC), 69.24 (ArCH₂O), 66.01 (OCH₂CH₂N), 64.55 (OCH₂(CH₂)₂S), 60.99 (SCH₂CH₂OH), 47.20 (d, $J = 46.3$ Hz, OCH₂CH₂N), 35.00 (SCH₂CH₂OH), 29.20 (O(CH₂)₂CH₂S), 28.45 (OCH₂CH₂CH₂S). FTIR-ATR: 3433cm^{-1} (O-H, stretch), 1744cm^{-1} (C=O_{carbonate, stretch}), 1687cm^{-1} (C=O_{carbamate, stretch}), 1230cm^{-1} (C-O, stretch).

Thiol-ene reaction with AIBN

A solution containing the polymer was first prepared with a concentration of 100 mg of polymer per 1 mL of 1,4-dioxane. For a typical thiol-ene reaction with AIBN as a radical source, a 27mL vial was charged with a stir bar, 1mL of the polymer containing solution, butanethiol (1.48 mL), and AIBN (7.61mg). The solution was

heated to 90°C for 18 hr, and the resulting product was precipitated in cold methanol.

Chapter 6



Polycarbonate ion gels as electrodes for electrophysiology

Chapter 6. Polycarbonate iongels as electrodes for electrophysiology

6.1. Introduction

Electrical activities of the brain, heart, and muscles are all particularly important signals in determining the status of one's health. These electrophysiological measurements are made possible through the implementation of electrodes that are able to measure electrical activities around the areas of interest. Currently, standard medical procedures for cutaneous readings utilize electrodes based on Ag/AgCl. However, these electrodes require the use of water based electrolytes to lower the impedances across the electrode and skin interface, which in turn improves the signal to noise ratio. The minimization of impedance is of importance; however, such water based electrolytes are prone to drying out over time and cause the impedance to rise.¹¹⁷ The increase in impedance reduces the ability of the electrodes to work properly and thus the refilling of the electrolyte gel is necessary to maintain the electrodes in working order. Such procedures can be time consuming and may cause discomfort amongst the patients. Therefore, new biocompatible electrolyte systems with low evaporation rates are of great interest for electrodes in cutaneous electrophysiology.

Previous work in our group by Isik *et al.*, demonstrated the potential of iongels for exactly such applications.⁶⁵ Their confidence in these gels containing ionic liquids stemmed the fact that these materials have negligible vapor pressure and evaporation rates, and are thus less prone to drying out.¹¹⁸ Ionic liquids can be broadly defined as organic and inorganic salts with melting points lower than 100 °C. The cholinium lactate based ion gels they reported were capable of providing accurate electrocardiography measurements up to 72 hours without the need of

a 'refill'. Though this work was a step in the right direction, these materials were still acrylate based and offered low biodegradability.

As stated earlier, aliphatic polycarbonates are known to have low toxicity, biocompatibility, and biodegradability properties.^{34,39,119} In our previous work, we reported the preparation of non-charged polycarbonate gels using the eight membered cyclic carbonates. These materials exhibited acceptable mechanical properties, biocompatibility, and were able to degrade back into their starting materials rapidly in water.³⁷ In this section, we wanted to combine the promising features of ionic liquids and polycarbonates to produce biodegradable and biocompatible solid electrolytes for electrodes for cutaneous electrophysiology. Here in our work, we produced ion gels by ROP of *N*-substituted eight membered cyclic carbonates in the presence of ionic liquids. Biodegradability, rheological, and electrical properties of the gels were studied. Finally, the ion gels were mounted onto PEDOT:PSS based electrodes and used in the recording of heartbeats from the skin.

6.2. Results and discussion

6.2.1. Preparation of ion gels

Non-charged polycarbonate gels were prepared from ***N*-8-C**, **bis *N*-8-C**, and PEG_{8k} diol using the same methodology outlined in the previous chapter. We opted for a simple "one-pot synthesis" approach which allowed us to target specific quantities of ionic liquids (Figure 35).

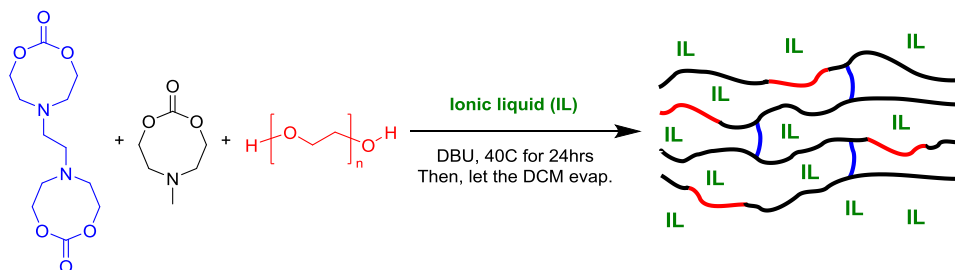


Figure 35. Polycarbonate ion gels were prepared in a one post synthesis approach. In doing so, we were able to control the amount of ionic liquid inside the iongels.

A range of ionic liquids were prepared using the anion exchange resin procedure as reported by Alcalde *et al.*¹²⁰ For this, a glass column was packed with the commercially available Amberlyst™ A-26(OH) ion exchange resin (Figure 36). Acidic solutions carrying the desired anion were then passed over the ion exchange resin to ‘charge’ the resin. In our case, the desired anions were lactate, acetate, and butyrate. Therefore, lactic acid, acetic acid, and butyric acid solutions were respectively used in charging of the ion exchange resins. Once a column was ‘charged’ with the desired anion, a solution of cholinium or imidazolium salt was then passed over the resin to exchange their original anions for the desired anions. A range of ionic liquids were prepared in this manner and depicted in (Figure 36).

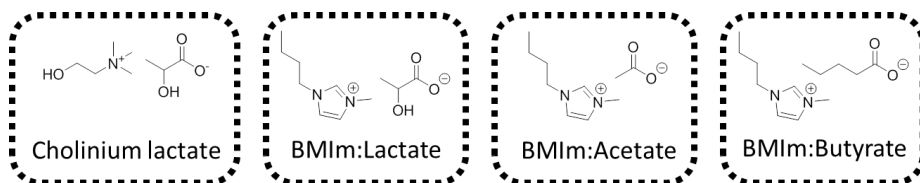


Figure 36. Here we show the chemical structures of the ionic liquids that we prepared and surveyed in the preparation of polycarbonate iongels for electrodes.

With the ionic liquids on hand, we then first tried to prepare ion gels with cholinium lactate, so that we would obtain analogous materials to the work of Isik *et al.*⁶⁵ A range of 10 to 30 wt% of cholinium lactate with respects to the other

starting materials of the gels were surveyed. However, none of them yielded a gel like material, and all trials afforded semi-viscous liquids. We suspect the reason for this was that the primary alcohol group in the cholinium acted as an initiator during the polymerization process. The presence of excess initiators would drastically reduce the ability to form long and networked polycarbonate chains that would make up the gels. As for comparison sake, Isik *et al.*⁶⁵ were able to produce gels up to 60 wt% cholinium lactate. But it is important to note that these gels were acrylate based and the reactions were not nearly as susceptible to alcohol and water. In addition, it is generally better to have higher ionic liquid content within the gels, because it allows for higher conductivities essential for electrode applications.

A number of 1-butyl-3-methylimidazolium (BMIm) based ionic liquids were also prepared and tested. Out of the three BMIm ionic liquids that we prepared, the version with the lactate anion (BMIm:Lactate) was the most promising. We were able to consistently prepare ion gels up to 35 wt% BMIm:Lactate, however these gels were extremely delicate and difficult to handle. Polycarbonate gels with 30 wt% BMIm:Lactate (**Gel-Lac-30**) were much more favorable, they were mechanically stronger and much easier to handle (Figure 37). We were also able to prepare ion gels with BMIm:Butyrate, but we were unable to surpass 10 wt%. As for the BMIm:Acetate, we were unable to obtain any gels and the experiments only yielded viscous materials.

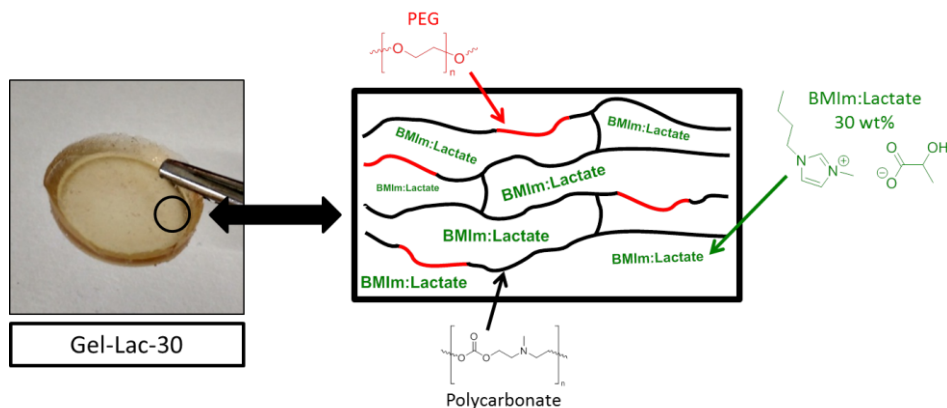


Figure 37. A photograph of a polycarbonate gel loaded with 30 wt% BMIm:Lactate (Gel-Lac-30).

6.2.2. Characterization of the iongels with FTIR-ATR

A series of FTIR-ATR characterizations were carried out for BMIm:Lactate, **Gel-Lac-30**, and a polycarbonate gel without ionic liquid (Figure 38). For BMIm:Lactate, we observed peaks at 1598cm^{-1} and 1736cm^{-1} that corresponded to the C=O (stretch) of the lactate anion in its conjugated and protonated forms respectively. The lactate (C=O, conjugate) was observed in the FTIR spectrum for **Gel-Lac-30**, and expectedly absent for the polycarbonate gel without ionic liquid. The C=O and C-O stretching bands originating from the polycarbonate structure were clearly observable at 1736cm^{-1} and 1248cm^{-1} respectively. In summary, we can observe characteristic BMIm:Lactate and polycarbonate signals within our **Gel-30-Lac** samples. This indicated that we were able to successfully ROP our **N-8-C** and **bis N-8-C** monomers in the presence of BMIm:Lactate.

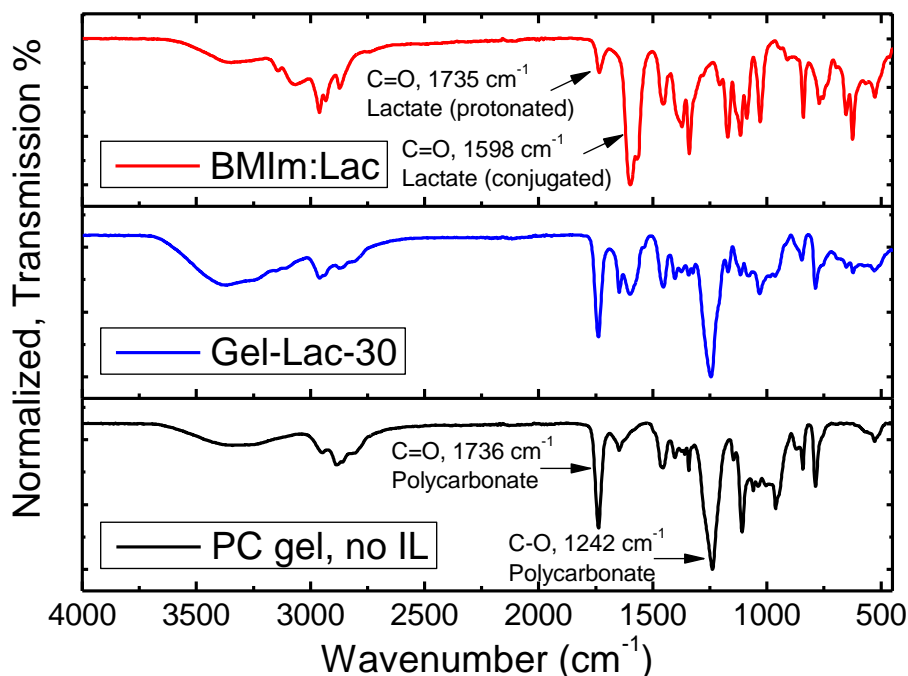


Figure 38. FTIR-ATR characterization of the BMIm:Lactate ionic liquid (top), polycarbonate gel with 30wt% BMIm:Lactate (Gel-Lac-30, middle), and just the polycarbonate gel without any ionic liquids (bottom).

6.2.3. Rheology testing

A series of polycarbonate ion gels were prepared with different amounts of BMIm:Lactate (10-30 wt%). Their rheological properties were studied using oscillatory tests, and their elastic (G') and loss (G'') moduli were plotted against angular frequency (Figure 39). When $G' > G''$, the material is said to be elastic and gel-like. On the other hand, when $G'' > G'$, the material behaves as a viscous liquid. For **Gel-Lac-10**, the ion gel with the least amount of ionic liquid (10 wt%), we observed G' dominating G'' for the entire range of angular frequencies tested. Interestingly, we can observe the G'' converge towards the G' at higher angular frequencies. If we were to continue testing this material at higher frequencies, perhaps we can expect to observe a cross-over point, in which the material

would stop behaving as a gel and instead behave as a viscous liquid. However, these extreme angular frequencies are not very applicable for our gels as electrodes, but it's still interesting to note.

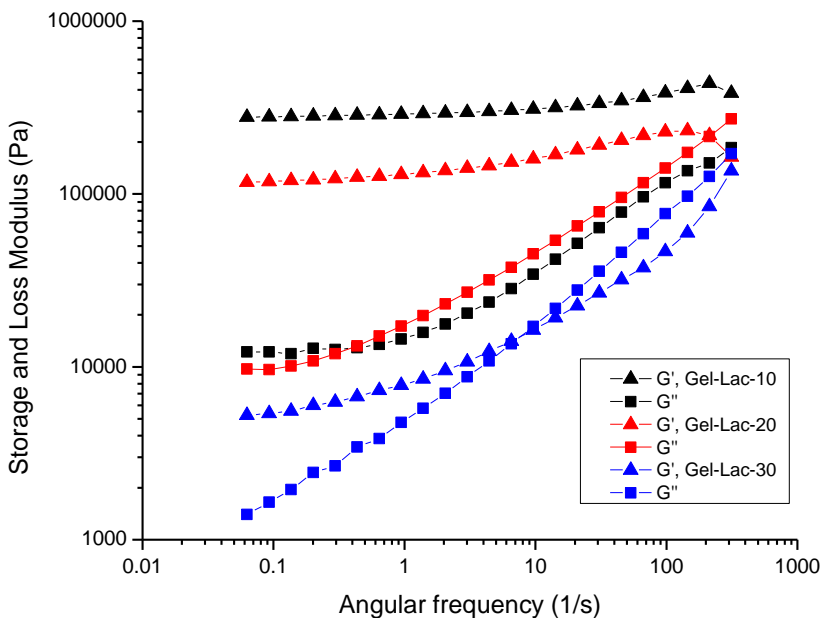


Figure 39. Rheological studies using oscillatory tests were performed for **Gel-Lac-10** (black), **Gel-Lac-20** (red), and **Gel-Lac-30** (blue). Elastic moduli (G') are marked with triangles and loss moduli are marked with squares.

As we increased the ionic liquid content from 10 to 20 wt%, we can see that **Gel-Lac-20** behave as an elastic gel for almost the entirety of range of frequencies. At the angular frequency of 213 s^{-1} , there is a cross-over point in which the material ceases to behave as a gel and begins to behave as a viscous liquid. As we arrive to the 30 wt% **Gel-Lac-30**, we see this cross-over point shift further to the left from 213 s^{-1} to $\sim 6 \text{ s}^{-1}$. We expect that the cross-over point would continue shifting to the left if we increase the ionic liquid content. If true, this would certainly help to explain why we were only able to obtain viscous materials at $> 35 \text{ wt}\%$.

Although **Gel-Lac-30** behaves as a viscous material at higher angular frequencies ($>10\text{ s}^{-1}$), the gel-like behavior at lower angular frequencies ($<10\text{ s}^{-1}$) is more than sufficient for our application. Our intended applications of these materials are for electrodes to be placed on areas of the body with much less movement. In addition, the G' and G'' curves of **Gel-Lac-30** were considerably lower than those of **Gel-Lac-10**. This indicated that the gels were softer as we increased the ionic liquid content, and indeed is what we observed while handling the materials.

6.2.4. Biodegradability study

The biodegradability of **Gel-Lac-30** was assessed by completely submerging it in deionized water at room temperature, and the material appeared to significantly degrade within two hours (Figure 40). To clarify, we were not able to visually observe any pieces of gels after two hours. The water was removed and the residues were characterized with ^1H NMR (Figure 41) and FTIR-ATR (Figure 42) spectroscopy. A comparable study was performed using polycarbonate gels without ionic liquids; these materials lasted much longer and degraded after ~ 30 hours. We believe this large difference in longevity was mainly attributed to the presence of BMIm:Lactate. Ionic liquids such as the one used here are known to be hydrophilic, in which case this could accelerate the uptake of water throughout the entirety of the gel. This can then allow for the polycarbonate linkages to rapidly hydrolyze from both inside and outside of the gels.

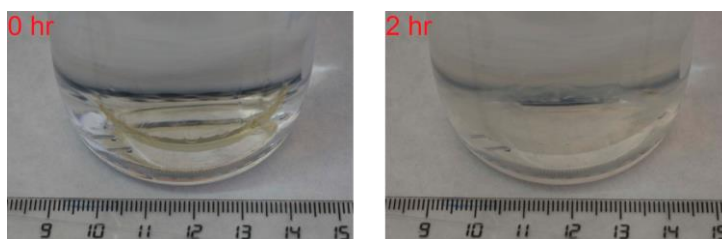


Figure 40. Photographs of the biodegradability experiment with **Gel-Lac-30** in water at room temperature. An initial photograph was taken right when the gel was added to the water (left), and an additional photo was taken two hours later (right).

As mentioned previously, the residues of the degraded **Gel-Lac-30** were characterized with ^1H NMR. We were able to determine **Gel-Lac-30** degraded back to its starting materials: *N,N,N',N'*-tetrakis(2-hydroxyethyl)ethylenediamine, *N*-methyldiethanolamine, polyethylene glycol, and BMIm:Lactate. This result was consistent to a similar work published previously.³⁷ The degradation of the polycarbonate structure was further evidenced by the absence of the carbonyl signal by ^{13}C NMR spectroscopy.

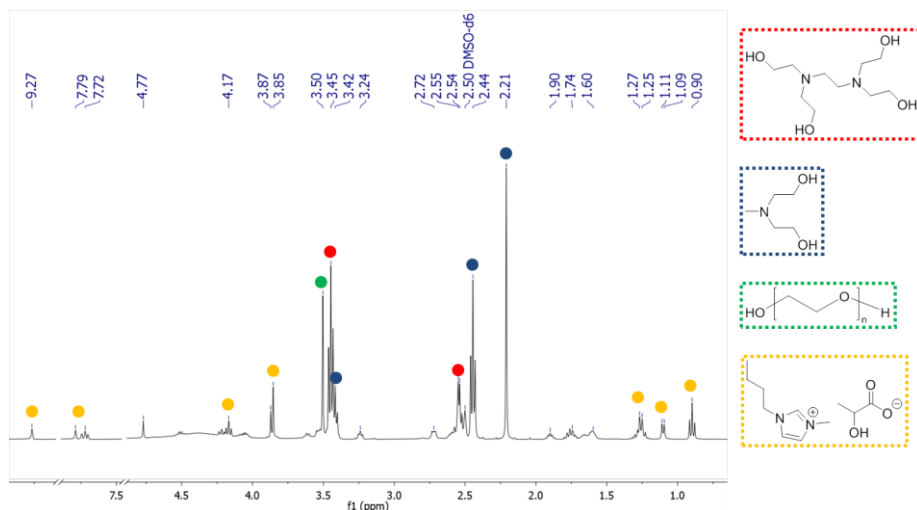


Figure 41. Residues from the biodegradability testing of **Gel-Lac-30** were characterized with ^1H NMR in d_6 -DMSO. Here we can observe that the gels have degraded back into its respective starting materials: *N,N,N',N'*-tetrakis(2-hydroxyethyl)ethylenediamine (red), *N*-methyldiethanolamine (blue), polyethylene glycol (green), and BMIm:Lactate (yellow).

Characterizations of the residues were also carried out with FTIR-ATR (Figure 42). Surprisingly, we observed signals at 1741 cm^{-1} and 1254 cm^{-1} that corresponded exactly to the polycarbonates' C=O and C-O stretching bands. If they are indeed polycarbonate signals, their reduced intensity compared to the pristine **Gel-Lac-30** suggests that much of the polycarbonates have been degraded and that there may be some oligomers left behind. Additional evidence

suggesting the successful degradation of the carbonate linkages was the presence of the C-O stretching band at 1030 cm^{-1} , which was previously absent in the pristine ion gel. This particular band was attributed to primary alcohols originating from the starting materials. In addition, we were able to identify BMIm:Lactate amongst the residues by its characteristic C=O band at 1598 cm^{-1} . Though the NMR and FTIR-ATR data suggests different degrees of degradation, both techniques provide the evidence for the degradation of polycarbonates back into its starting materials.

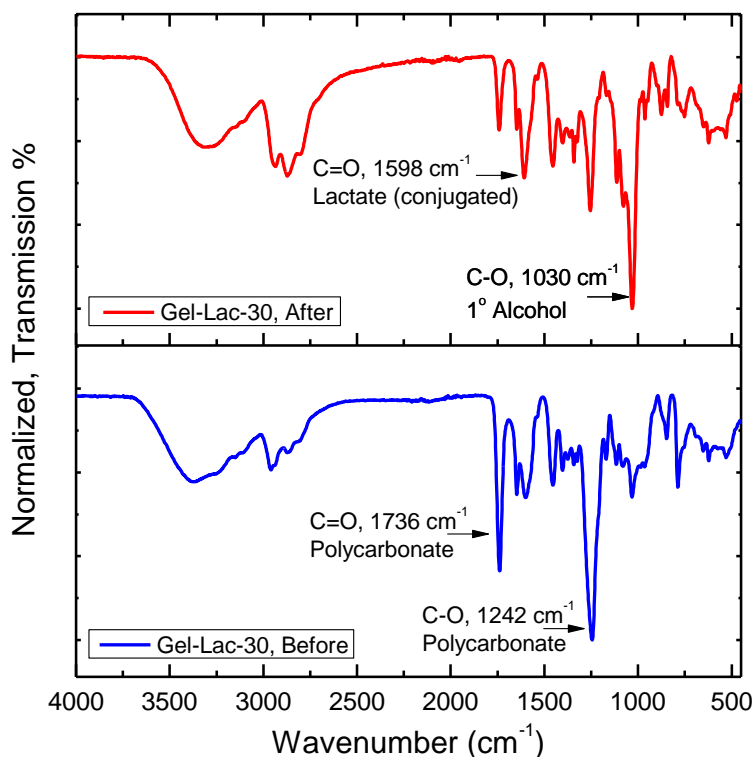


Figure 42. FTIR-ATR characterization of the Gel-Lac-30 after its biodegradability study in water (red) and before (blue).

6.2.5. Ionic conductivity measurements

Before incorporating these iongels into devices, we needed to be confident that the materials would provide high enough ionic conductivity to be suitable for electrode applications. As mentioned previously, ionic liquids are particularly hygroscopic and the slight presence of water can have an enormous impact on the conductivity measurements. To account for this, all the iongels were meticulously dried using a combination of a conventional oven and a Buchi® oven under vacuum prior to measuring their ionic conductivities (Figure 43).

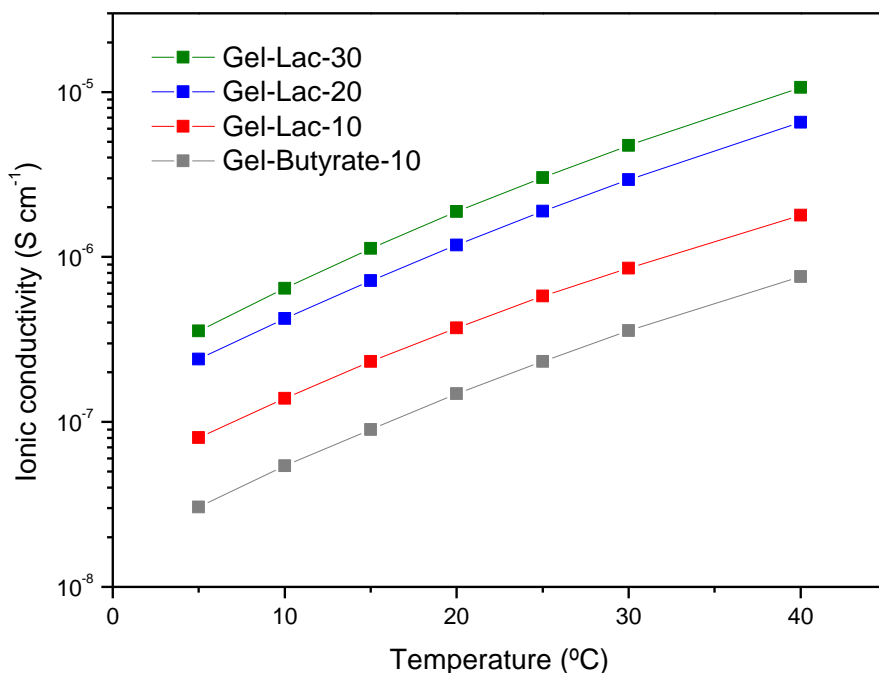


Figure 43. Ionic conductivities measurements were carried for Gel-Lac-30 (green), Gel-Lac-20 (blue), Gel-Lac-10 (red), and Gel-Butyrate-10 (grey). A temperature range of 5 to 40 °C was surveyed and the ionic conductivities were given as S cm⁻¹.

Ionic conductivities across a temperature range of 5 to 40 °C was surveyed for ion gels with 10, 20, and 30 wt% BMIm:Lactate (**Gel-Lac-10**, **Gel-Lac-20**, and **Gel-Lac 30**, respectively) and 10 wt% BMIm:Butyrate (**Gel-Butyrate-10**). A table

listing the ionic conductivities for the gels at 25 °C was prepared (Table 10). For each of the samples, we observed a positive correlation between ionic conductivity and temperature. This phenomenon was to be expected, because the additional thermal energy allows for ionic liquid molecules to move around faster and easier, which is then represented in the increase of ionic conductivity.

Table 10. Ionic conductivities of the dried gels at room temperature (25 °C).

Material	Ionic conductivity at 25 °C
Gel-Lac-30	$3.03 \times 10^{-6} \text{ S cm}^{-1}$
Gel-Lac-20	$1.89 \times 10^{-6} \text{ S cm}^{-1}$
Gel-Lac-10	$5.79 \times 10^{-7} \text{ S cm}^{-1}$
Gel-Butyrate-10	$2.33 \times 10^{-7} \text{ S cm}^{-1}$

For the gels with BMIm:Lactate, we observed a rise in ionic conductivities as the ionic liquid content increased from 10 to 30 wt%. The largest increase of ionic conductivity was by about half an order of magnitude that occurred between 10 to 20 wt% in **Gel-Lac-10** and **Gel-Lac-20**, respectively. Results with **Gel-Butyrate-10** were the least promising, and provided the lowest ionic conductivities amongst all the materials tested. Even with the same wt% of ionic liquid, **Gel-Lac-10** offered half an order of magnitude greater ionic conductivities than **Gel-Butyrate-10**.

Amongst the tested materials, **Gel-Lac-30** was the most promising. Under the dried conditions, it had an ionic conductivity of $3.03 \times 10^{-6} \text{ S cm}^{-1}$ at 25 °C. Though this was much inferior to the 60 wt% cholinium lactate gels that offered $10^{-3} \text{ S cm}^{-1}$ at 20 °C that Isik *et al.* reported⁶⁵, it didn't represent a "real world" measurement where moisture would be present. As we commented before, ionic liquids are very hygroscopic and the mere presence of water can influence the ionic conductivity measurements. To demonstrate the 'doping' effect of water, dried **Gel-Lac-30** were left out in the laboratory and ionic conductivities were followed over time. In addition, moisture uptake, given in weight %, was also

followed by measuring the mass of the gel versus its original dried state (Figure 44).

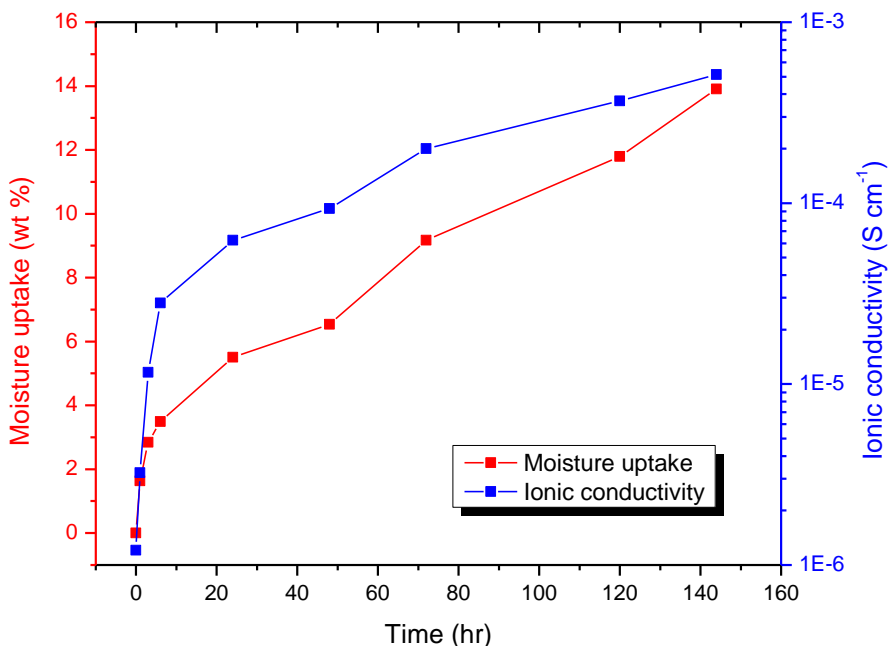


Figure 44. Dried Gel-Lac-30 samples were left out in the laboratory and we tracked the moisture uptake (red, wt%) and ionic conductivities (blue) over a period of time.

As we expected, **Gel-Lac-30**'s ionic conductivity increased dramatically from $1.21 \times 10^{-6} \text{ S cm}^{-1}$ to $5.14 \times 10^{-4} \text{ S cm}^{-1}$ after leaving the gels out in the laboratory for six days. Even just after leaving the gels out for two days, we were able to observe a large improvement in ionic conductivities by two orders of magnitudes, and this was attributed to ~14 wt% absorption of moisture. Other ion gels from Figure 43 were also subjected to similar testing and exhibited an increase of ionic conductivities by one or two orders of magnitude (Figure 45). However, **Gel-Lac-30** remained the most promising amongst the materials and the conductivities in its 'doped' state were high enough to be used for our electrode applications.

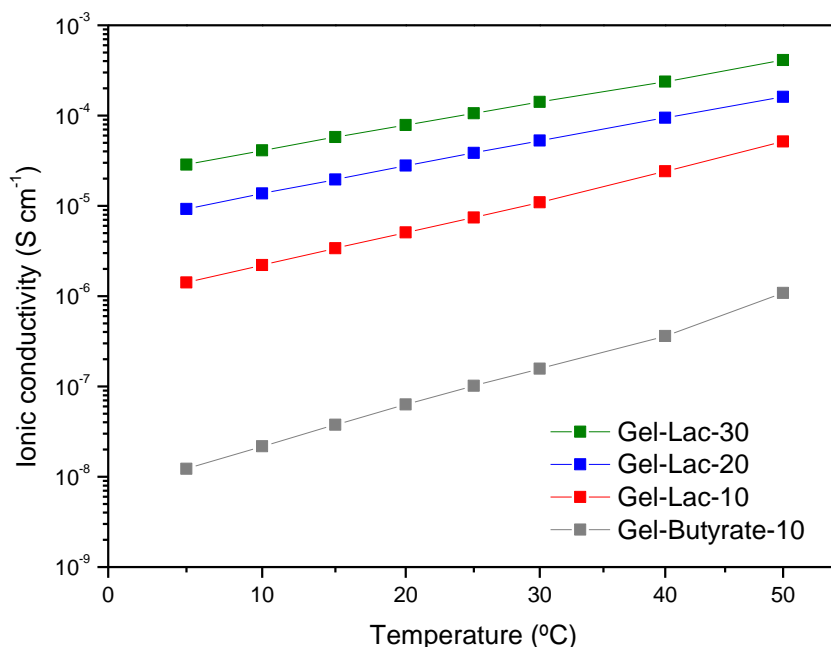


Figure 45. Polycarbonate gels loaded with ionic liquids were left in the open inside the laboratory for one week. The ionic conductivities were then measured across a range of temperatures.

6.2.6. Electrode fabrication and testing

Electrode fabrication

In order to improve the contact between skin and the electrodes, polycarbonate ion gels loaded with 30 wt% BMIm:Lactate (**Gel-Lac-30**) were incorporated onto electrodes made of gold and PEDOT:PSS conducting polymer (Figure 46). As discussed previously, the main advantages of the ion gels are its low toxicity and biodegradability. The electrodes were made with thin polyimide films that allowed the electrodes to be flexible and conformable to the skin.



Figure 46. An exploded view of the electrode and all of the different materials used (left). A photograph of the electrode with the ion gel deposited on top (right).

Impedance measurements

Impedance measurements of the electrode/skin interface were carried using a three-electrode configuration on a healthy volunteer (Figure 47). The working and counter electrodes were placed on the subject's forearm, and the reference electrode was placed on the elbow. For this study, commercially available Ag/AgCl electrodes were used for both the counter and reference electrodes. Moreover, our electrodes that we prepared were used as the working electrodes. To compare our electrodes to the standard medical ones, an additional impedance measurement was made with an Ag/AgCl working electrode.

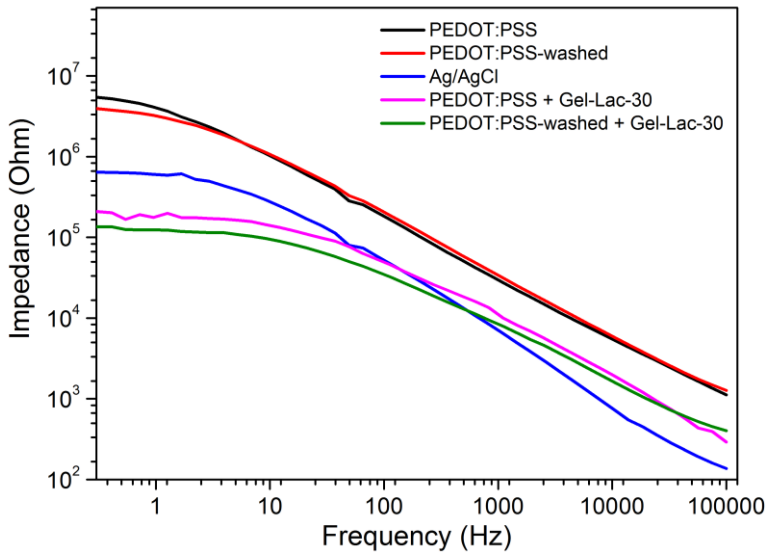


Figure 47. Comparison of the impedance on skin recordings with different working electrodes at a frequency range between 0.1 and 100000 Hz. Medical electrode (blue), PEDOT:PSS electrodes (black and red), and PEDOT:PSS with iongel electrodes (pink and green).

In Figure 47, we observed a clear difference in impedance when the polycarbonate ion gel was present (**pink**) or absent (**black**) from the electrode. When the ion gel was present, we saw a decrease in impedance by approximately one order of magnitude across the entire range of frequencies tested. This was particularly favorable, because lower impedances generally allows for better signal to noise ratios for cutaneous electrophysiological (ECG) recordings.¹³¹ Impedance measurements were also taken using standard medical electrodes (Ag/AgCl electrode, **blue**). If we were to compare our electrodes (**pink**) with the Ag/AgCl electrodes, our electrodes displayed lower impedances at frequencies below ~100 Hz, but not at higher frequencies (~100 to 10^5 Hz). This was acceptable because the ECG electrodes generally operate in the range of 1-100 Hz.

Additional impedance measurements were taken to demonstrate the idea of a 'washable' and 'refillable' electrode. For this, an electrode bearing a polycarbonate ion gel was washed with deionized water to remove the ion gel layer and expose the PEDOT:PSS. An impedance measurement was taken (**red**) and the curve that we obtained was nearly the same as our initial measurement when the ion gel was absent (**black**). Next, the washed electrode was 'refilled' with a new ion gel (**green**) and the impedance was nearly identical prior to washing the electrodes (**pink**).

Electrocardiography (ECG) measurements

Electrocardiography (ECG) measurements were taken from a healthy volunteer using both the **Gel-Lac-30** electrode and the standard medical electrode (Figure 48). The recording performance of the **Gel-Lac-30** electrode was comparable with the standard medical electrode, and the QT intervals could be obtained for both materials. The QT interval represents the time taken for ventricular depolarization and repolarization, and can be used to identify numerous heart conditions, such as arrhythmias or hypertrophy. Recordings of approximately 10 minutes were taken for each material, and the volunteer reported no redness or irritation of the skin.

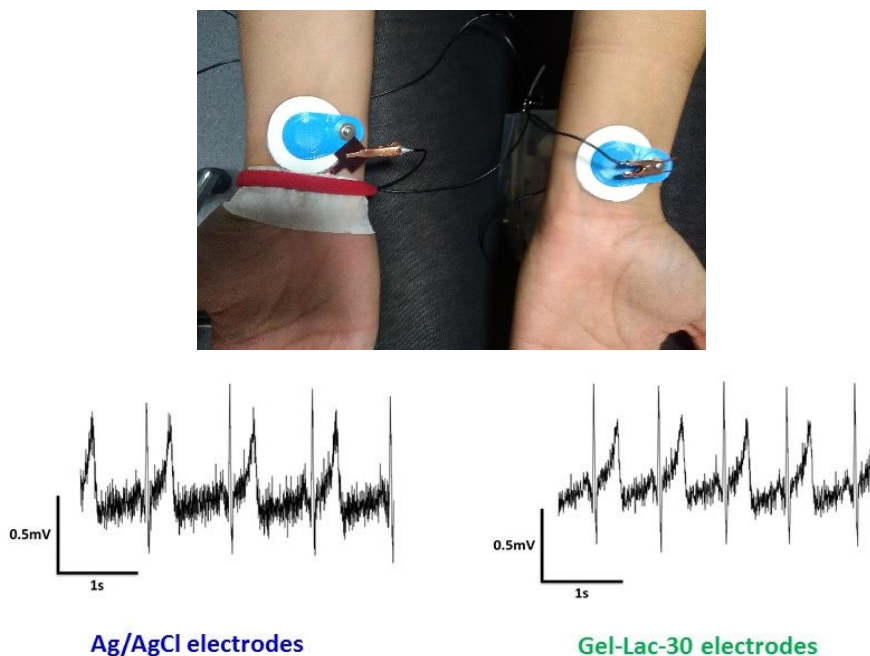


Figure 48. Electrocardiogram recordings were taken from the wrists of the volunteer (Top center). The standard medical Ag/AgCl electrode (bottom left) and the Gel-Lac-30 electrode (in green) were evaluated.

6.3. Conclusions

A series of biodegradable polycarbonate iongels loaded with ionic liquids were prepared for electrophysiological applications. A number of ionic liquids were tested, and we found that iongels consisting of 30 wt% BMIm:Lactate (**Gel-Lac-30**) to be the most promising. Using FTIR-ATR and rheological measurements, we were able to determine the successful organocatalyzed ring opening polymerization of our cyclic carbonate monomers. Indeed, these iongels showed fast degradability in water at room temperature. Ionic conductivities of the gels in their 'dried' states were measured, and we later demonstrated that these gels

were extremely hygroscopic. The trace amounts water absorbed by the iongels from the atmosphere led to huge gains in ionic conductivities. With the 'wet' iongels showing promising conductivities, electrodes were fabricated with **Gel-Lac-30**. Impedance measurements showed a slight advantage of our electrodes with lower impedances over the standard medical Ag/AgCl electrodes. Lastly, we used our electrodes for electrocardiography and were able to produce recordings comparable to the standard medical electrodes.

6.4. Experimental part

Materials and equipment

^1H and ^{13}C NMR spectra were recorded with Bruker Avance DPX 300, Bruker FourierTM 300, and Bruker Avance 400 spectrometers. The NMR chemical shifts were reported as δ in parts per million (ppm) relative to the traces of non-deuterated solvent (eg. $\delta = 2.50$ ppm for d_6 -DMSO or $\delta = 7.26$ for CDCl_3). Fourier transform infrared - attenuated total reflection (FTIR-ATR) spectroscopy was performed with a Bruker Alpha. Gel permeation chromatography size exclusion chromatography (SEC) was performed on a system consisting of a Shimadzu LC-20A pump, Waters 717 autosampler, Waters 2410 differential refractometer, and three columns in series (Styragel HR2, HR4 and HR6). The SEC system ran on THF (HPLC grade) at 35 °C using a flow rate of 1 mL min⁻¹ and was calibrated using polystyrene standards ranging from 595 to 3.95x10⁶ Da. All SEC samples were diluted to 5mg/mL, filtered with 0.45 micron PTFE filter, and lastly toluene was added as a flow marker.

Triethylamine ($\geq 99\%$), lactic acid solution ($\geq 85\%$), allyl chloride (98%), 1-butyl-3-methylimidazolium chloride ($\geq 99\%$), ethylene glycol ($\geq 99\%$), polyethylene glycol 8000 (USP), 4-dodecylbenzenesulfonic acid ($\geq 95\%$), 3-methacryloxypropyltrimethoxysilane ($> 98\%$), and 1,8-diazabicyclo[5.4.0]undec-7-ene ($\geq 99\%$) were purchased from Sigma Aldrich and used as is. AmberlystTM A-26(OH), *N,N,N',N'*-tetrakis(2-hydroxyethyl)ethylenediamine (99%), *N*-128

methyldiethanolamine (>98%), *N*-butyric acid (SLR), *N,N,N',N'*-tetramethyl-1,8-naphthalenediamine (99%), and potassium carbonate (ACS grade, anhydrous) were purchased and used as is from Fisher Scientific. Triphosgene (>98%) were purchased from TCI and used as is. Poly(3,4-ethylenedioxythiophene):poly(styrene sulfonate) (PEDOT:PSS) from Clevis PH-1000 were purchased and used as is from Heraeus Holding GmbH. Analytical grade solvents were purchased and used as is from Fisher Scientific. For solvents used within the glovebox, extra dried solvents were purchased from Fisher Scientific and stored over molecular sieves. Deuterated solvents were purchased from Deutero and were used as is.

Preparation of ionic liquid (BMIm:Lactate)

A glass column was packed with 16g of Amberlyst™ A-26(OH) ion exchange resin and washed with 100mL of methanol. Next, a solution of lactic acid (5g) in 50mL of methanol was passed over the ion exchange resin. As the acidic solution passed over the resin, the color of the resin would change from a dark red to a bright yellow. The pH of the solution exiting the column was constantly monitored. Once the resin was fully charged with the desired anion, the pH of the exiting material would equate to the acidic solution. The column and resin would then be washed with excess methanol until a pH of 7 was obtained. Next, a solution of BMIm:Chloride (2g) in 100mL MilliQ water was then slowly passed over the resin so that the chloride anions would exchange for the lactate anions (Figure 49). The product was collected, carefully dried (rotary evaporator and Schlenk line), and stored in a N₂ filled glovebox.

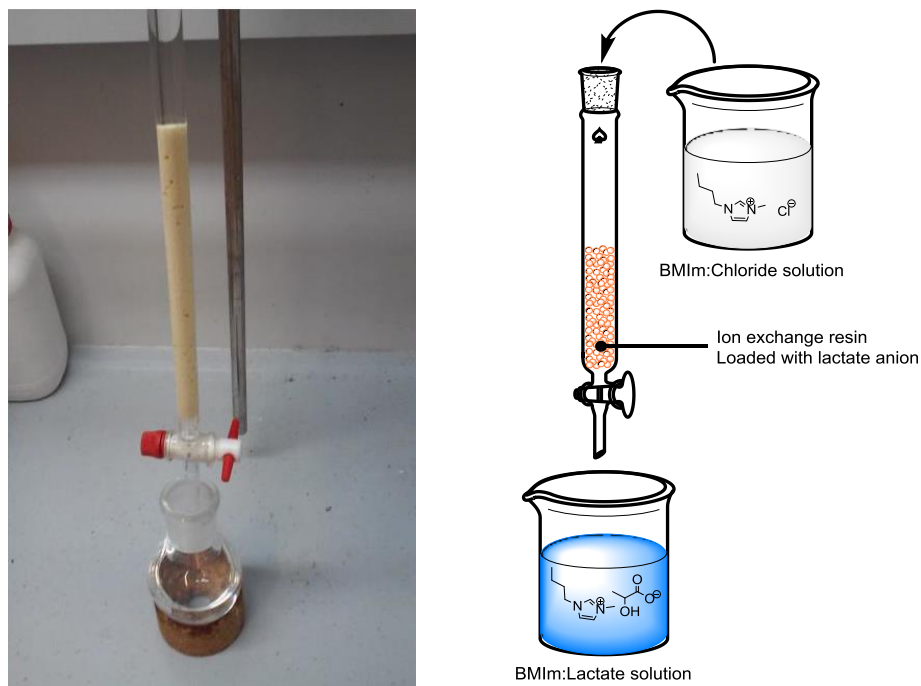


Figure 49. Left, a photograph depicting the ion exchange process (photo credit: Jordan Ochs). Right, a cartoon showing the anion exchange of chloride for lactate to prepare the BMIm:Lactate ionic liquid.

Preparation of polycarbonate ion gel (Gel-30-Lac)

A 12mL vial was charged with **N-8-C** (0.310g, 2.2mmol), **bis N-8-C** (0.120g, 0.42mmol), PEG₈₀₀₀ end capped diol (0.030g), and BMIm:Lactate (0.138g) were dissolved in 2mL of DCM. Next, DBU (0.036g) was added to the solution, and the vial was sealed and placed into an oil bath at 40 °C for 24 hr. The vial was then taken out of the oil bath and placed on a flat surface. The cap was then removed for the DCM to evaporate slowly at room temperature. The gels were then carefully dried in a conventional oven at 50 °C (~12 hr) and later a Buchi® oven at 50 °C (24 hr) under vacuum.

Rheology testing

Rheology measurements on the ion gels were conducted on Anton Paar Physica MCR 101 rheometer using oscillatory tests with parallel plate geometry. Angular frequency sweeps from 0.0628 s^{-1} to 314 s^{-1} at constant strain amplitude ($\gamma = 1\%$) were applied at $25\text{ }^{\circ}\text{C}$. Later, G' and G'' values were plotted versus frequency.

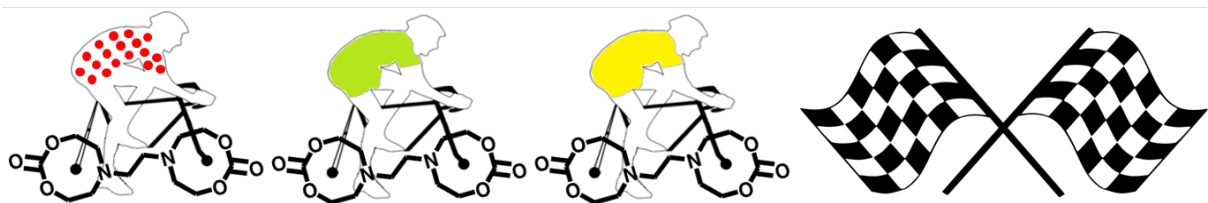
Biodegradability assessment

A 250mL bottle was filled to the maximum with MilliQ deionized water. Next, the polycarbonate gel was placed flat at the bottom-center of the bottle. The bottle was then sealed and kept at room temperature. Once the gel(s) had degraded or was no longer visible, the water was removed using a rotary evaporator. The remaining residues were then characterized by NMR and FTIR-ATR.

Device fabrication

Fabrication of the electrodes were prepared in a similar fashion as Leleux et al.¹²² In short, plastic polyimide (Kapton HN) electrodes were laser-cut to a thickness of 125 μm and an active area of 0.5 cm^2 . Then, 10 nm of chromium and 100 nm of gold were evaporated onto the electrodes. A solution of PEDOT:PSS, ethylene glycol, 4-dodecylbenzenesulfonic acid, and 3-methacryloxypropyltrimethoxysilane (ratio of 80/10/0.4/1) was then drop casted ($5\text{ }\mu\text{L}$) onto the active area of the electrode. The PEDOT:PSS film was then baked at $110\text{ }^{\circ}\text{C}$. **Gel-Lac-30** was then deposited on top of the PEDOT:PSS layer of the recording area and left overnight at room temperatures and conditions. To finish the device, a connection terminal was added to the other side of the electrode using a snap button, and the insulation for the device was provided from a protective paint.

Chapter 7



Conclusions

Chapter 7. Conclusions

The scope of this PhD thesis was aimed at exploring the versatility of the *N*-substituted eight membered cyclic carbonate platforms. Through this thesis work, these cyclic carbonates were utilized as starting materials towards poly(hydroxyurethane)s, antimicrobial polycarbonates, and even solid electrolytes for electrodes.

Firstly, we demonstrated that **bis N-8-C** was an excellent candidate for the synthesis of isocyanate free poly(hydroxyurethane)s. Kinetic studies of the mono-functional **N-8-C** and bi-functional **bis N-8-C** demonstrated their superior reactivity over the smaller and well known five and six membered cyclic carbonates. Furthermore, high molecular weight NIPUs were formed by the polyaddition of **bis N-8-C** and 1,6-hexamethylenediamine at room temperature without any catalysts. The results from this study indicated that **bis N-8-C** to be an ideal candidate for sustainable synthesis of industrially relevant non-isocyanate poly(hydroxyurethane)s.

Next, linear polycarbonates and polycarbonate hydrogels were prepared using the ROP of eight membered cyclic carbonates. These materials were quaternized with iodomethane to afford cationic structures suitable for bactericidal activity. The materials were shown to be effective against both *E. coli* and *S. aureus*. Further hemolysis testing showed that both materials exhibited very low hemolytic activity. These properties make these materials of interest in treating biofilms contaminated with pathogens or even possibly wound dressings. However, the materials in this section utilized a post-polymerization quaternization step that does not allow for precise control of the quaternization of the tertiary amines present within the polymers.

To remedy this, we then synthesized and polymerized cationic aliphatic cyclic carbonates. By polymerizing charged cyclic carbonates, this would help control the degree of quaternization in the final material without a need for a post-quaternization procedure. The charged monomers showed very high reactivity rates and were polymerizable in conditions that are generally unfavorable for ROP processes. A computational study was conducted and confirmed that the cationic cyclic monomers were indeed orders of magnitude more reactive than their non-charged analogs. Polycarbonate gels were also prepared and their swelling and the biodegradability properties were studied. The polycarbonate hydrogels demonstrated very high bactericidal activity against *E. coli* and *S. aureus* by disrupting the membrane of the bacteria. However, these materials also suffered from quite high hemolysis activities.

Allyl functionalized eight membered cyclic carbonates based on diethanolamines were also prepared. Our kinetic studies revealed the superior reactivity of **8-ACfm** over **8-ACI**, and obtained high conversions after one hour despite the low organocatalyst loading of 2.5 mol%. Homopolymers with **8-ACfm** were also prepared and the allyl functionalities were modified with three different thiols. We also copolymerized **8-ACfm** with two commercially available cyclic monomers (L-Lactide and TMC) and functionalized them with 1-butanethiol with similar success.

Finally, a series of biodegradable polycarbonate iongels were prepared and tested as solid electrolytes for electrophysiological applications. Ion gels consisting of 30 wt% BMIm:Lactate were found to be the most promising. Using FTIR-ATR and rheological measurements, we determined that we were able to successfully polymerize our cyclic carbonate monomers in the presence of ionic liquids and organocatalysts. Ionic conductivities of the ion gels showed that trace amounts water absorbed by the ion gels from the atmosphere led to huge

gains in ionic conductivity. With the iongels showing promising conductivities, electrodes were fabricated and tested. Impedance measurements showed a slight advantage of our electrodes with lower impedances over the standard medical Ag/AgCl electrodes. Lastly, we used our electrodes for electrocardiography and were able to produce heartbeat recordings comparable to that of the standard medical electrodes.

In conclusion, the versatility of the *N*-substituted eight membered cyclic carbonates was demonstrated in this thesis. Using these monomers and materials, we were able to prepare both polycarbonates and poly(hydroxyurethane)s. Furthermore, we synthesized gels from these monomers and studied them in two separate applications (antibacterial hydrogels and electrophysiology). The *N*-substituted eight membered cyclic carbonate platform is a rather new compared to its smaller cousins, and this thesis work demonstrated it has great potential to produce new functional materials for a wide variety of applications.

Chapter 8

References and lists

Chapter 8. References and lists

8.1 References

- 1 J. H. Clements, *Ind. Eng. Chem. Res.*, 2003, **42**, 663–674.
- 2 US5449474 A, 1995.
- 3 US6239090 B1, 2001.
- 4 US6187108 B1, 2001.
- 5 G. Gachot, S. Grugeon, M. Armand, S. Pilard, P. Guenot, J.-M. Tarascon and S. Laruelle, *J. Power Sources*, 2008, **178**, 409–421.
- 6 US5993787 A, 1999.
- 7 H. Tomita, F. Sanda and T. Endo, *J. Polym. Sci. Part Polym. Chem.*, 2001, **39**, 162–168.
- 8 H. Sardon, A. Pascual, D. Mecerreyes, D. Taton, H. Cramail and J. L. Hedrick, *Macromolecules*, 2015, **48**, 3153–3165.
- 9 G. Beniah, X. Chen, B. E. Uno, K. Liu, E. K. Leitsch, J. Jeon, W. H. Heath, K. A. Scheidt and J. M. Torkelson, *Macromolecules*, 2017, **50**, 3193–3203.
- 10 L. Maisonneuve, O. Lamarzelle, E. Rix, E. Grau and H. Cramail, *Chem. Rev.*, , DOI:10.1021/acs.chemrev.5b00355.
- 11 A. Bossion, G. O. Jones, D. Taton, D. Mecerreyes, J. L. Hedrick, Z. Y. Ong, Y. Y. Yang and H. Sardon, *Langmuir*, 2017, **33**, 1959–1968.
- 12 T. Lebarbé, A. S. More, P. S. Sane, E. Grau, C. Alfos and H. Cramail, *Macromol. Rapid Commun.*, 2014, **35**, 479–483.
- 13 A. S. More, T. Lebarbé, L. Maisonneuve, B. Gadenne, C. Alfos and H. Cramail, *Eur. Polym. J.*, 2013, **49**, 823–833.
- 14 H. Sardon, A. C. Engler, J. M. W. Chan, D. J. Coady, J. M. O'Brien, D. Mecerreyes, Y. Y. Yang and J. L. Hedrick, *Green Chem.*, 2013, **15**, 1121–1126.
- 15 Renewable Non-Isocyanate Based Thermoplastic Polyurethanes via Polycondensation of Dimethyl Carbamate Monomers with Diols - Unverferth - 2013 - Macromolecular Rapid Communications - Wiley Online Library, <http://onlinelibrary.wiley.com/doi/10.1002/marc.201300503/full>, (accessed August 24, 2017).
- 16 O. Kreye, H. Mutlu and M. A. R. Meier, *Green Chem.*, 2013, **15**, 1431–1455.
- 17 J. Guan, Y. Song, Y. Lin, X. Yin, M. Zuo, Y. Zhao, X. Tao and Q. Zheng, *Ind. Eng. Chem. Res.*, 2011, **50**, 6517–6527.
- 18 E. Delebecq, J.-P. Pascault, B. Boutevin and F. Ganachaud, *Chem. Rev.*, 2013, **113**, 80–118.
- 19 R. H. Lambeth and T. J. Henderson, *Polymer*, 2013, **54**, 5568–5573.
- 20 B. Ochiai, H. Kojima and T. Endo, *J. Polym. Sci. Part Polym. Chem.*, 2014, **52**, 1113–1118.
- 21 H. Matsukizono and T. Endo, *RSC Adv.*, 2015, **5**, 71360–71369.

- 22 H. Tomita, F. Sanda and T. Endo, *J. Polym. Sci. Part Polym. Chem.*, 2001, **39**, 851–859.
- 23 B. Ochiai, M. Matsuki, T. Miyagawa, D. Nagai and T. Endo, *Tetrahedron*, 2005, **61**, 1835–1838.
- 24 B. Ochiai, Y. Satoh and T. Endo, *Green Chem.*, 2005, **7**, 765–767.
- 25 O. Lamarzelle, P.-L. Durand, A.-L. Wirocius, G. Chollet, E. Grau and H. Cramail, *Polym. Chem.*, 2016, **7**, 1439–1451.
- 26 D. J. Fortman, J. P. Brutman, C. J. Cramer, M. A. Hillmyer and W. R. Dichtel, *J. Am. Chem. Soc.*, 2015, **137**, 14019–14022.
- 27 H. Tomita, F. Sanda and T. Endo, *J. Polym. Sci. Part Polym. Chem.*, 2001, **39**, 860–867.
- 28 H. Tomita, F. Sanda and T. Endo, *J. Polym. Sci. Part Polym. Chem.*, 2001, **39**, 162–168.
- 29 L. Maisonneuve, A. S. More, S. Foltran, C. Alfos, F. Robert, Y. Landais, T. Tassaing, E. Grau and H. Cramail, *RSC Adv.*, 2014, **4**, 25795–25803.
- 30 V. Caló, A. Nacci, A. Monopoli and A. Fanizzi, *Org. Lett.*, 2002, **4**, 2561–2563.
- 31 T. Ema, Y. Miyazaki, S. Koyama, Y. Yano and T. Sakai, *Chem. Commun.*, 2012, **48**, 4489–4491.
- 32 V. Besse, G. Foyer, R. Auvergne, S. Caillol and B. Boutevin, *J. Polym. Sci. Part Polym. Chem.*, 2013, **51**, 3284–3296.
- 33 M. Blain, L. Jean-Gérard, R. Auvergne, D. Benazet, S. Caillol and B. Andrioletti, *Green Chem.*, 2014, **16**, 4286–4291.
- 34 S. Tempelaar, L. Mespouille, P. Dubois and A. P. Dove, *Macromolecules*, 2011, **44**, 2084–2091.
- 35 L. Mespouille, O. Coulembier, M. Kawalec, A. P. Dove and P. Dubois, *Prog. Polym. Sci.*, 2014, **39**, 1144–1164.
- 36 Z. Zhang, R. Kuijter, S. K. Bulstra, D. W. Grijpma and J. Feijen, *Biomaterials*, 2006, **27**, 1741–1748.
- 37 A. Pascual, J. P. K. Tan, A. Yuen, J. M. W. Chan, D. J. Coady, D. Mecerreyes, J. L. Hedrick, Y. Y. Yang and H. Sardon, *Biomacromolecules*, 2015, **16**, 1169–1178.
- 38 Z. Zhang, D. W. Grijpma and J. Feijen, *J. Controlled Release*, 2006, **111**, 263–270.
- 39 A. Y. Yuen, E. Lopez Martinez, E. Gomez-Bengoia, A. L. Cortajarena, R. H. Aguirresarobe, A. Bossion, D. Mecerreyes, J. L. Hedrick, Y. Y. Yang and H. Sardon, *ACS Biomater. Sci. Eng.*, , DOI:10.1021/acsbiomaterials.7b00335.
- 40 J. P. K. Tan, D. J. Coady, H. Sardon, A. Yuen, S. Gao, S. W. Lim, Z. C. Liang, E. W. Tan, S. Venkataraman, A. C. Engler, M. Fevre, R. Ono, Y. Y. Yang and J. L. Hedrick, *Adv. Healthc. Mater.*, n/a-n/a.
- 41 J. Feng, R.-X. Zhuo and X.-Z. Zhang, *Prog. Polym. Sci.*, 2012, **37**, 211–236.
- 42 L. Meabe, H. Sardon and D. Mecerreyes, *Eur. Polym. J.*, , DOI:10.1016/j.eurpolymj.2017.06.046.
- 43 S. Inoue, H. Koinuma and T. Tsuruta, *Makromol. Chem.*, 1969, **130**, 210–220.
- 44 D. J. Darensbourg, *Chem. Rev.*, 2007, **107**, 2388–2410.

- 45 O. Nuyken and S. D. Pask, *Polymers*, 2013, **5**, 361–403.
- 46 B. D. Mullen, C. N. Tang and R. F. Storey, *J. Polym. Sci. Part Polym. Chem.*, 2003, **41**, 1978–1991.
- 47 X. Hu, X. Chen, S. Liu, Q. Shi and X. Jing, *J. Polym. Sci. Part Polym. Chem.*, 2008, **46**, 1852–1861.
- 48 J. M. W. Chan, X. Zhang, M. K. Brennan, H. Sardon, A. C. Engler, C. H. Fox, C. W. Frank, R. M. Waymouth and J. L. Hedrick, *J. Chem. Educ.*, 2015, **92**, 708–713.
- 49 T. Ariga, T. Takata and T. Endo, *Macromolecules*, 1997, **30**, 737–744.
- 50 S. H. Kim, J. P. K. Tan, K. Fukushima, F. Nederberg, Y. Y. Yang, R. M. Waymouth and J. L. Hedrick, *Biomaterials*, 2011, **32**, 5505–5514.
- 51 R. C. Pratt, F. Nederberg, R. M. Waymouth and J. L. Hedrick, *Chem. Commun.*, 2008, **0**, 114–116.
- 52 Z. Y. Ong, K. Fukushima, D. J. Coady, Y.-Y. Yang, P. L. R. Ee and J. L. Hedrick, *J. Controlled Release*, 2011, **152**, 120–126.
- 53 X. Zhang, Z. Zhong and R. Zhuo, *Macromolecules*, 2011, **44**, 1755–1759.
- 54 S. Tempelaar, L. Mespouille, O. Coulembier, P. Dubois and A. P. Dove, *Chem. Soc. Rev.*, 2013, **42**, 1312–1336.
- 55 P. G. Parzuchowski, M. Jaroch, M. Tryznowski and G. Rokicki, *Macromolecules*, 2008, **41**, 3859–3865.
- 56 F. He, Y.-P. Wang, G. Liu, H.-L. Jia, J. Feng and R.-X. Zhuo, *Polymer*, 2008, **49**, 1185–1190.
- 57 D. P. Sanders, K. Fukushima, D. J. Coady, A. Nelson, M. Fujiwara, M. Yasumoto and J. L. Hedrick, *J. Am. Chem. Soc.*, 2010, **132**, 14724–14726.
- 58 B. B. Uysal, U. S. Gunay, G. Hizal and U. Tunca, *J. Polym. Sci. Part Polym. Chem.*, 2014, **52**, 1581–1587.
- 59 X. Hu, X. Chen, H. Cheng and X. Jing, *J. Polym. Sci. Part Polym. Chem.*, 2009, **47**, 161–169.
- 60 S. C. D. Smedt, J. Demeester and W. E. Hennink, *Pharm. Res.*, 2000, **17**, 113–126.
- 61 I. Tabujew and K. Peneva, 2014, pp. 1–29.
- 62 H.-F. Wang, W. Su, C. Zhang, X. Luo and J. Feng, *Biomacromolecules*, 2010, **11**, 2550–2557.
- 63 X. Zhang, M. Cai, Z. Zhong and R. Zhuo, *Macromol. Rapid Commun.*, 2012, **33**, 693–697.
- 64 D. Mecerreyes, *Prog. Polym. Sci.*, 2011, **36**, 1629–1648.
- 65 M. Isik, T. Lonjaret, H. Sardon, R. Marcilla, T. Herve, G. G. Malliaras, E. Ismailova and D. Mecerreyes, *J. Mater. Chem. C*, 2015, **3**, 8942–8948.
- 66 V. Besse, F. Camara, F. Méchin, E. Fleury, S. Caillol, J.-P. Pascault and B. Boutevin, *Eur. Polym. J.*, 2015, **71**, 1–11.
- 67 J. Guan, Y. Song, Y. Lin, X. Yin, M. Zuo, Y. Zhao, X. Tao and Q. Zheng, *Ind. Eng. Chem. Res.*, 2011, **50**, 6517–6527.
- 68 N. von der Assen and A. Bardow, *Green Chem.*, 2014, **16**, 3272–3280.

- 69 E. Delebecq, J.-P. Pascault, B. Boutevin and F. Ganachaud, *Chem. Rev.*, 2013, **113**, 80–118.
- 70 A. Boyer, E. Cloutet, T. Tassaing, B. Gadenne, C. Alfos and H. Cramail, *Green Chem.*, 2010, **12**, 2205–2213.
- 71 B. Grignard, J.-M. Thomassin, S. Gennen, L. Poussard, L. Bonnaud, J.-M. Raquez, P. Dubois, M.-P. Tran, C. B. Park, C. Jerome and C. Detrembleur, *Green Chem.*, , DOI:10.1039/C5GC02723C.
- 72 R. H. Lambeth and T. J. Henderson, *Polymer*, 2013, **54**, 5568–5573.
- 73 B. Ochiai, H. Kojima and T. Endo, *J. Polym. Sci. Part Polym. Chem.*, 2014, **52**, 1113–1118.
- 74 H. Matsukizono and T. Endo, *RSC Adv.*, 2015, **5**, 71360–71369.
- 75 H. Tomita, F. Sanda and T. Endo, *J. Polym. Sci. Part Polym. Chem.*, 2001, **39**, 851–859.
- 76 B. Ochiai, M. Matsuki, T. Miyagawa, D. Nagai and T. Endo, *Tetrahedron*, 2005, **61**, 1835–1838.
- 77 B. Ochiai, S. Inoue and T. Endo, *J. Polym. Sci. Part Polym. Chem.*, 2005, **43**, 6282–6286.
- 78 B. Ochiai, S. Inoue and T. Endo, *J. Polym. Sci. Part Polym. Chem.*, 2005, **43**, 6613–6618.
- 79 B. Ochiai, Y. Satoh and T. Endo, *Green Chem.*, 2005, **7**, 765–767.
- 80 O. Lamarzelle, P.-L. Durand, A.-L. Wirotius, G. Chollet, E. Grau and H. Cramail, *Polym. Chem.*, , DOI:10.1039/C5PY01964H.
- 81 D. J. Fortman, J. P. Brutman, C. J. Cramer, M. A. Hillmyer and W. R. Dichtel, *J. Am. Chem. Soc.*, 2015, **137**, 14019–14022.
- 82 H. Tomita, F. Sanda and T. Endo, *J. Polym. Sci. Part Polym. Chem.*, 2001, **39**, 860–867.
- 83 L. Maisonneuve, A. S. More, S. Foltran, C. Alfos, F. Robert, Y. Landais, T. Tassaing, E. Grau and H. Cramail, *RSC Adv.*, 2014, **4**, 25795.
- 84 H. Tomita, F. Sanda and T. Endo, *J. Polym. Sci. Part Polym. Chem.*, 2001, **39**, 4091–4100.
- 85 S. Venkataraman, V. W. L. Ng, D. J. Coady, H. W. Horn, G. O. Jones, T. S. Fung, H. Sardon, R. M. Waymouth, J. L. Hedrick and Y. Y. Yang, *J. Am. Chem. Soc.*, 2015, **137**, 13851–13860.
- 86 L. Maisonneuve, A.-L. Wirotius, C. Alfos, E. Grau and H. Cramail, *Polym. Chem.*, 2014, **5**, 6142–6147.
- 87 H. Tomita, F. Sanda and T. Endo, *J. Polym. Sci. Part Polym. Chem.*, 2001, **39**, 3678–3685.
- 88 M. V. Zabalov, R. P. Tiger and A. A. Berlin, *Russ. Chem. Bull.*, 2012, **61**, 518–527.
- 89 V. D. Nemirovsky and S. S. Skorokhodov, *J. Polym. Sci. Part C Polym. Symp.*, 2007, **16**, 1471–1478.
- 90 F. Camara, S. Benyahya, V. Besse, G. Boutevin, R. Auvergne, B. Boutevin and S. Caillol, *Eur. Polym. J.*, 2014, **55**, 17–26.

- 91 T. Ariga, T. Takata and T. Endo, *J. Polym. Sci. Part Polym. Chem.*, 1993, **31**, 581–584.
- 92 J. L. J. van Velthoven, L. Gootjes, D. S. van Es, B. A. J. Noordover and J. Meuldijk, *Eur. Polym. J.*, 2015, **70**, 125–135.
- 93 T. D. Gootz, *Crit. Rev. Immunol.*, DOI:10.1615/CritRevImmunol.v30.i1.60.
- 94 R. P. Mishra, E. Oviedo-Orta, P. Prachi, R. Rappuoli and F. Bagnoli, *Curr. Opin. Microbiol.*, 2012, **15**, 596–602.
- 95 G. D. Wright, *Chem. Commun.*, 2011, **47**, 4055–4061.
- 96 F. Nederberg, Y. Zhang, J. P. K. Tan, K. Xu, H. Wang, C. Yang, S. Gao, X. D. Guo, K. Fukushima, L. Li, J. L. Hedrick and Y.-Y. Yang, *Nat. Chem.*, 2011, **3**, 409–414.
- 97 A. C. Engler, N. Wiradharma, Z. Y. Ong, D. J. Coady, J. L. Hedrick and Y.-Y. Yang, *Nano Today*, 2012, **7**, 201–222.
- 98 A. S. Hoffman, *Adv. Drug Deliv. Rev.*, 2012, **64**, 18–23.
- 99 S. Sarabahi, *Indian J. Plast. Surg.*, 2012, **45**, 379.
- 100 C. Zhao, X. Li, L. Li, G. Cheng, X. Gong and J. Zheng, *Langmuir*, 2013, **29**, 1517–1524.
- 101 A. C. Engler, J. P. K. Tan, Z. Y. Ong, D. J. Coady, V. W. L. Ng, Y. Y. Yang and J. L. Hedrick, *Biomacromolecules*, 2013, **14**, 4331–4339.
- 102 Hössel, Dieing, Nörenberg, Pfau and Sander, *Int. J. Cosmet. Sci.*, 2000, **22**, 1–10.
- 103 M. Isik, A. M. Fernandes, K. Vijayakrishna, M. Paulis and D. Mecerreyes, *Polym. Chem.*, 2016, **7**, 1668–1674.
- 104 S. Venkataraman, J. P. K. Tan, V. W. L. Ng, E. W. P. Tan, J. L. Hedrick and Y. Y. Yang, *Biomacromolecules*, DOI:10.1021/acs.biomac.6b01463.
- 105 Z. Zheng, J. Guo, H. Mao, Q. Xu, J. Qin and F. Yan, *ACS Biomater. Sci. Eng.*, DOI:10.1021/acsbiomaterials.7b00165.
- 106 A. W. Thomas and A. P. Dove, *Macromol. Biosci.*, 2016, **16**, 1762–1775.
- 107 Z. X. Voo, M. Khan, K. Narayanan, D. Seah, J. L. Hedrick and Y. Y. Yang, *Macromolecules*, 2015, **48**, 1055–1064.
- 108 A. C. Engler, J. M. W. Chan, D. J. Coady, J. M. O'Brien, H. Sardon, A. Nelson, D. P. Sanders, Y. Y. Yang and J. L. Hedrick, *Macromolecules*, 2013, **46**, 1283–1290.
- 109 R. J. Williams, I. A. Barker, R. K. O'Reilly and A. P. Dove, *ACS Macro Lett.*, 2012, **1**, 1285–1290.
- 110 C. E. Hoyle, A. B. Lowe and C. N. Bowman, *Chem. Soc. Rev.*, 2010, **39**, 1355–1387.
- 111 K. Olofsson, M. Malkoch and A. Hult, *J. Polym. Sci. Part Polym. Chem.*, 2016, **54**, 2370–2378.
- 112 A. Yuen, A. Bossion, E. Gómez-Bengoia, F. Ruipérez, M. Isik, J. L. Hedrick, D. Mecerreyes, Y. Y. Yang and H. Sardon, *Polym. Chem.*, 2016, **7**, 2105–2111.
- 113 A. Pascual, H. Sardón, F. Ruipérez, R. Gracia, P. Sudam, A. Veloso and D. Mecerreyes, *J. Polym. Sci. Part Polym. Chem.*, 2015, **53**, 552–561.

-
- 114 Y. A. Chang, A. E. Rudenko and R. M. Waymouth, *ACS Macro Lett.*, 2016, **5**, 1162–1166.
- 115 R. C. Pratt, B. G. G. Lohmeijer, D. A. Long, P. N. P. Lundberg, A. P. Dove, H. Li, C. G. Wade, R. M. Waymouth and J. L. Hedrick, *Macromolecules*, 2006, **39**, 7863–7871.
- 116 X. Zhang, G. O. Jones, J. L. Hedrick and R. M. Waymouth, *Nat. Chem.*, 2016, **8**, 1047–1053.
- 117 L.-D. Liao, I.-J. Wang, S.-F. Chen, J.-Y. Chang and C.-T. Lin, *Sensors*, 2011, **11**, 5819–5834.
- 118 M. Galiński, A. Lewandowski and I. Stępniaik, *Electrochimica Acta*, 2006, **51**, 5567–5580.
- 119 T. Artham and M. Doble, *Macromol. Biosci.*, 2008, **8**, 14–24.
- 120 E. Alcalde, I. Dinarès, A. Ibáñez and N. Mesquida, *Molecules*, 2012, **17**, 4007–4027.
- 121 E. S. Kappenman and S. J. Luck, *Psychophysiology*, DOI:10.1111/j.1469-8986.2010.01009.x.
- 122 P. Leleux, C. Johnson, X. Strakosas, J. Rivnay, T. Hervé, R. M. Owens and G. G. Malliaras, *Adv. Healthc. Mater.*, 2014, **3**, 1377–1380.

8.2 List of figures

Figure 1. Applications of cyclic carbonates are far and wide ranging. The work in this thesis will focus on using cyclic carbonates as starting materials for polymers.	2
Figure 2. Examples of five, six, and seven membered cyclic carbonates (from left to right). As the ring size increases, the overall trend is higher reactivity and lower stability.	3
Figure 3. The four most studied synthetic pathways in obtaining polyurethanes without isocyanates. ⁸	5
Figure 4. Here we show cyclic carbonates bearing a number of different functional pendant groups, including: azide, amine, alkyl, allyl, halide, etc. Aside from the first two cyclic carbonates (from the left), the rest of the cyclic carbonates were derived from bis-MPA.	9
Figure 5. Visual representation of how the thesis was structured.	12
Figure 6. Kinetics plot from the aminolysis of various cyclic carbonates with <i>n</i> -hexylamine.	19
Figure 7. Conversions from reactions with <i>N</i> -8-C, 6-C, and 5-C with less reactive amines. Reactions were carried out at 50 °C for 6 hours.	20
Figure 8. Reaction energy profile for <i>N</i> -8-C and its Gibbs Free energies computed at m062x/6-31+G(d,p) (pcm, solvent =DMSO) level.	22
Figure 9. Comparison of the Free Gibbs activation energies for the ring opening process computed at m062x/6-31+G(d,p) (pcm, solvent =DMSO) level.	23
Figure 10. ¹ H NMR of NIPU1 after 24 h at 25 °C. Proton signals attributed to the starting material bis <i>N</i> -8-C have been labeled with "*"	25
Figure 11. FTIR-ATR spectra of (a) bis <i>N</i> -8-C monomer and (b) lyophilized NIPU1.	26
Figure 12. Polycarbonates were prepared via the ROP of <i>N</i> -8-C (top line) and later quaternized using iodomethane (bottom line).	40

Figure 13. ^1H NMR of the monomer <i>N</i> -8-C (bottom) and the ROP of 8M PDMEA 100 (top) in its crude after 40 hours of reaction time in CDCl_3 . The conversion was followed by using the relative integral values of the methyl pendant groups.	41
Figure 14. ^{13}C NMR of <i>N</i> -8-C (bottom), 8M PDMEA 100 (mid), and 8M PDMEA 100 Mel (top).	41
Figure 15. FTIR-ATR of the non-charged cyclic carbonate <i>N</i> -8-C (bottom) and the polymer 8M PDMEA 100 (top).....	42
Figure 16. FTIR-ATR of 8M PDMEA 100 Mel after quaternization with iodomethane.....	43
Figure 17. ^1H NMR in d_6 -DMSO of the polymer 8M PDMEA 100 Mel after the quaternization with iodomethane.....	44
Figure 18. Cationic polycarbonate hydrogels were prepared using the non-charged <i>N</i> -8-C. An additional post-polymerization step with iodomethane was required to obtain the charged structures.....	45
Figure 19. Antimicrobial studies of 8M PDMEA 200 Mel (inset) towards <i>S. aureus</i> were conducted using different minimum inhibitory concentrations (MIC) at 37 °C. Survivability measurements of the bacteria were taken at different time intervals (1, 5, 15, and 30min). ⁴⁰	47
Figure 20. Charged linear polycarbonates showed no hemolysis activities regardless of DPs tested and concentrations up to 1000 $\mu\text{g}/\text{mL}$ after 1 hr of incubation at 37 °C.....	48
Figure 21. Homopolymerizations of 8-Met (DP: 50) were carried out and characterized with ^1H NMR in d_6 -DMSO. Depicted above is of the homopolymer, and below is the monomer 8-Met.	61
Figure 22. FTIR-ATR of 8-Met (bottom) and its homopolymer at DP50 (top).	62
Figure 23. Depicted here are the substrates used in the computational study, neutral amine monomer (<i>N</i> -8-C, left) and the ammonium species (A-1, right). ..	64

- Figure 24. Reaction energy profile for substrate A-1 and its Gibbs Free energies computed at M062X/6-311+G(d,p) (iefpcm, solvent =DMSO) level. 65
- Figure 25. A representative scheme used to create the polycarbonate ion gels using the 8-Met (black, monomer), bis *N*-8-C (blue, crosslinker), and PEG (red, initiator). 67
- Figure 26. Rheological studies using oscillatory tests were performed on Gel-8-Met re-swollen with water. Here we have plotted the elastic modulus (G' , ▲) and the loss modulus (G'' , ■). The $G' > G''$ trend indicates that we have a three dimensionally covalently bonded network throughout the gel. 68
- Figure 27. We used FTIR-ATR to characterize the Gel-8-Met in its initial state (black) and after leaving the gel in water after eight hours at room temperature (red); an additional intermediary scan was also performed (blue). Polycarbonate signals at 1744 and 1244 cm^{-1} decreased with time in water, and carboxylic acid signal at 1702 cm^{-1} was observed upon the degradation of the polycarbonate. . 70
- Figure 28. Antibacterial efficacy of the hydrogels measured at different times (15 min, 30 min, 1 hr, 2 hrs, and 8 hrs) against *E. coli* (left) and *S. aureus* (right). The CFU/mL values were calculated from counting the number of colonies on agar plates when different dilutions were plated. 71
- Figure 29. Scanning electron microscopy (SEM) images of *E. coli* were taken before (left) and after (right) eight hours of treatment with Gel-8-Met; scale bars corresponds to 1 μm . The micrograph after the hydrogel treatment suggests that the bacteria underwent membrane disruption. 73
- Figure 30. Model polymerizations were carried out with monomers 8-ACfm (red) and 8-ACI (blue) with DBU (10 mol%) at room temperature. The monomer 8-Acfm was able to reach full conversion within 10 minutes, whereas 8-ACI only achieved 14% conversion after one hour. 87
- Figure 31. MALDI-TOF of the ROP of Polymer 2 (DP50). Here we observed signals that corresponded to both linear and cyclic polycarbonates. 90

Figure 32. ^1H NMR in CDCl_3 of polymer 2 in its crude (above) and after the radical thiol-ene functionalization with 1-butanethiol (below).	93
Figure 33. Here we show the ^1H NMRs of the two copolymers in CDCl_3 and their corresponding proton assignments; the copolymers with L-Lactide (above) and TMC (below).	96
Figure 34. ^1H NMR of Polymer 7a (top) and 8a (bottom) in CDCl_3 after thiol-ene modification with 1-butanethiol.	97
Figure 35. Polycarbonate ion gels were prepared in a one post synthesis approach. In doing so, we were able to control the amount of ionic liquid inside the iongels.	112
Figure 36. Here we show the chemical structures of the ionic liquids that we prepared and surveyed in the preparation of polycarbonate iongels for electrodes.	112
Figure 37. A photograph of a polycarbonate gel loaded with 30 wt% BMIm:Lactate (Gel-Lac-30).	114
Figure 38. FTIR-ATR characterization of the BMIm:Lactate ionic liquid (top), polycarbonate gel with 30wt% BMIm:Lactate (Gel-Lac-30, middle), and just the polycarbonate gel without any ionic liquids (bottom).	115
Figure 39. Rheological studies using oscillatory tests were performed for Gel-Lac-10 (black), Gel-Lac-20 (red), and Gel-Lac-30 (blue). Elastic moduli (G') are marked with triangles and loss moduli are marked with squares.	116
Figure 40. Photographs of the biodegradability experiment with Gel-Lac-30 in water at room temperature. An initial photograph was taken right when the gel was added to the water (left), and an additional photo was taken two hours later (right).	117
Figure 41. Residues from the biodegradability testing of Gel-Lac-30 were characterized with ^1H NMR in d_6 -DMSO. Here we can observe that the gels have degraded back into its respective starting materials: <i>N,N,N',N'</i> -tetrakis(2-	

hydroxyethyl)ethylenediamine (red), *N*-methyldiethanolamine (blue), polyethylene glycol (green), and BMIm:Lactate (yellow)..... 118

Figure 42. FTIR-ATR characterization of the Gel-Lac-30 after its biodegradability study in water (red) and before (blue). 119

Figure 43. Ionic conductivities measurements were carried for Gel-Lac-30 (green), Gel-Lac-20 (blue), Gel-Lac-10 (red), and Gel-Butyrate-10 (grey). A temperature range of 5 to 40 °C was surveyed and the ionic conductivities were given as $S\ cm^{-1}$ 120

Figure 44. Dried Gel-Lac-30 samples were left out in the laboratory and we tracked the moisture uptake (red, wt%) and ionic conductivities (blue) over a period of time. 122

Figure 45. Polycarbonate gels loaded with ionic liquids were left in the open inside the laboratory for one week. The ionic conductivities were then measured across a range of temperatures..... 123

Figure 46. An exploded view of the electrode and all of the different materials used (left). A photograph of the electrode with the ion gel deposited on top (right). 124

Figure 47. Comparison of the impedance on skin recordings with different working electrodes at a frequency range between 0.1 and 100000 Hz. Medical electrode (blue), PEDOT:PSS electrodes (black and red), and PEDOT:PSS with iongel electrodes (pink and green). 125

Figure 48. Electrocardiogram recordings were taken from the wrists of the volunteer (Top center). The standard medical Ag/AgCl electrode (bottom left) and the Gel-Lac-30 electrode (in green) were evaluated. 127

Figure 49. Left, a photograph depicting the ion exchange process (photo credit: Jordan Ochs). Right, a cartoon showing the anion exchange of chloride for lactate to prepare the BMIm:Lactate ionic liquid. 130

8.3 List of tables

Table 1. Synthesis of NIPUs from bis <i>N</i> -8-C and diamines after 24 h.	28
Table 2. Molecular weight measurements of linear non-charged polycarbonates	42
Table 3. Exploration of homopolymerization of charged eight-membered cyclic monomers via ROP in DMSO.....	60
Table 4. Comparison of the Gibbs Free energy values for the three different substrates, computed at M062X/6-311+G(d,p) (iefpcm, solvent =DMSO) level. 66	66
Table 5. Summary of different compositions used to prepare the gels and their swelling behaviors in H ₂ O.....	69
Table 6. Polymerization conditions and SEC results from ROP of 8-ACfm and 8- ACI.....	91
Table 7. Post-polymerization radical thiol-ene functionalization of polycarbonates.	94
Table 8. Copolymerization of with 8-ACfm to access functional copolymers.....	95
Table 9. Post-polymerization radical thiol-ene functionalization with 1-butanethiol of copolymers	97
Table 10. Ionic conductivities of the dried gels at room temperature (25°C).....	121

8.4 List of publications from this thesis

1. Broad-spectrum antimicrobial polycarbonate hydrogels with fast degradability, A. Pascual, J. P. K. Tan, **A. Yuen**, J. M. W. Chan, D. J. Coady, D. Mecerreyes, J. L. Hedrick, Y. Y. Yang and H. Sardon, *Biomacromolecules*, 2015, 16, 1169–1178.

2. Room temperature synthesis of non-isocyanate polyurethanes (NIPUs) using highly reactive N-substituted 8-membered cyclic carbonates, **A. Yuen**, A. Bossion, E. Gómez-Bengoa, F. Ruipérez, M. Isik, J. L. Hedrick, D. Mecerreyes, Y. Y. Yang and H. Sardon, *Polym. Chem.*, 2016, 7, 2105–2111.

3. Preparation of Biodegradable Cationic Polycarbonates and Hydrogels Through the Direct Polymerization of Quaternized Cyclic Carbonates, **A. Yuen**, E. Lopez Martinez, E. Gomez-Bengoa, A. L. Cortajarena, R. H. Aguirresarobe, A. Bossion, D. Mecerreyes, J. L. Hedrick, Y. Y. Yang and H. Sardón, *ACS Biomater. Sci. Eng.*, DOI:10.1021/acsbiomaterials.7b00335.

4. Broad Spectrum Macromolecular Antimicrobials with Biofilm Disruption Capability and In Vivo Efficacy, J. P. K. Tan, D. J. Coady, H. Sardon, **A. Yuen**, S. Gao, S. W. Lim, Z. C. Liang, E. W. Tan, S. Venkataraman, A. C. Engler, M. Fevre, R. Ono, Y. Y. Yang and J. L. Hedrick, *Adv. Healthc. Mater.*, DOI:10.1002/adhm.201601420.

The works in Chapters 5 and 6 are currently being prepared for publication.